

181981



no.596, 1960

USGS LIBRARY - RESTON



3 1818 00083247 5

20)

290

0.596

960

60-162

Do not copy
this page

UNITED STATES
✓ DEPARTMENT OF THE INTERIOR
U.S. Geological Survey

[Reports - Open file series]

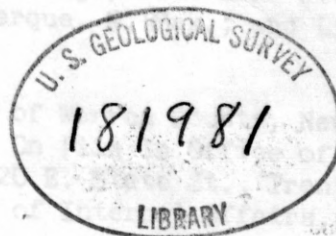
PETROGRAPHY OF THE UPPER CAMBRIAN DOLOMITES OF WARREN COUNTY.

NEW JERSEY

by

Valentine E. Zadnik

1934-



4 JAN 1963

This report and/or map is preliminary and has not been edited or reviewed for conformity with Geological Survey standards or nomenclature.

OPEN-FILE REPORT

7787

Contents

	Page
Abstract-----	4
Introduction-----	5
Acknowledgements-----	5
Physiographic setting and location-----	6
Stratigraphy-----	6
Structure-----	22
Location and general description-----	24
Description of microfacies-----	25
Methods and techniques of the investigation-----	29
The ideal cycle-----	35
Description of section 1-----	38
Generalized parameter variations for section 1-----	42
Description of section 2-----	46
Generalized parameter variations for section 2-----	59
Conclusions-----	62
Bibliography-----	64
Appendix-----	67

Dark zone under stromatolites is collitic dolarenite----- 15

6.--Road cut along north side of U. S. Route 22 near
 cloverleaf at west end of Easton, Pa. Well preserved,
 small Cryptozoon fieldii on top bedding surface----- 14

7.--Carpentersville section, unit 278. Rather large
 cabbagelike stromatolite colony showing thinly
 laminated character----- 1

- Figure 1.--Carpentersville section, unit 317. View of two large bowl-shaped stromatolite colonies near the southeast corner of the fifth quarry from the north. Scales are 8 inches.----- 13
- 2.--Carpentersville section, unit 334. Nicely preserved Cryptozoon fieldii showing knobby, thinly laminated top surface (bedding surface).----- 13
- 3.--Carpentersville section, unit 139. Very large stromatolite colony in overturned strata measuring 6 feet across, 1 foot high. Within large arcuate structure are fine, conformable, wavy laminae----- 14
- 4.--Railroad cut at junction U. S. Routes 22 and 24 east of Phillipsburg, N. J. Large stromatolite colony exhibiting knobby top bedding surface.----- 14
- 5.--Abandoned quarry behind sewage disposal plant at Phillipsburg, N. J. Close-up view of Cryptozoon fieldii with well-developed, conformable laminae. Dark zone under stromatolites is oolitic dolarenite- 15
- 6.--Road cut along north side of U. S. Route 22 near cloverleaf at west end of Easton, Pa. Well preserved, small Cryptozoon fieldii on top bedding surface----- 15
- 7.--Carpentersville section, unit 278. Rather large cabbagelike stromatolite colony showing thinly laminated character.----- 16

Figure 8.--Reigelsville section, unit 89. Close-up view of

- Anamalophycus compactus displaying small digitate-like structures----- 16
- 9.--Carpentersville section, unit 73. Irregular distribution of quartz grains in desiccation dolerudite. Embedded lithic fragments weather in negative relief. Strata overturned----- 17
- 10.--Carpentersville section, unit 73. Irregular distribution of quartz grains in desiccation dolerudite. Strata overturned----- 17
- 11.--Carpentersville section, unit 258. Small oscillation ripple marks on overturned strata. Crests are 2 inches apart----- 18
- 12.--Abandoned quarry opposite Locks 22 and 23 of the Delaware Canal along U. S. Route 611, Pa. Large oscillation ripple marks on north wall of quarry in overturned strata. Crests are 16 inches apart----- 18
- 13.--Carpentersville section, unit 258. "Fucoids" measuring 1/4 inch in diameter and 8 or 10 inches long. Strata overturned----- 19
- 14.--Carpentersville section, unit 149. Desiccation polygons in dolarenite----- 19
- 15.--Abandoned quarry behind sewage disposal plant at Phillipsburg, New Jersey. Desiccation brecciation of stromatolite colony. Dark Massive beds below stromatolites are oolitic dolarenite----- 36

Figure 16.--Abandoned quarry behind sewage disposal plant at Phillipsburg, New Jersey. Desiccation brecciation of stromatolites. Note superposition of small digitate and funnel-shaped colonies over large dome-shaped variety. Note inverted lunate fragments in desiccation dolorudite near top of photograph-----	43 44 45-5 59-6 61 36
17.--Abandoned quarry behind sewage disposal plant at Phillipsburg, New Jersey. Close-up showing transition from oolitic dolarenite (dark platy beds at bottom of photograph) to cryptozoan dolomite (light beds which thin and thicken) and overlying arenaceous desiccation dolorudite with cross bedding directly above stromatolites-----	37
18.--Road cut along south side of U. S. Route 22 near cloverleaf at west end of Easton, Pennsylvania. Relationship of oolitic dolarenite (lower dark bed), cryptozoan dolomite and arenaceous desiccation dolorudite with tabular and lunate fragments oriented parallel to bedding-----	37
Plate 1.--Location Map of Investigated Sections-----	7
2.--Table of Symbols-----	25
3.--Column Showing Parameter Variations of Microfacies Section 1-----	35
4.--Column Showing Parameter Variations of Microfacies Section 2-----	35
5-8.--Detailed Parameter Variations - Section 1-----	38-42

	Page
Plate 9.--Generalized Parameter Variations - Section 1-----	43
10.--Parameter Variations for Groups of Cycles - Section 1--	44
11-24.--Detailed Parameter Variations - Section 2-----	46-54
25-26.--Generalized Parameter Variations - Section 2-----	59-60
27.--Parameter Variations for Groups of Cycles - Section 2--	61

Table 1.--Chemical analyses for five samples from investigated environment. In order of decreasing relative depth these microfossils are: dololite, sections-----, dolomite, and dehydrated dolorudite.

Over 1,200 samples spaced at an average interval of 1.8 feet were collected from two measured sections, one at Riegelsville, N. J., and another at Carpentersville, N. J. Thin sections, cut perpendicular to the bedding were made and analyzed according to the method used by Albert V. Carozzi which consists of the statistical measurement of the sizes and frequencies of detrital, authigenic and organic components of a sedimentary rock. In this investigation, three general types of parameters were investigated: detrital components, degree of crystallinity and chemical composition. The detrital components present in sufficient abundance for study are quartz, pyrite, calcite and reworked lithic fragments. The maximum size of the largest optically continuous dolomite crystals for each thin section was measured to obtain the degree of crystallinity. Chemical composition was investigated by means of an X-ray diffractometer.

The results of the statistical measurements are interpreted by means of a bathymetrical curve showing the variations of relative depth as a function of thickness. The oscillations in the bathymetrical curve exhibit superposed asymmetrical cycles of sedimentation. The ideal cycle begins with structureless dololite (deepest water facies) and grades upward through progressively shallower facies and terminates with desiccation doloredite. Immediately overlying this doloredite is a dololite which begins the superjacent cycle. The bathymetrical curve also displays a rhythmic occurrence of series of cycles or megacycles. Within each megacycle, each superposed cycle terminates in a progressively shallower microfacies.

The two investigated sections do not overlap stratigraphically and therefore correlation could not be attempted. Although correlation on the basis of individual cycles is probably limited to short distances, the megacycles and the major groups of cycles could provide a valuable means of correlation in this general area.

PETROGRAPHY OF THE UPPER CAMBRIAN DOLOMITES OF WARREN COUNTY,

NEW JERSEY

by Valentine E. Zadnik

Abstract

Petrographic investigation of the Upper Cambrian dolomites along the Delaware River in Warren County, New Jersey, has led to the distinction of six different microfacies each representing a specific sedimentary environment. In order of decreasing relative depth these microfacies are: dololutite, dolarenite, oolitic dolarenite, dolorudite, cryptozoan dolomite and desiccation dolorudite.

Over 1,200 samples spaced at an average interval of 1.8 feet were collected from two measured sections, one at Riegelsville, N. J., and another at Carpentersville, N. J. Thin sections, cut perpendicular to the bedding were made and analyzed according to the method used by Albert V. Carozzi which consists of the statistical measurement of the sizes and frequencies of detrital, authigenic and organic components of a sedimentary rock. In this investigation, three general types of parameters were investigated: detrital components, degree of crystallinity and chemical composition. The detrital components present in sufficient abundance for study are quartz, pyrite, oolites and reworked lithic fragments. The maximum size of the largest optically continuous dolomite crystals for each thin section was measured to obtain the degree of crystallinity. Chemical composition was investigated by means of an X-ray diffractometer.

The results of the statistical measurements are interpreted by means of a bathymetrical curve showing the variations of relative depth as a function of thickness. The oscillations in the bathymetrical curve exhibit superposed asymmetrical cycles of sedimentation. The ideal cycle begins with structureless dololutite (deepest water facies) and grades upward through progressively shallower facies and terminates with desiccation dolorudite. Immediately overlying this dolorudite is a dololutite which begins the superjacent cycle. The bathymetrical curve also displays a rhythmic occurrence of series of cycles or megacycles. Within each megacycle, each superposed cycle terminates in a progressively shallower microfacies.

The two investigated sections do not overlap stratigraphically and therefore correlation could not be attempted. Although correlation on the basis of individual cycles is probably limited to short distances, the megacycles and the major groups of cycles could provide a valuable means of correlation in this general area.

Introduction

The Upper Cambrian carbonate rocks of eastern Pennsylvania and New Jersey have been the subject of considerable geologic work in the past. Much of this work however, was devoted to description of rock types and the recognition and tracing of gross lithologic features. Very little attention has been paid to the detailed petrography of these rocks which were deposited in a very shallow environment and display a great variety of sedimentary textures. Through their statistical analysis it is possible to reconstruct the environment of deposition of the rocks and to attempt correlation between widely separated sections.

The particular purpose of this investigation has been the petrographic and statistical analysis of the Upper Cambrian dolomites along the east side of the Delaware River in Warren County, N. J. Over 1,200 thin sections were made from samples collected at an average interval of 1.8 feet from two separated sections. The two sections do not overlap stratigraphically and therefore variations of the parameters were traced only through time and could not be used in this particular case for correlation purposes.

Acknowledgements

The author is deeply indebted to Professor Albert V. Carozzi for guidance during this entire project. Professor Carozzi offered many valuable suggestions and criticisms particularly for the interpretation of the petrographic findings. Professor Harold W. Scott is thanked for helpful comments during the initial phases of the investigation. The writer also wishes to acknowledge the assistance of Professors Jack L. Hough, Ralph E. Grim and Donald U. Deer^e for critical reading of the thesis.

Structural data and their interpretations presented herein are the result of current work, as yet unpublished, of Avery A. Drake, Jr., Robert E. Davis and Donald C. Alvord of the U. S. Geological Survey. Mr. Drake deserves special consideration for synthesis of these data and for summer field supervision. The writer also wishes to acknowledge with gratitude financial assistance and field equipment received from the U. S. Geological Survey during the summer of 1959. The U. S. Geological Survey is also thanked for chemical and laboratory data and for the preparation of some of the thin sections.

Physiographic setting and location

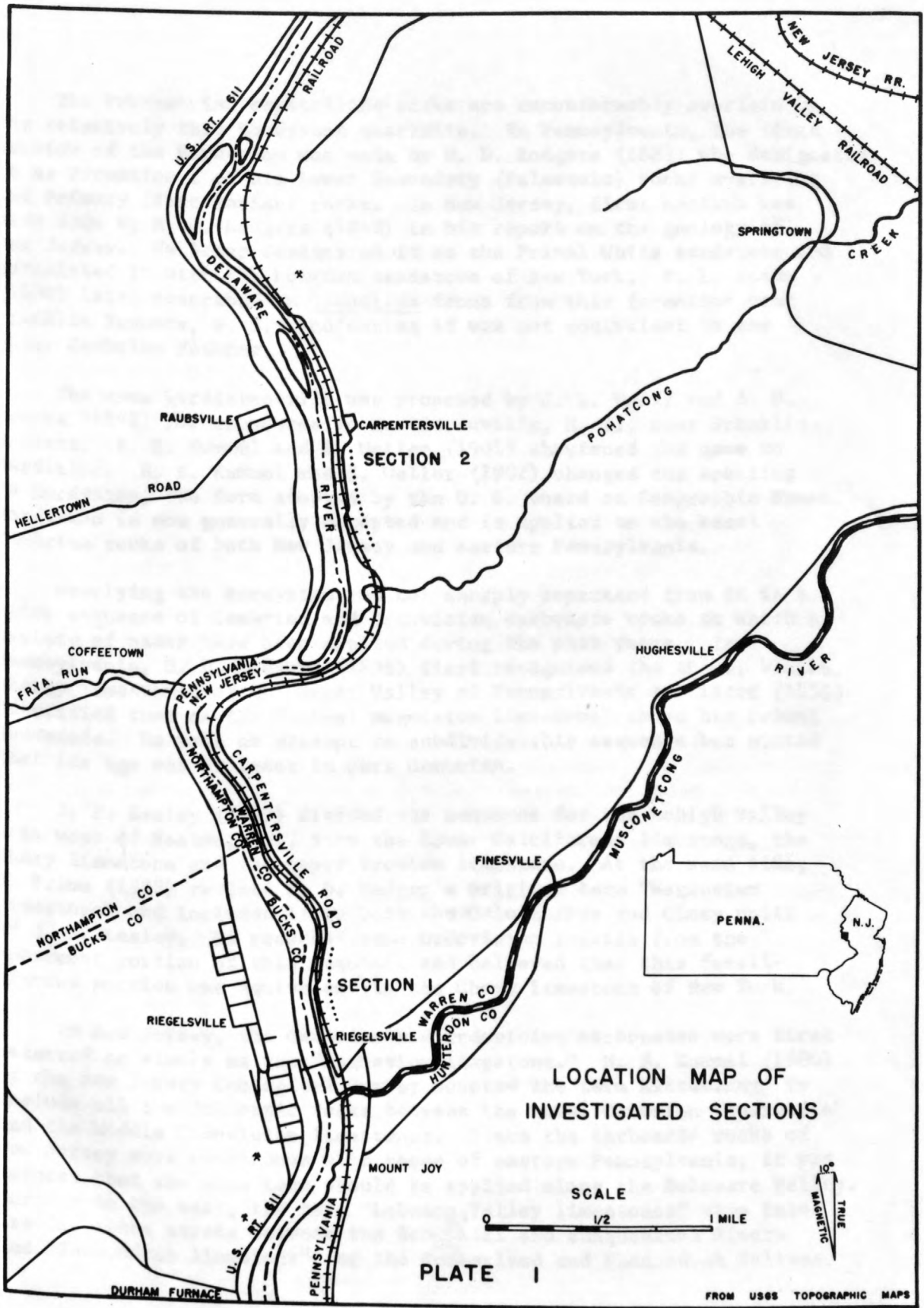
Cambrian and Ordovician carbonate rocks *crop out* in a belt extending from north-central New Jersey southwestward through Pennsylvania. These rocks form part of the Great Valley of Pennsylvania which extends from New York to the Shenandoah Valley. At the Delaware River between Easton and Riegelsville, Pa., this belt is broken into several small elongated valleys interrupted by northeast-trending ridges of Precambrian crystalline rocks.

Physiographically, the area is part of the Reading Prong which widens to the northeast to form the New England Physiographic Province. The Prong narrows considerably toward the southwest and in the vicinity of Reading, Pa., the Triassic rocks completely overlap the Precambrian crystalline rocks. The crystalline rocks reappear again southwest of the Susquehanna River and continue southward as the Blue Ridge Province. Immediately north of the area of study is the Slate Belt developed in Ordovician (Martinsburg) slate. The northern boundary of the Slate Belt is Blue (Kittatinny) Mountain which forms the southeastern boundary of the folded Appalachians of the Ridge and Valley Province. South of the area of study lies the Triassic Lowlands of the Piedmont Province with its lower and more subdued topography.

The area included in the present investigation is *situated* along the Delaware River in Warren County, N. J. (pl. I). Two sections were measured and samples were collected at about 1.8 foot intervals. Section 1 contains 253 samples and is located near the northern boundary of the Riegelsville quadrangle at longitude $75^{\circ}11'27''$ W. and latitude $40^{\circ}35'57''$ N. This section begins immediately north of Riegelsville, N. J., and extends north along the Pennsylvania Railroad and Carpentersville Road which parallels the railroad. Section 2 contains 945 samples and is located near the southern boundary of the Easton quadrangle at longitude $75^{\circ}11'17''$ W. and latitude $40^{\circ}07'55''$ N. This section begins one-half mile south of Carpentersville, N. J., and extends southward along the Pennsylvania Railroad and Carpentersville Road through a series of abandoned quarries almost to Pohatcong Creek.

Stratigraphy

Many stratigraphic problems exist in the lower Paleozoic section of the Delaware Valley in spite of the fact that much geologic work has been done in the area. Examination of the literature reveals considerable disagreement regarding nomenclature and correlation particularly of the Cambrian and Ordovician carbonate rocks. This is due principally to the structural complexity of the strata, lack of paleontologic evidence and the local nature of detailed stratigraphic work.



The Precambrian crystalline rocks are unconformably overlain by the relatively thin Hardyston quartzite. In Pennsylvania, the first mention of the Hardyston was made by H. D. Rodgers (1883) who designated it as Formation I of his Lower Secondary (Paleozoic) rocks overlying the Primary (Precambrian) rocks. In New Jersey, first mention was also made by H. D. Rodgers (1840) in his report on the geology of New Jersey. He later designated it as the Primal White sandstone and correlated it with the Potsdam sandstone of New York. F. L. Nason (1890) later described an Olenellus fauna from this formation near Franklin Furnace, N. J., indicating it was not equivalent to the Upper Cambrian Potsdam.

The name Hardistonville was proposed by J. E. Wolff and A. H. Brooks (1898) for exposures in Hardistonville, N. J., near Franklin Furnace. H. B. Kummel and S. Weller (1901) shortened the name to Hardiston. H. B. Kummel and S. Weller (1902) changed the spelling to Hardyston, the form adopted by the U. S. Board on Geographic Names. Hardyston is now generally accepted and is applied to the basal Cambrian rocks of both New Jersey and eastern Pennsylvania.

Overlying the Hardyston and not sharply separated from it is a thick sequence of Cambrian and Ordovician carbonate rocks to which a variety of names have been applied during the past years. In Pennsylvania, H. D. Rodgers (1836) first recognized the thick, bluish, cherty limestones of the Great Valley of Pennsylvania and later (1858) identified them as the "Auroal Magnesium limestone" above his Primal sandstone. He made no attempt to subdivide this sequence but hinted that its age was at least in part Cambrian.

J. P. Lesley (1883) divided the sequence for the Lehigh Valley area west of Easton, Pa., into the lower Calciferous limestone, the Chazy limestone and the upper Trenton limestone. At the same time, F. Prime (1883) revised H. D. Rodger's original term "Magnesium limestone" and included it in both the Calciferous and Chazy units of J. P. Lesley. He recorded some Ordovician fossils from the uppermost portion of this sequence and believed that this fossiliferous portion was equivalent to the Chazy limestone of New York.

In New Jersey, the Cambrian and Ordovician carbonates were first referred to simply as the "Magnesium limestone." H. B. Kummel (1900) of the New Jersey Geological Survey adopted the term Kittatinny to include all the dolomitic rocks between the basal Cambrian "quartzite" and the Middle Ordovician limestones. Since the carbonate rocks of New Jersey were continuous with those of eastern Pennsylvania, it was natural that the same term should be applied along the Delaware Valley. Farther to the west, the term "Lebanon Valley limestones" came into use for these strata between the Schuylkill and Susquehanna Rivers and "Shenandoah limestone" for the Cumberland and Shenandoah Valleys.

To the present day, the New Jersey Geological Survey lumps the entire Cambrian and Lower Ordovician carbonate sections into the "Kittatinny limestone."

E. T. Wherry (1909) first suggested a breakdown for the limestones in the Lehigh Valley of Pennsylvania and proposed the terms Leithsville for the Middle(?) Cambrian dolomites above the Hardyston, and Coplay for the Lower Ordovician limestone. Eventually E. T. Wherry's term "Coplay" was changed to Beekmantown because of its supposed correlation with the New York type section. B. L. Miller (1939, 1941) in his reports on Lehigh and Northampton Counties, Pa., essentially retains E. T. Wherry's nomenclature but uses the term Tomstown for Leithsville because of its supposed correlation with the Tomstown of southeastern Pennsylvania. The name Tomstown was originally proposed by G. W. Stose (1909) from exposures at Tomstown, Franklin County, Pa.

In the Reading quadrangle, near the Schuylkill River, J. P. Hobson (1957) recently established four mappable rock formations in the Beekmantown thus raising the name Beekmantown from formational to group status. The four formations named in ascending order are: Stonehenge formation, Rickenbach formation (new name), Epler formation (new name), and Ontelaunee formation (new name). G. W. Stose (1908) originally named the Stonehenge from exposures near Chambersberg, Franklin County Pa., and designated it as the basal member of the Beekmantown limestone. In addition, J. P. Hobson also delineated 10 members of the formations within the Beekmantown group. In general, workers to the west and southwest subdivided the Cambrian and Ordovician into numerous units but geologists have been reluctant to correlate these formations with those in eastern Pennsylvania and New Jersey because of the lithologic differences, lack of paleontologic evidence and reduced thicknesses in the east.

A. A. Drake and associates of the U. S. Geological Survey are remapping the Middle Delaware Valley rocks and recognize the following Cambrian and Ordovician formations:

ORDOVICIAN

Upper-Middle	{	Martinsburg shale
		Hershey limestone of C. E. Prouty (1959)
Middle	{	Myerstown limestone of C. E. Prouty (1959)
		Beekmantown group of J. P. Hobson (1957)
Lower	{	Epler formation of J. P. Hobson (1957)
		Rickenbach formation of J. P. Hobson (1957)

CAMBRIAN

Upper	{	Allentown dolomite of B. L. Miller (1939)
Middle	{	Leithsville formation
Lower	{	Hardyston "quartzite"

PRECAMBRIAN

The Allentown dolomite of B. L. Miller (1939) to which the present designation is confined, is composed of light-medium gray or light-gray to dark-medium gray, fine- to medium-grained dolomite. Some widely scattered sparsely crystalline beds occur where quartz is present. The weathered rock surface is usually light to medium or chalk white. Bedding varies considerably and changes more or less rhythmically from poorly laminated massive beds averaging 3 feet to platy or shaly beds. The alternating character of color and texture, topographically suggests the cyclic nature of this formation and is evidence of the rhythmic variations of its detrital component.

The lithology of the Hardyston quartzitic pure quartz sandstone ("quartzite") is extremely variable but in the Easton and Riegelsville quadrangles quartzite with feldspathic phases is most common. The typical nonfeldspathic phase is dominantly light to medium gray, weathering brown, vitreous, and massive. Quartz grains are more or less well rounded and commonly show secondary enlargement; the cementing material is very fine-grained quartz. This phase often contains lenses of white to purple quartz pebble conglomerate in a quartz matrix. The feldspathic phase is composed largely of poorly sorted, angular quartz grains and feldspar, both potassic feldspar and plagioclase. This phase bears a strong similarity in appearance to the subjacent Precambrian crystalline rocks. The feldspathic phase is normally cemented by silica but in places by hydrous iron oxides. Conglomeratic phases of this rock contain well-rounded quartz pebbles and at places a few pink potassic feldspar phenoclasts.

The quartzitic pure quartz phases of the formation grade upward into siliceous and dolomitic, buff-colored shales, which in turn grade into the overlying Leithsville formation.

The Leithsville formation consists of interbedded light-medium gray to dark gray, fine- to coarse-grained dolomite and calcitic dolomite, and light-gray to tan sericitic shale, occasionally calcareous. Quartz sandstone beds are present locally and some of the dolomite is more or less argillaceous. The beds normally weather to a light gray or chalk white but the more argillaceous rock weathers yellowish to buff. No true oolites have been recorded in the formation, but pisolitelike calcareous bodies have been recognized in its upper part. The formation is rhythmically bedded; massive beds give way to platy bedded zones which in turn pass into shale. The massive beds average 5 feet in thickness and are commonly laminated. Mud cracks, ripple marks, graded bedding and crossbedding are common features of the formation. The Leithsville grades into the overlying Allentown dolomite of B. L. Miller (1939), the contact being placed at the bottom of the first Allentown cycle. In mapping, the first appearance of stromatolites or oolites is a useful marker.

The Allentown dolomite of B. L. Miller (1939) to which the present investigation is confined, is composed of light-medium gray or light-olive gray to dark-medium gray, fine- to medium-grained dolomite. Some thin widely scattered coarsely crystalline beds occur where quartz grains are absent. The weathered rock surface is usually light to medium gray or chalk white. Bedding varies considerably and changes more or less rhythmically from poorly laminated massive beds averaging 3 feet thick to platy or shaly beds. The alternating character of color and bedding, megascopically suggests the cyclic nature of this formation and gives evidence of the rhythmic variations of its detrital components.

Cycle details are discussed elsewhere in this paper but in general, the massive beds are composed of fine-grained textureless dolomite and dolarenite. The more thinly bedded material is composed of dolorudite or well-sorted oolitic zones.

Several varieties of cryptozoons are present throughout the formation, although they are generally more abundant in the lower and middle parts of the formation. Specific varieties are not confined to particular stratigraphic intervals which indicates that the cryptozoons stratigraphically appear to be of little diagnostic value.

Oolites are much more abundant than is suggested by megascopic inspection, particularly in the lower and middle portions of the formation. They are well sorted and occur in lenses or beds up to 2 feet in thickness or as part of a poorly sorted detrital matrix in somewhat thicker dolorudite zones. Some oolites show intense tectonic deformation in the a-direction of the megastructures. There are also scattered occurrences of oolites showing deformation that occurred probably during sedimentation when they were still in a soft condition. Such oolites are ruptured or squashed and are generally floating in a fine-grained matrix.

The top part of the Allentown contains considerable dar-gray[✓] chert in lenses or irregular beds. Variable quantities of detrital quartz are present throughout the formation. Largest and most abundant quartz grains occur in the dolorudite[✓] particularly in the desiccation dolorudite where quartz grains often are the dominant matrix material. ^(Figures 9-10) Quartz is generally scattered uniformly throughout the dolarenite zones although concentrations occur as lenses, bands or streaks. All detrital quartz grains display undulose extinction.

In general, quartz grains in the top portion of the Allentown show jagged boundaries due to replacement by carbonate material in a manner similar to that described by T. R. Walker (1957). In the lower part of the formation, which contains no chert, many quartz grains show secondary enlargement. Potassic feldspar also occurs in relatively small quantities where quartz is abundant. Argillaceous material does not constitute a significant component of this formation.

Local disconformities, ripple marks, mud cracks, and crossbedding and graded bedding are common features of the dolarenitic and dolorudite zones. ^(Figures 11-14) The Allentown is transitional with the overlying Rickenbach dolomite of J. P. Hobson (1957). The top of the Allentown is marked by the disappearance of the shallow episodes of the typical cycle. For mapping purposes the contact is placed at the first appearance of medium-coarse to coarse grained, thin bedded, calcareous dolarenite or the last appearance of cryptozoons, oolites or desiccation dolorudite.



Figure 1.--Carpentersville section, unit 317. View of two large bowl-shaped stromatolite colonies near the southeast corner of the fifth quarry from the north. Scales are 8 inches.



Figure 2. Carpentersville section, unit 334. Nicely preserved Cryptozoon fieldii showing knobby, thinly laminated top surface (bedding surface).



Figure 3. Carpentersville section, unit 139. Very large stromatolite colony in overturned strata measuring 6 feet across, 1 foot high. Within large arcuate structure are fine, conformable, wavy laminae.



Figure 4. Railroad cut at junction U. S. Routes 22 and 24 east of Phillipsburg, N. J. Large stromatolite colony exhibiting knobby top bedding surface.



Figure 5.--Abandoned quarry behind sewage disposal plant at Phillipsburg, N. J. Close-up view of Cryptozoon fieldii with well-developed, conformable laminae. Dark zone under stromatolites is oolitic dolarenite.



Figure 6.--Road cut along north side of U. S. Route 22 near cloverleaf at west end of Easton, Pa. Well preserved, small Cryptozoon fieldii on top bedding surface.



Figure 7. Carpentersville section, unit 278. Rather large cabbagelike stromatolite colony showing thinly laminated character.



Figure 8. Reigelsville section, unit 89. Close-up view of Anamalophycus compactus displaying small digitate-like structures.



Figure 9.--Carpentersville section, unit 73. Irregular distribution of quartz grains in desiccation dolorudite. Embedded lithic fragments weather in negative relief. Strata overturned.



Figure 10.--Carpentersville section, unit 73. Irregular distribution of quartz grains in desiccation dolorudite. Strata overturned.



Figure 11.--Carpentersville section, unit 258. Small oscillation ripple marks on overturned strata. Crests are 2 inches apart.



Figure 12.--Abandoned quarry opposite Locks 22 and 23 of the Delaware Canal along U. S. Route 611, Pa. Large oscillation ripple marks on north wall of quarry in overturned strata. Crests are 16 inches apart.

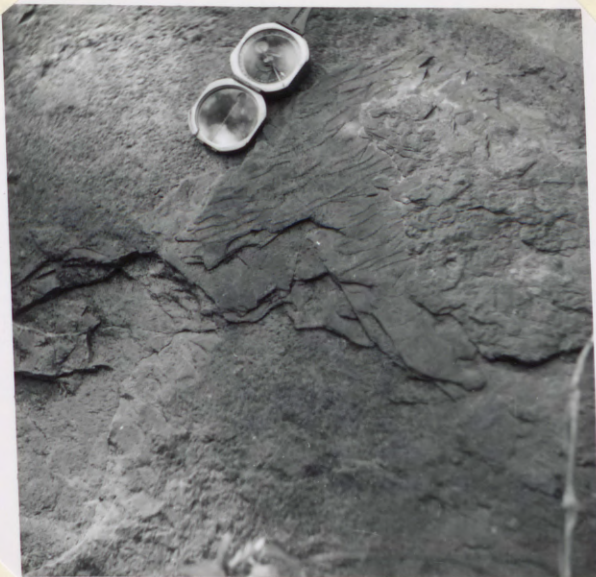


Figure 13.--Carpentersville section, unit 258. "Fucoids" measuring $\frac{1}{4}$ inch in diameter and 8 or 10 inches long. Strata overturned.



Figure 14.--Carpentersville section, unit 149. Desiccation polygons in dolarenite.

The lower part of J. P. Hobson's Rickenbach ^{formation} dolomite consists of light-medium gray to medium-dark gray, medium-fine to coarsely crystalline dolomite. The coarsely crystalline material is calcareous and both bedded and nodular cherts are present. This part of the formation is characterized by a ruditic texture that is well shown on weathered surfaces but is nearly invisible in freshly broken rock. Phenoclasts composed of tiny crystals of dolomite, and rarely, calcite, are present and are enclosed by more coarsely crystalline dolomite. Many of these phenoclasts may be the result of recrystallized fossils. True dolomite conglomerate or sedimentary breccia is also present in this part of the formation.

The upper part of the formation is light to medium gray, medium-fine to very fine grained dolomite. This part is generally similar to the lower part of the formation but is finer grained and occurs in beds 1 to 3 feet thick. The upper part of the formation has a "dirty" appearance because of its silt and sand content. The Rickenbach dolomite grades into the overlying Epler formation of J. P. Hobson (1957). The contact is placed below the lowest recognized limestone bed.

J. P. Hobson's Epler formation is a heterogeneous assemblage of interbedded limestone and dolomite. The limestone is light gray to medium gray, very fine grained to cryptogranular and occurs in beds that average less than 1 foot thick. Often it is so finely laminated as to simulate shale. Dolomite in this formation is fine grained to cryptogranular and medium-light gray to dark-medium gray. It is commonly laminated or mottled. Nodular or bedded chert is present throughout the formation, but a very chert-rich zone is present near the base which serves as a useful criteria in mapping the Rickenbach-Epler contact.

Unconformably overlying the Epler formation is a series of dark colored Middle Ordovician limestones which have been used extensively for the manufacture of portland cement. In New Jersey they have been referred to as the Jacksonburg limestone (R. L. Miller, 1937) but recently C. E. Prouty (1959) recognized two mappable facies of this unit: the Myerstown limestone, a dark gray to black, fine to medium grained, pure limestone, and the Hershey limestone, a black, fine grained, argillaceous limestone. The two formations are probably separated by an unconformity.

Above the Middle Ordovician limestones is the thick Martinsburg shale, ~~of Upper Ordovician age~~. On the basis of lithology, this formation can be subdivided into several members, none of which have been named. The lower part is characteristically a thin-bedded slate, the middle part of the formation contains numerous arenaceous beds and the uppermost part is thin bedded and devoid of arenaceous material. The Martinsburg, in turn, is overlain unconformably by the Lower Silurian Shawangunk conglomerate (Tuscarora).

Little is known regarding the thicknesses of the Cambrian formations in eastern Pennsylvania and New Jersey. Estimates vary considerably but the entire section is known to thicken to the west and southwest. In Lebanon County, C. Gray and associates (1958) of the Pennsylvania Geological Survey recognize five members of the Conococheaque formation, which is the standard Upper Cambrian formation of the Central Appalachians. (1) Buffalo Springs member consisting of alternating gray crystalline limestone and gray to olive-gray dolomite and calcareous dolomite, locally oolitic; (2) Snitz Creek member composed of thick to very thick bedded light gray to medium gray dolomite, commonly oolitic, with some limestone and shaly limestone interbeds; (3) Schaefferstown member, consisting of medium-light gray to medium gray limestone with shaly bands and laminae; (4) Millback member, a unit similar to the Buffalo Creek member but containing thin sandstones and arenaceous limestones or dolomites; (5) Richland member composed of a lower massive cryptozoon- and chert-bearing dolomite zone and an upper zone displaying cycles. These cycles begin with gray siliceous dolomite which passes upward into calcareous dolomite, magnesian limestone or banded limestone and dolomite, the bands often being broken into conglomerate. The cycles are terminated by medium gray to light gray dolomite with shaly partings.

The Allentown dolomite of B. L. Miller (1939) in the Delaware Valley area is equivalent to at least part of this sequence. However, numerous stratigraphic changes occur along the strike between Reading and Allentown, Pa. In Lebanon County, the Conococheaque is underlain by the Tomstown dolomite which is largely equivalent to the Leithsville of the Easton area, although in Lebanon County the Tomstown is regarded as Early Cambrian in age with no recognizable Middle Cambrian present.

Farther to the southwest, the Elbrook limestone underlies the Conococheaque which in turn is underlain by the Waynesboro formation which in turn is underlain by the Tomstown dolomite, Antietam "quartzite," Harpers phyllite and Chickies "quartzite." The section continues to thicken, until in Virginia, an extremely thick sequence is recognized and all the Cambrian(?) and Precambrian(?) clastics are present.

The thickness of the Lower Ordovician carbonate rocks varies in a similar manner. The thickness of the Beekmantown group is ~~more than~~ *over* 2,000 feet in Lebanon County where J. P. Hobson recognized all of its four formations. Eastward these formations are reduced in thickness and in the Delaware Valley area, only Hobson's Rickenbach ~~dolomite~~ *formation* and his Epler formation are present. The stratigraphy of Hobson's Stonehenge is not well understood toward the east but it apparently pinches out toward the northeast as it approaches the highlands. The stratigraphic details of the Ontelaunee ~~dolomite~~ *formation* of Hobson (1957) are also unknown but the marked unconformity at the top of the Beekmantown group in the Delaware Valley area could explain its absence.

The depositional history of the Myerstown-Hershey interval of C. E. Prouty (1959) is not understood in this area and the Martinsburg shale presents even more complex problems.

Structure

The structures of the rocks in the Delaware Valley area vary considerably in complexity. In the area of the present investigation the Cambrian and Ordovician carbonate rocks are tightly folded and complexly faulted into northeast trending structures. Precambrian ridges composed of metasedimentary gneisses and intrusive igneous rocks separate valleys of limestone and dolomite in which the structures are predominantly faulted, asymmetrical synclines. The synclines are gently plunging and many of their southeast limbs are overturned. Major anticlinal axes cannot be traced in the sedimentary rocks of the area as their positions are always occupied by Precambrian crystalline ridges or are broken by thrust faults.

The Silurian and Devonian rocks at the Delaware Water Gap and northward are much less deformed. The rather open, asymmetrical folds are characterized by short southeast limbs. The folds in these rocks become more complex along the strike toward the southwest until they reach recumbent attitudes at the Lehigh Water Gap. Further north, the strata are much less deformed and pass into the essentially flat-lying beds of the massif of the Pocono Plateau. Disturbed strata are not again encountered until the Hudson Valley is reached. Symmetry of the structural pattern is completed by the relatively simple structures of the Triassic rocks which lie to the south and the essentially flat-lying Tertiary coastal plain sediments farther to the south.

Considerable disagreement exists regarding the details of the deformation of the Precambrian crystalline rocks. Recent work by A. A. Drake, Jr. of the U. S. Geological Survey (written communication, 1960) indicates that in general, the Precambrian rocks were not concentrically folded with the Paleozoic sedimentary rocks and therefore the crystalline ridges are not anticlinal in nature. Studies of the compositional layering, platy mineral foliation and minor folds of the crystalline cores reveal that their internal structure may be anticlinal or synclinal and in general is independent of the structure of the overlying Paleozoic rocks. Most of the Precambrian ridges are bounded by faults, probably thrusts, on their northern margins and the general structural pattern may be that of crystalline cored nappes complicated by high-angle thrusts. A few small nappe structures have been recognized near Easton, Pa.

During deformation, the Lower Paleozoic strata were detached from the Precambrian probably along the Hardyston-Leithsville contact. Such a decollement would explain the strongly cataclastic nature of the Precambrian crystalline rocks along the southeast sides of the ridges. Here the Precambrian is granulated and mylonized. Cleavage locally is developed parallel to the Paleozoic trends indicating a superposition of Paleozoic deformation on the Precambrian structure.

Precambrian deformation occurred at least 900 million years ago as dated by zircon and Potassium/Argon ages from undeformed syntectonic granites.

One of the major problems of the Precambrian of the area is the type of faulting bounding the crystalline ridges. Fault contacts are seldom exposed and the distribution of strata where evidence of faulting exists permits interpretation as high-angle reverse faults or high-angle normal faults. It is possible that these ridges are related to complex nappe structures which as yet are not well delineated.

Aeromagnetics and some gravity data are available for the Reading Prong area (Bromery, 1959) but it will take considerable time to gather sufficient information to form reliable conclusions regarding the basement complex in this area.

The deformation of the sedimentary rocks in the immediate area of investigation has been very complex and in general the Cambrian and Ordovician dolomites have been deformed primarily by concentric folding. In areas of strongest stress and upon overturning, shear folding with strong development of cleavage replaces simple flexure folding. At least part of the movement occurred along cleavage planes as shown by the well developed a-axis lineations present on these surfaces. Incompetent beds in the sequence were deformed by both shear folding and flowage as shown by the incompetent Hershey limestone and Martinsburg formation which show classic examples of these types of deformation. Bedding in these formations is nearly completely obliterated and shows as color bands, if at all.

The major structure recognizable in the immediate area, except for a poorly delineated major synclinorium in the Martinsburg shale farther to the north, is the Alpha syncline southeast of Easton. The Hershey limestone of C. E. Prouty (1959) which occupies the keel of this syncline is perhaps the most strongly deformed rock in the area and appears to be isoclinally folded. Bedding, where discernable, is essentially parallel to the flow cleavage.

The complex overturned and recumbent folds in the pre-Silurian rocks are almost certainly the result of the Taconic orogeny although this conclusion cannot be confirmed because post-Ordovician rocks are absent in the area. The Silurian and Devonian rocks at the Delaware Water Gap and northward were deformed primarily during the Appalachian orogeny. The Appalachian event produced certain structural features as overprints on the Taconic structures such as folded cleavage present in the Hershey limestone in the Alpha syncline and in the Martinsburg formation. A cleavage arch has apparently formed in the keel of the

Alpha syncline and a new slip cleavage parallels the axial plane of this arch. This later folding subjected the pre-Silurian rocks to regional shear, perhaps partly due to decollement. The thrusts are more difficult to date and may be due to either or both ages.

Toward the south, the Triassic formations were later involved in the Palisades disturbance. Normal faults which transect earlier folds and thrust blocks beyond the present northern limit of the Triassic formations give indication that the Palisades disturbance superposed a third deformational phase on parts of the Lower Paleozoic formations.

Location and general description

Selection of Geological sections for sampling.--The original purpose of this investigation was to study the entire Upper Cambrian section by means of statistical petrographic analysis. However, a complete section of the Allentown is not exposed in the area and estimates regarding its thickness vary considerably. As a result, two sections were selected and sampled in order to obtain as complete a section as possible. Because the Allentown exhibits similarity throughout its thickness, it was necessary to select sections which displayed contacts with either the subjacent or superjacent formations. Section 1 begins approximately at the Leithsville-Allentown contact and proceeds stratigraphically upward as far as exposures permit. This section passes through several abandoned quarries along the Pennsylvania Railroad immediately north of Riegelsville, N. J. Section 2 begins about 90 feet above the Allentown-Rickenbach contact and extends stratigraphically downward as far as the outcrop permits. This section also passes through a series of abandoned quarries 1 mile south of Carpentersville, N. J. The composite thickness of the two sections is 2,202.3 feet.

The Riegelsville section is structurally on the inverted (southeast) limb of an overturned syncline. The Carpentersville section is on the inverted (southeast) limb of an overturned synclinorium that is complicated in the keel area by later cleavage arching and thrusting. Both synclinal structures trend northeast and are separated by Pohatcong Mountain which trends parallel to the synclinal axes.

Sampling procedure.--The general lithologic characters, sequence and structure of numerous exposures of the area were first investigated in order to determine which sections were best suited for the proposed study. The best exposed sections were selected. Sampling was accompanied by a detailed description of rock types, succession and structures. Sections were measured by means of a 5-foot steel tape and Brunton compass.

4 The sampling interval was set at approximately 1.5 feet. However, effort was made to sample each megascopically visible variation in lithology. The number of samples, therefore, is proportional to the variability in the observed composition, texture and structural aspects of the strata. In order to avoid omission of any significant sedimentary variations, the sampling interval rarely exceeded 2 feet even in massive strata that megascopically appeared uniform. Each sample measured about 8 cubic inches and its stratigraphic top was indicated by means of a red crayon.

A total of 2,202 feet of section was described and 1,198 samples were collected resulting in an average sampling interval of 1.8 feet. Section 1, 516 feet thick, contains 253 samples. Section 2, 1,686 feet thick, contains 945 samples.

Description of microfacies

The microscopic and hand lens examination of the thin sections combined with the megascopic study of the field samples has led to the distinction of six different microfacies which build up by their cyclic alternations the two investigated columns. The extremely recrystallized nature of the rocks complicated the microscopic examination and required a combination of study in transmitted light and in reflected light. In many cases the megascopic observations were essential in identifying the cryptozoan-bearing dolomites and the desiccation dolorudites. Recrystallization also prohibited any photographic reproductions of the microfacies.

Microfacies 1.--Microfacies 1 is a dololutite and appears in transmitted light as a microcrystalline mosaic of interlocking anhedral dolomite crystals relatively uniform in size within the limits of each thin section. The average size of the dolomite crystals is approximately .08 mm but ranges from .03 mm to .12 mm in diameter. Sedimentary structures are absent except for occasional poorly defined laminae which are best displayed under reflected light.

Detrital quartz is uniformly scattered throughout this microfacies; its size averages .08 mm but ranges from .02 mm to .10 mm in diameter. Pyrite is rather abundant and appears as very fine pigments evenly distributed.

This microfacies represents the dolomitized equivalent of a calcilutite.

Microfacies 2.--Microfacies 2 is a dolarenite and appears in transmitted light as a mosaic of anhedral dolomite crystals larger than those of microfacies 1. The crystals average .15 mm but range from .05 mm to .19 mm in diameter. In reflected light this microfacies appears composed of fragments derived from pre-existing carbonate sediments showing bedding traces, crossbedding or graded bedding, of oolites, or of textureless grains which may have been formed by aggregational processes during sedimentation. The oolites are relatively small ranging from .23 mm in diameter to .44 mm and show only faint concentric texture. The size of the fragments averages .80 mm but ranges from .03 mm to 2.00 mm in diameter. The shape of the fragments is variable and their long dimension is generally parallel to the bedding. Usually, crystal outlines are developed without regard for original detrital particle outlines and optically continuous crystals of dolomite transect fragment boundaries.

Detrital quartz is slightly larger and more abundant than in microfacies 1. Its average diameter is .13 mm but ranges from .04 mm to .18 mm. The quartz grains are scattered uniformly throughout the thin section or concentrated in thin streaks, bands or lenses. Most of the quartz "floats" in a carbonate matrix. This is a strong indication in favor of the primary calcarenitic nature of the latter. The quartz grains show jagged boundaries due to replacement by the surrounding carbonate material. Grains or cubes of pyrite are uniformly scattered throughout the rock.

This microfacies represents the dolomitized equivalent of a calcarenite.

Microfacies 3.--Microfacies 3 is an oolitic dolarenite and appears in transmitted light as a mosaic of interlocking dolomite crystals considerably larger than in microfacies 1 or 2. The size of the crystals averages .25 mm in diameter and ranges from .11 mm to .36 mm. In reflected light this microfacies shows pseudoolites, and moderately to well-sorted oolites in a clear to white cement. The pseudoolites, which are elliptical or spheroidal microcrystalline grains with no coating of concentric layers, represent reworked and abraded lithic fragments. They are generally equal in size or slightly larger than the oolites although those subequal in size also occur. The oolites appear as rounded, darker bodies vaguely showing a concentric texture and their size averages .57 mm in diameter but ranges from .12 mm to 1.20 mm. The dolomite crystals of the cement are the same size or somewhat larger than those composing the oolites. Seldom is there a sharp optical boundary between oolites and the cement visible under transmitted light. In some cases, a single large crystal of twinned dolomite occupies most of the surface area of the oolite but the crystal and oolite boundaries do not coincide.

In addition to the normal oolites are three types of deformed oolites. In a first type oolites are tectonically stretched; all show the same degree of stretching in a given thin section. In a second type oolites are brecciated and appear shattered along radial or concentric lines. They are penetrated by numerous, irregular wedgelike veins of clear to white microcrystalline dolomite which displace the oolite fragments but do not replace them. In a third type isolated, "floating" oolites appear ruptured, squashed or drawn out suggesting deformation before compaction while their cores were still in a plastic condition (A. V. Carozzi, in press).

In two instances, large oolites with peculiar bipartite texture were noted similar to those described by E. T. Wherry (1915) from the Upper Cambrian of Northampton County, Pa. Both of these oolite zones occur in sec. 2, one 37 feet and the other 193 feet above the base of the section (pls. 9 and 10 respectively). Their average diameter is over 2.0 mm and they constitute the largest oolites observed in the investigated sections. In a thin section cut perpendicular to the bedding, these oolites show a "half-moon" appearance and are divided into a light and dark portion, the latter being the lower. The dividing line between the two parts is straight or slightly convex upward. The upper part is white and contains no impurities. The lower part contains the nucleus and other residues that dropped down when the original interior of the oolite was dissolved away. The crystallinity of both parts is similar and is coarser than the groundmass of the rock. The average diameter of the dolomite crystals in thin sections displaying these peculiar oolites is .70 mm.

Detrital quartz frequency is relatively low in this microfacies but its average clasticity of .16 mm and its range from .06 mm to .47 mm is higher than microfacies 1 or 2. Pyrite is relatively rare.

This microfacies represents the dolomitized equivalent of an oolitic calcarenite.

Microfacies 4.--Microfacies 4 is a dolorudite and appears in transmitted light as a mosaic of anhedral dolomite crystals approximately the same size as those of microfacies 3. The size of the crystals averages .25 mm in diameter but ranges from .05 mm to .37 mm. Occasional darker areas may be seen in the groundmass which in reflected light appear as subangular to rounded fragments ranging in size from 2.0 mm to more than 6.0 mm. These fragments consist of dololutite, dolarenite or oolitic dolarenite derived from microfacies 1, 2, and 3 respectively. Generally one kind of fragment is present in each thin section although particles of several types occasionally occur together. The fragments are well rounded, poorly sorted and show random orientation.



In reflected light, the fragments generally appear to be embedded in an interstitial matrix of lighter dolarenite or oolitic dolarenite although occasionally they are scattered in a clear to white cement. The oolites are relatively large and average .60 mm in diameter but range from .12³ mm to 1.00 mm. They appear as rounded darker areas rarely showing good concentric or radial texture. The lithic fragments and oolites sometimes show tectonic stretching or shattering.

Detrital quartz is abundant particularly in slides with dolarenitic or dololutitic matrix but occurs in small quantities (~~because of winnowing action~~) if the matrix is oolitic. The clasticity of the quartz averages .25 mm in diameter but ranges from .07 mm to .65 mm.

This microfacies represents the dolomitized equivalent of a calcirudite.

Microfacies 5.--Microfacies 5 is a cryptozoan dolomite which bears a similarity in microscopic appearance to the dololutite of microfacies 1. It is composed of a mosaic of extremely small anhedral dolomite crystals that average .13 mm in diameter but range from .03 mm to .20 mm. The thin sections display no recognizable bio-constructed aspect under transmitted light and in general megascopic confirmation of the presence of stromatolites is necessary for the identification of this microfacies. Low power magnification in reflected light sometimes reveals essentially parallel wavy laminae of organic origin that are arched upward. Between laminae which correspond to phases of the matlike growth of the algae, small detrital particles have accumulated. These fine detrital carbonate particles are also concentrated in the "V"-shaped voids between adjacent domes of growth.

Some slides show that oolites were formed in the same environment as the stromatolite colonies. They built up the substratum of the colonies and in the case where oolite accumulation exceeded organic growth, they completely engulfed fingerlike organic growths. The oolites associated with the Cryptozoons are generally very small and uniform in size; their clasticity averages only .12 mm.

Extremely small detrital quartz grains are present between the organic laminae and their size averages .10 mm in diameter but ranges from .02 mm to .20 mm.

Microfacies 6.--Microfacies 6 is a coarse dessication dolorudite which appears in transmitted light to be composed of large lithic fragments and detrital quartz "floating" in a cement of small interlocking dolomite crystals. The fragments which range from 2.0 mm to over 6.0 mm in diameter are predominantly elongated and oriented subparallel to the bedding. They appear either as structureless masses or as particles exhibiting bedding, graded bedding or cross-bedding. The size of the dolomite crystals of the cement averages only .12³ mm in diameter but ranges from .06 mm to .28 mm; in the fragments, it is slightly smaller.

In reflected light, the large lithic fragments appear scattered in a dolarenitic groundmass composed of reworked carbonate particles, of oolites and of detrital quartz grains in a clear to white cement. The large lithic fragments are composed of structureless dololomite, dolarenite and rarely oolitic dolarenite and are desiccation products of microfacies 1, 2, and 3 respectively. In general, only one type of fragment is present in each thin section. Sometimes, large lunate fragments are present which exhibit the parallel wavy laminae characteristic of the cryptozoan dolomite of microfacies 5.

Detrital quartz is very large and abundant compared to the other microfacies. Its clasticity averages .51 mm and ranges from .13 mm to .92 mm. Occasionally quartz is so abundant that it constitutes nearly all the matrix material surrounding the large lithic fragments. In such instances, the thin sections reveal a quartzitic texture in which the irregular quartz grains are interlocked and welded together by solution of the silica at the grain contacts. Grains of pyrite are particularly abundant in this microfacies.

This microfacies represents the dolomitized equivalent of a desiccation calcirudite.

Methods and techniques of the investigation

Over 1,200 thin sections were cut perpendicular to the bedding and analyzed according to the method used by A. V. Carozzi (1950, 1958). This method consists of the statistical measurement of sizes and frequencies of detrital, authigenic and organic components of sedimentary rocks. The results are interpreted by means of a bathymetrical curve showing the variations of relative depth as a function of thickness.

One such measure is the index of clasticity which is defined as the apparent maximum diameter of the largest visible detrital element in a thin section. It can be statistically demonstrated that by the measurement of a minimum of 100 particles the apparent maximum diameter is very close to the true maximum diameter which may be obtained by mechanical analysis. The index of clasticity, expressed in millimeters, is an indicator of the intensity and distribution of marine currents during sedimentation. Clasticity values are computed for each detrital component that occurs in sufficient abundance to be significant. The numerical clasticity values are plotted on an appropriate scale along the lithological column opposite the thin section locations. The points are then joined to produce a smooth curve for each component measured to express variations in current intensity through time.

A second quantitative measure is that of frequency or the absolute number of grains of a given detrital or authigenic element in a standard area of the slide. For each component, the area of counting must be kept constant throughout the series of slides. In rocks containing large detrital components, it is apparent that a small area will produce a value much below the true frequency value. To reduce this error, it is necessary that the area of counting be at least ten times the diameter of the component measured. In general, about 100 particles should be counted to produce reliable frequency values.

Frequency is a direct indication of the development of an authigenic component and the supply of a detrital one reflecting then the load of the currents during sedimentation. It varies parallel to clasticity or in opposition to it if the supply is respectively normal or deficient. The numerical frequency values are also plotted as points opposite thin section locations along the lithologic column. The points are connected with a smooth curve that expresses variations in supply of the component through time. It is a common practice to superpose clasticity and frequency curves of each component to show their reciprocal relations.

In this investigation, four general types of parameters were investigated: detrital and authigenic components, degree of crystallinity and chemical composition. The detrital components present in sufficient abundance for study in both sections were quartz, oolites and reworked lithic fragments: pyrite was the only authigenic element.

Detrital quartz is present in large quantities and serves as an excellent parameter. In general quartz grains show considerable solution features particularly in parts of the section containing chert. Where chert is absent, dissolution effects appear reduced and many grains even show slight secondary enlargement. The clasticity of quartz was calculated by selecting the six largest quartz grains of the several hundred present on each slide and averaging their apparent maximum diameters. Quartz frequency was determined by counting the total number of grains present in six randomly-selected fields of view using a relatively high power objective. The total surface area examined on each slide was 19.79 square mm.

Pyrite is uniformly disseminated as extremely fine grains or cubes. Only in shear zones do pyrite crystals reach relatively large dimensions suggesting a secondary origin. Pyrite frequency was calculated by counting the total number of grains present in five randomly-selected fields of view using a medium power objective. The total area of the surface examined was 56.71 square mm.

Oolites occur in considerable abundance and constitute a good parameter. They are generally concentrated in rhythmically-spaced, relatively thin zones or in lenticular bodies. Due to the intense recrystallization of the rocks however, their radial or concentric structure is rarely discernible in transmitted light. The oolitic character is best displayed if the slides are placed on a glossy white card and illuminated by means of reflected light. Both clasticity and frequency measurements were determined in reflected light.

Oolite clasticity was calculated by averaging the apparent maximum diameter of the six largest oolites of at least 200 present on each slide. For oolites showing intense tectonic deformation, the average of the maximum and minimum diameters of each of the six largest oolites was determined. This average was used as the maximum diameter of each respective oolite to compute a general average value. Oolite frequency was determined by counting the number of oolites present in three randomly selected fields of view with a low power objective. The total area of the surface examined in each thin section was 105.75 square mm.

Oolites, in a strict sense, are not detrital components but were chosen because their clasticity and frequency bear the same relationship to the environment as detrital minerals in a nonsaturated environment. Oolites are accretionary bodies originating at the site of deposition by oolitization processes operating in a supersaturated environment. The oolite clasticity corresponds to the maximum intensity of local turbulence or agitation. This agitation selects the grain size of potential nuclei around which concentric layers develop and governs the ultimate size of the oolites (Carozzi, 1960).

Reworked oolites however, occur frequently in the matrix of dolerudites (microfacies 4 and 6) in which the dimension of the lithic fragments greatly exceed those of the oolites. These oolites which are not significant features for the reconstruction of the depositional conditions of the rock in which they occur result from the reworking and redeposition of preexisting or contemporaneous oolitic deposits. This is indicated by the fact that some oolites are broken or abraded during transportation and are not recoated or "healed" indicating that the environment was not supersaturated. Also lithic fragments with which the oolites are associated are well abraded. In this study reworked oolites were recorded but no attempt was made to measure their index of clasticity or frequency.

As already pointed out the investigated sections are largely of detrital origin and contain abundant lithic fragments derived from pre-existing carbonate deposits. These fragments vary considerably in size, shape, composition and relative abundance within small vertical intervals. The clasticity curve of these fragments, referred to as the general clasticity, revealed marked variation in the various microfacies and proved to be the most valuable parameter because of its sensitivity in recording slight changes in relative depth and current intensity. The general clasticity was calculated by selecting the five largest fragments from about 50 on each slide and averaging their apparent maximum diameters. In the bioconstructed microfacies the index of general clasticity becomes infinite and loses its practical value.

Dolomitization prevents recognition of those detrital fragments which might have been of organic origin. Accordingly, they have all been classified as lithic fragments and entered in the computation of the general clasticity. The original presence of organic debris is demonstrated megascopically by the fact that some of the desiccation dolorudite units contain lunate fragments resulting from the reworking and redeposition of pre-existing Cryptozoons.

An index of crystallinity has been devised to measure the variation in the size of the dolomite crystals of the various microfacies. The numerical values of crystallinity are not as precise as the other clasticity measurements because of the irregular and interlocking nature of the carbonate crystal outlines, but the variations in crystal size throughout the section are of such a magnitude that very precise measurements are unnecessary. Measurements were made with crossed nicols in order to determine the boundaries of the crystals on the basis of optical continuity.

For slides showing nearly uniform crystal size, the index of crystallinity was determined by computing the average diameter of several of the largest crystals. In slides exhibiting an association of different crystal sizes in approximately equal proportions, the average diameter of the largest crystals was again used as the crystallinity value. The occurrence of isolated crystals very much larger than the average maximum crystal size was considered due to local variations and their diameters were not entered in the computation of the crystallinity. For slides which displayed zones or bands of different crystal size an average diameter was computed for each zone from which a general average could be determined. Thin bands of extremely small crystals were disregarded if it was evident that these zones were tectonically induced by shearing stresses. In general, rocks that were severely sheared had a fine texture.

The composition of the carbonate rocks was investigated by the X-ray diffraction method proposed by C. B. Tennant and R. W. Berger (1957). This method utilized X-rays of a single known wave length to reveal difference in the d-spacings of the lattice of a diffracting crystalline substance. Approximate dolomite percentages were calculated by computing the ratio of the maximum peak heights for calcite and dolomite and comparing these ratios to peak ratios obtained from a series of mixtures of known percentages of these materials.

A part of each field sample was ground in a hand mortar for six minutes to produce a fine powder. The powder was placed in an aluminum holder and mounted in a General Electric SRD-3 diffractometer in such a manner that X-rays could be directed at it at various angles. A copper X-ray tube with a 1° slit was used and permitted to rotate through an angle (2θ) of 7° (26 to 33°). The goniometer speed was set at 2° per minute and the reflections were automatically recorded by a General Electric Speedomax unit. The maximum calcite peak occurred at 29.39° and dolomite at 30.96° .

Several important errors are introduced in this type of calculation due to the non-uniformity of grain size, preferred directions of breakage along cleavage, differential packing, nature and relative amount of noncarbonate material, interference of various reflections and instrumental variations. Despite these limitations the reliability of this method is sufficient for the purpose of this study. Several field samples were X-rayed three times and it was found that results could be duplicated to within a few percent. To serve as a check on the X-ray data, chemical analyses were obtained for five widely-separated samples in the section (Table 1).

The results of the X-ray diffraction are not graphically represented with the other parameters because the percentage of dolomite shows no significant variation. Such a striking uniformity in composition is in favor of a bed-by-bed dolomitization probably penecontemporaneous with sedimentation. Approximately 1200 samples were analyzed and their diffraction patterns indicate that both sections are virtually pure dolomite. Scattered samples show calcite percentages as high as 5 percent but this figure is insignificant since it lies within the range of probable error of the diffractometer. The only exception occurs at the base of the Lower Ordovician Rickenbach formation (J. P. Hobson, 1957) where several beds show percentages as high as 25 or 30 percent. For mapping purposes, this change in composition is important in locating the contact between the Cambrian and Ordovician rocks.

The six microfacies determined on the basis of textures and parameter variations have been interpreted and classified with respect to relative depth and agitation. Microfacies 1 represents the environment of deepest water and microfacies 6 represents the shallowest. This classification is the basis for the relative bathymetrical curve constructed by plotting the microfacies numbers as points on an arithmetic scale ranging from one to six. These points were connected by a smooth curve representing variations of relative depth of deposition as a function of thickness.

It should be stressed here that the entire range of microfacies described above has been deposited in a very shallow general environment. Wherever the word "deep" is used to qualify microfacies 1 it means only the deepest position within the general very shallow conditions.

The oscillations in the bathymetrical curve exhibit superposed asymmetrical cycles of sedimentation. Each cycle begins with a deep water facies and gradually grades upward to shallower water facies which is overlain immediately by the deep water facies beginning a new cycle. The bathymetrical curve also shows a rhythmic occurrence of series of cycles. In other words, there are cycles of cycles, or megacycles. Within each megacycle, each successively higher cycle terminates in a progressively shallower facies. The cycles and megacycles are discussed in detail in subsequent chapters.

TABLE 1

CHEMICAL ANALYSES FOR FIVE SAMPLES FROM INVESTIGATED SECTIONS

Lab. No.	155100	155099	155098	155097	155096
Strati- graphic location	Section (1) 61.0'	Sec. (2) 128.6'	Sec. (2) 492.7'	Sec. (2) 1571.5'	Sec. (2) 1624.5'
SiO ₂	2.6	8.6	3.7	5.2	7.5
Al ₂ O ₃	.59	2.1	.45	1.2	1.6
Fe ₂ O ₃	.38	.51	.51	.55	.41
FeO	.31	.40	.29	.06	.22
MgO	20.8	18.7	20.3	19.4	16.9
CaO	29.1	26.5	28.6	28.8	29.6
Na ₂ O	.04	.07	.06	.06	.07
K ₂ O	.44	1.5	.33	.88	1.2
H ₂ O	.16	.27	.30	.32	.38
TiO ₂	.04	.12	.04	.07	.10
P ₂ O ₅	.03	.03	.02	.02	.03
MnO	.01	.02	.02	.01	.02
CO ₂	<u>45.1</u>	<u>40.7</u>	<u>44.9</u>	<u>43.5</u>	<u>41.6</u>
Sum	100	100	100	100	100

Note: Samples were analysed by the *Geochemistry and Petrology* Branch of the U. S. Geological Survey according to methods described in U. S. Geological Survey Bulletin 1036-C.

The ideal cycle

Each microfacies which has been described has a definite position in the overall cyclic depositional pattern. Thus an ideal cycle (Plate 3) has been constructed to illustrate the changes of sedimentation by the variations of the parameter values in each succeeding microfacies. Since the ideal succession corresponds to a shallowing in time, the microfacies are arranged according to bathymetrical position with microfacies 1 at the bottom and microfacies 6 at the top.

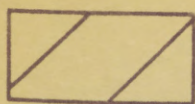
Plate 3 shows the variations in parameter values of the ideal cycle for section 1. The value of each parameter for each microfacies was calculated by averaging all the respective values for that microfacies. The points corresponding to each parameter were plotted on appropriate arithmetic scales and connected by smooth curves.

The general clasticity curve is asymmetrical and increases gradually from zero in the dololutite to a value of .707 mm in the oolitic dolarenite. It increases sharply in the dolorudite to 4.145 mm and then decreases abruptly to .373 mm in the cryptozoan dolomite where mat-like organic growth prohibited in-place reworking and transportation of large fragments. The cycle terminates with a desiccation dolorudite in which the general clasticity reaches its maximum value of 5.331 mm. The overall trend of the general clasticity is to increase from microfacies 1 to 6.

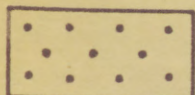
Detrital quartz clasticity and frequency curves vary in a parallel manner to each other indicating regular supply, and moreover are parallel to the general clasticity. This relation shows that the same currents that are responsible for bringing the quartz are also responsible for the pencontemporaneous reworking of the sediments. The quartz clasticity increases gradually from microfacies 1 where its value is .102 mm to microfacies 4 where it reaches a value of .272 mm. A marked decline to .116 mm occurs in microfacies 5 due to mat-like stromatolite growth which prevented the transportation of large detrital particles. This is followed by a peak value of .444 mm in microfacies 6. Quartz frequency in the dololutite is 163 and increases slightly to 170 in the dolarenite. The oolitic dolarenite microfacies shows a value of only 65 representing a deficient supply although the clasticity curve reveals that the current intensity does not diminish. The frequency increases to 201 in the dolorudite and then decreases to 68 in the cryptozoan dolomite. The maximum frequency is present in the desiccation dolorudite where its value is 404. The overall trend of quartz frequency and clasticity is to increase from microfacies 1 to 6 similar to general clasticity.

Oolite frequency and clasticity curves show parallel variation and a symmetrical aspect. The clasticity is zero in the dololutite but increases rapidly to .233 mm in the dolarenite and to a peak value of .514 mm in the oolitic dolarenite. This is followed by a zero value in the dolorudite and the appearance of a small secondary peak of .126 mm in the cryptozoan dolomite which in turn is followed by a third drop to zero in the desiccation dolorudite. The frequency curve shows values of 39, 187 and 26 in microfacies 2, 3 and 5 respectively.

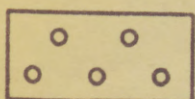
TABLE OF SYMBOLS



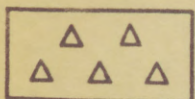
DOLOLUTITE



DOLARENITE



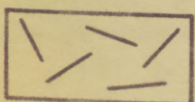
OOLITIC DOLARENITE



DOLORUDITE



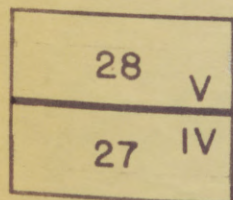
CRYPTOZOAN DOLOMITE



DESICCATION DOLORUDITE



THIN SECTION LOCATIONS

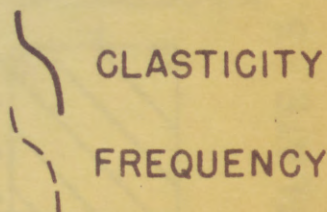


ARABIC NUMERALS INDICATE CYCLES

ROMAN NUMERALS INDICATE MEGACYCLES

R | REWORKED OOLITES

C | CHERT



CLASTICITY

FREQUENCY

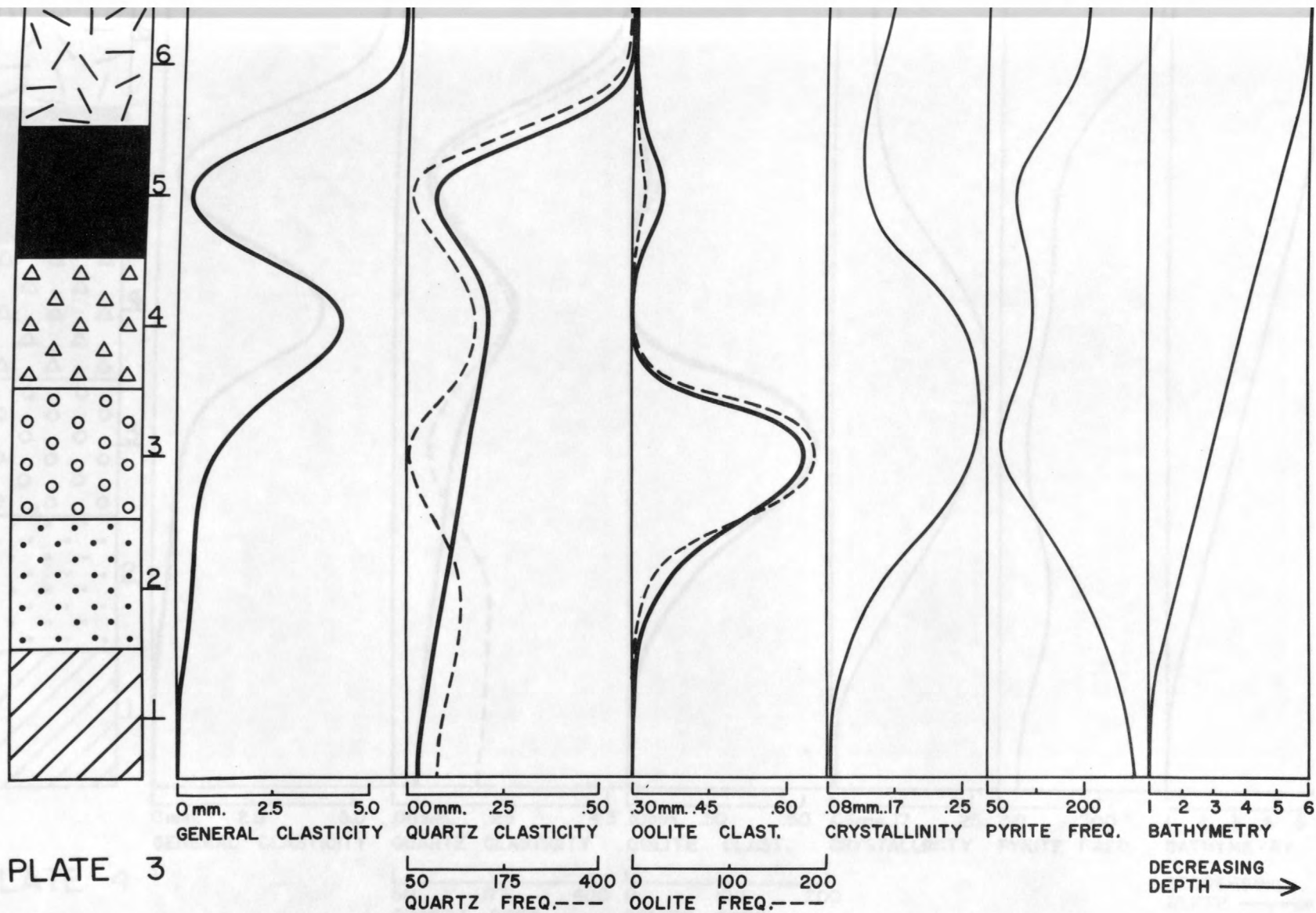


PLATE 3

COLUMN SHOWING PARAMETER VARIATIONS OF MICROFACIES — SECTION I



PLATE 4

COLUMN SHOWING PARAMETER VARIATIONS OF MICROFACIES — SECTION 2

The oolite parameters show zero values in the dolorudite and desiccation dolorudite because they reflect the frequency and clasticity of oolites only in the environments where they are forming. The oolites in the matrix of the dolorudites are reworked and are not significant in the reconstruction of their depositional conditions. The small secondary peak appearing in the cryptozoan dolomite is due to occasional oolite development contemporaneous with the upward growth of the stromatolites. Oolites are present between adjacent colonies or in pockets within colonies indicating that agitation and sea water concentration was locally favorable for their development.

The curve for the index of crystallinity is symmetrical. It begins with the minimum value of .088 mm/ in microfacies 1 and increases to .168 mm/ in microfacies 2 and reaches a broad peak that extends through microfacies 3 and 4 both of which have a crystallinity value of .249 mm/. The curve then gradually declines to .149 mm/ in microfacies 5 and .123 mm/ in microfacies 6. The size of the dolomite crystals appears to be primarily influenced by the original grain size of the carbonate debris. This is illustrated by the subparallel trend of the crystallinity curve to the general clasticity curve except at the top of the cycle in the desiccation dolorudite. In this microfacies, the supply of detrital quartz is so great and individual grains so large that carbonate crystal growth during recrystallization was inhibited. It is interesting to note that in the dolorudite where a secondary peak in the quartz curves occurs, quartz grains are neither large enough nor sufficiently abundant to have significant effect on the development of carbonate crystals.

The pyrite curve shows that a minimum value of 188 occurs at the base of the cycle in the dololutite. The curve oscillates upward to values of 224, 219 and 238 in microfacies 2, 3 and 4 respectively and reaches a peak value of 378 at the termination of the cycle. The general trend of pyrite frequency is an increase upwards parallel to quartz and general clasticity indicating that iron oxides, later changed to sulfide, were brought by the same currents that transported detrital quartz. Where tectonic shearing is present, pyrite frequency generally increases suggesting a secondary origin.

The bathymetrical curve shows that the ideal cycle begins in a relatively deep, quiet environment in which transportation of detrital particles is at a minimum. Extremely fine reworked carbonate material as well as products of chemical precipitation accumulate to form the structureless lutitic texture of microfacies 1. Gradually the environment shallows increasing the agitation and competency of the currents which rework and redeposit carbonate particles ^{of} sand size to produce the arenitic texture of microfacies 2. Locally the environment is also suitable for the formation of oolites. Shallowing continues primarily by the sedimentary upbuilding of materials. Agitation increases and the environment becomes sufficiently concentrated ⁱⁿ to produce well sorted oolitic deposits on a large scale. During oolite formation quartz frequency is low indicating deficient supply. As the environment

continues to become shallower a marked increase in the agitation and transporting power of the currents produces a corresponding increase in the frequency and clasticity values of the detrital particles. During this phase, relatively large lithic fragments are reworked from one or more of the subjacent microfacies and are redeposited to produce the ruditic texture of microfacies 4. In this agitated, relatively shallow environment, biostromal mats of stromatolites blanket the surface and inhibit further brecciation or transportation of large particles. This results in a sharp decline in quartz and general clasticity and also in quartz and pyrite frequency. Locally, isolated pockets within the stromatolite colonies continue to provide conditions favorable for oolite development. The stromatolites persist until conditions are so shallow and agitation so intense that growth ceases and brecciation is renewed on a large scale accompanied by temporary exposition to the air. In many cases, the stromatolites themselves are reworked and form many of the large fragments in the desiccation dolerudites (Figures 15-18). The termination of the ideal cycle corresponds to the period of most competent currents which are responsible for the peak values characteristic of microfacies 6.

A similar ideal cycle has been constructed for section 2 (Plate 4). The general clasticity, quartz and oolite curves are similar but in section 2 pyrite frequency shows an anomalous value in the dololutite where a maximum instead of a minimum value is present. This high value of pyrite in section 2 may be explained either by secondary enrichment in sheared zones of microfacies 1 or by the possibility that the dololutite microfacies includes products of complete recrystallization of other microfacies in which pyrite frequency was originally higher.



Figure 15. Abandoned quarry behind sewage disposal plant at Phillipsburg, New Jersey. Desiccation brecciation of stromatolite colony. Dark massive beds below stromatolites are oolitic dolarenite.



Figure 16. Abandoned quarry behind sewage disposal plant at Phillipsburg, New Jersey. Desiccation brecciation of stromatolites. Note superposition of small digitate and funnel-shaped colonies over large dome-shaped variety. Note inverted lunate fragments in desiccation dolerudite near top of photograph.



Figure 17. Abandoned quarry behind sewage disposal plant at Phillipsburg, New Jersey. Close-up showing transition from oolitic dolarenite (dark platy beds at bottom of photograph) to cryptozoan dolomite (light beds which thin and thicken) and overlying arenaceous desiccation dolorudite with cross bedding directly above stromatolites.



Figure 18. Road cut along south side of U. S. Route 22 near cloverleaf at west end of Easton, Pennsylvania. Relationship of oolitic dolarenite (lower dark bed), cryptozoan dolomite and arenaceous desiccation dolorudite with tabular and lunate fragments oriented parallel to bedding.

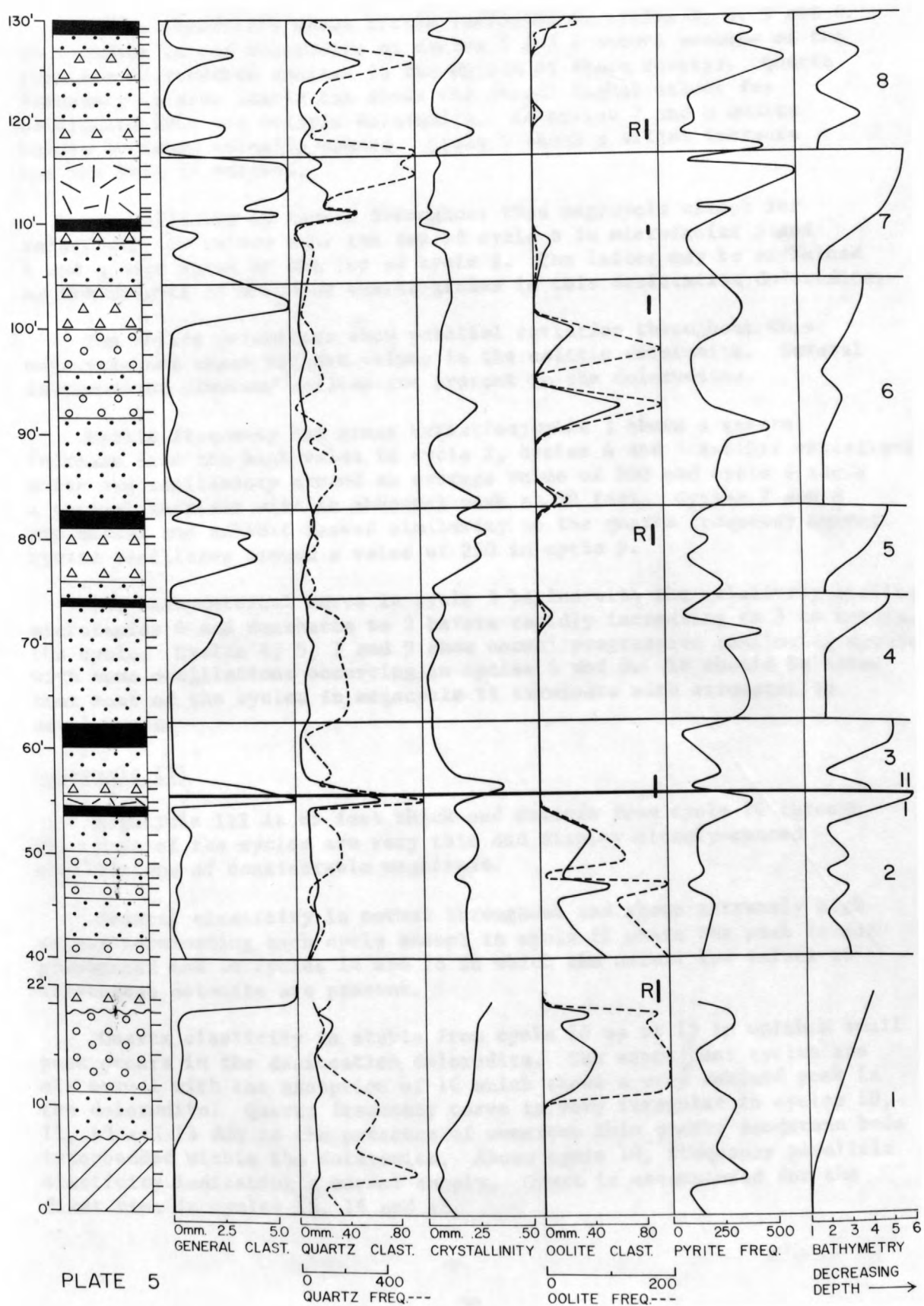


PLATE 5

Quartz clasticity shows little variation in cycles 3, 4, 5 and 6. No increase in the dolerudite of cycles 5 and 6 occurs because of the presence of reworked oolites in the matrix of these rudites. Quartz frequency is also stable but shows the normal higher values for dolarenite than for oolitic dolarenite. In cycles 7 and 8 quartz values increase normally upward. Cycle 9 shows a slight increase but the peak is subdued.

Crystallinity is normal throughout this megacycle except for relatively low values near the top of cycle 6 in microfacies 3 and 4 and a high value at the top of cycle 9. The latter may be explained by the absence of abundant quartz grains in this desiccation dolorudite.

The oolite parameters show parallel variation throughout this megacycle and reach highest values in the oolitic dolarenite. Several instances of reworked oolites are present in the dolorudites.

Pyrite frequency has great variation; cycle 3 shows a general increase from the high value in cycle 2, cycles 4 and 5 exhibit variations which are oscillatory around an average value of 200 and cycle 6 shows a general increase with an abnormal peak at 90 feet. Cycles 7 and 8 are normal and exhibit marked similarity to the quartz frequency curves. Pyrite oscillates around a value of 250 in cycle 9.

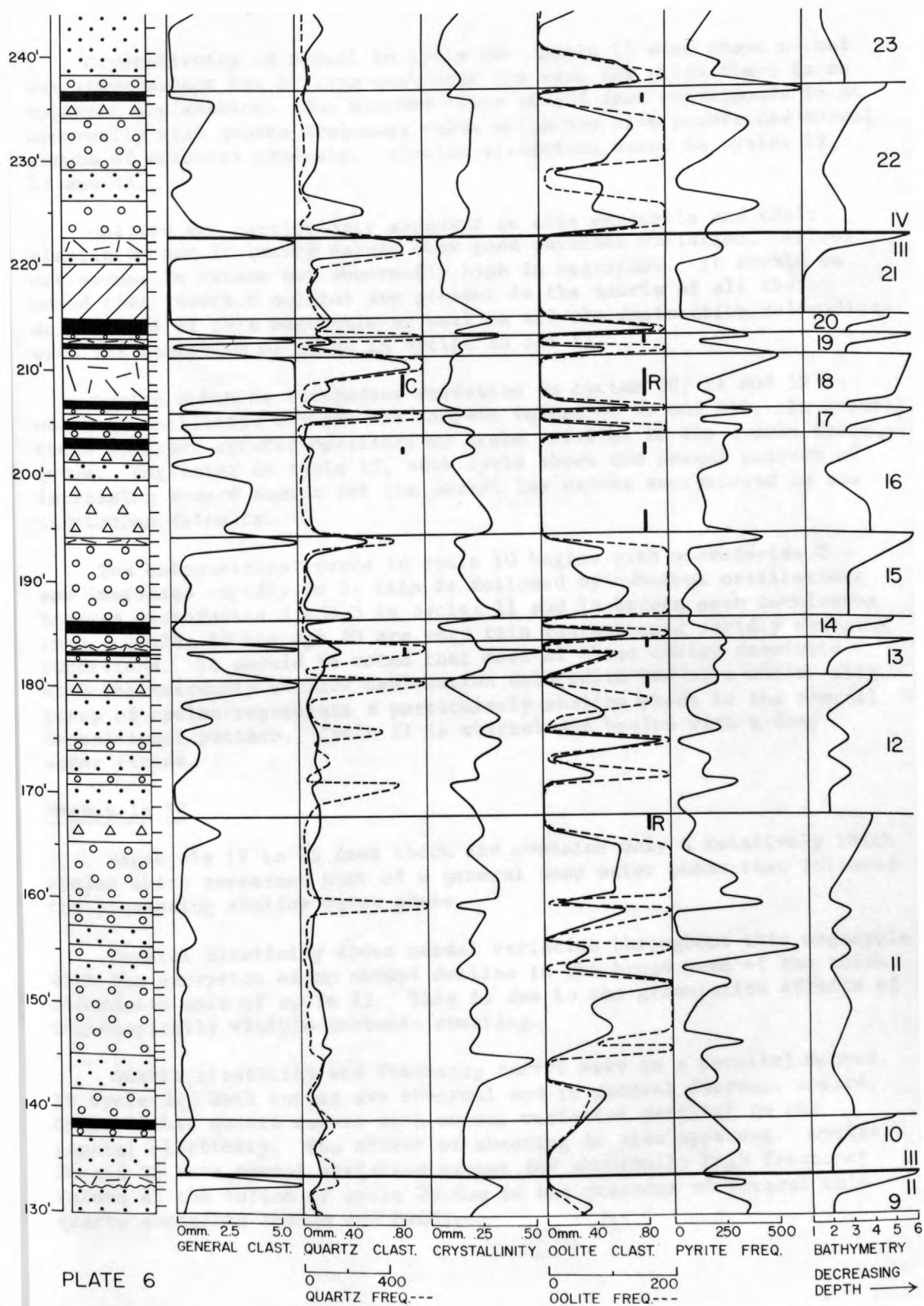
The bathymetrical curve in cycle 3 begins with the relatively shallow microfacies 4 and decreases to 2 before rapidly increasing to 5 to terminate the cycle. Cycles 4, 5, 7 and 9 show normal progressive shallowing upward with some oscillations occurring in cycles 6 and 8. It should be noted that most of the cycles in megacycle II terminate with stromatolite development.

Megacycle III

Megacycle III is 89 feet thick and extends from cycle 10 through 21. Most of the cycles are very thin and display closely-spaced oscillations of considerable magnitude.

General clasticity is normal throughout and shows extremely high values terminating each cycle except in cycle 11 where the peak is not pronounced and in cycles 14 and 16 in which the normal low values of cryptozoan dolomite are present.

Quartz clasticity is stable from cycle 10 up to 15 in which a small peak occurs in the desiccation dolorudite. The subsequent cycles are all normal with the exception of 16 which shows a very subdued peak in the dolorudite. Quartz frequency curve is very irregular in cycles 10, 11, 12 and 13 due to the presence of numerous thin quartz sandstone beds interbedded within the dolarenite. Above cycle 18, frequency parallels clasticity indicating a normal supply. Chert is encountered for the first time in cycles 13, 16 and 18.



Crystallinity is normal in cycle 10. Cycle 11 also shows normal variation except for a large peak near the base for which there is no apparent explanation. The minimum value at 159 feet corresponds to an abnormally high quartz frequency value which may have prohibited normal growth of dolomite crystals. Similar situations occur in cycles 12, 13 and 15.

Oolites are particularly abundant in this megacycle and their clasticity and frequency values show good parallel variation. Values are normal in nature but abnormally high in magnitude. It should be noted that reworked oolites are present in the matrix of all the dolorudites of this megacycle as well as all the desiccation dolorudites with the exception of those in cycles 15 and 17.

Pyrite exhibits tremendous variation in cycles 10, 11 and 12 in which it oscillates between the extreme values of 50 and 600. In general, these apparent erratic oscillations trend parallel to the quartz frequency curve. Beginning in cycle 13, each cycle shows the normal pattern of increasing upward except for the normal low values encountered in the cryptozoan dolomite.

The bathymetrical curve in cycle 10 begins with microfacies 2 and increases rapidly to 5; this is followed by numerous oscillations between microfacies 2 and 3 in cycles 11 and 12 before each terminates in 4. Cycles 13 through 20 are very thin representing rapidly changing conditions. It should be noted that most of these cycles terminate with the extremely shallow desiccation dolorudite and as a whole, this group of cycles represents a particularly shallow phase in the overall depositional pattern. Cycle 21 is thicker and begins with a deep water facies.

Megacycle IV

Megacycle IV is 75 feet thick and contains only 4 relatively thick cycles which represent part of a general deep water phase that followed the preceding shallow water phase.

General clasticity shows normal variation throughout this megacycle with the exception of an abrupt decline in the broad peak of the thick dolarenite unit of cycle 23. This is due to the granulation effects of megascopically visible tectonic shearing.

Quartz clasticity and frequency curves vary in a parallel manner. In cycle 22, both curves are abnormal and in general decrease upward. Cycle 23 has quartz curves with normal variation parallel to the general clasticity. The effect of shearing is also apparent. Cycles 24 and 25 have normal variation except for abnormally high frequency values at the bottom of cycle 24 due to the presence of several thin quartz sandstone lenses and bands.

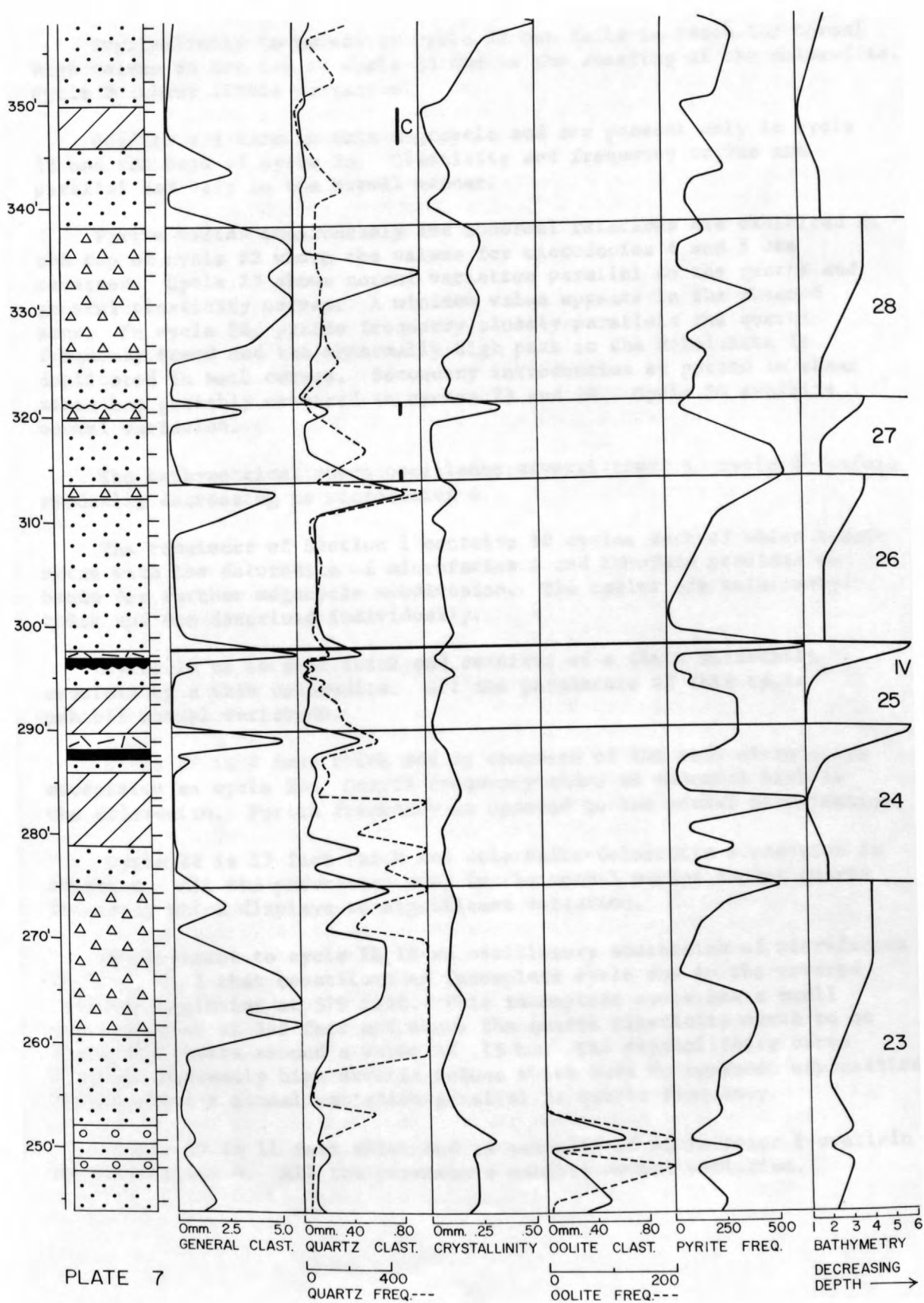


PLATE 7

Crystallinity is normal in cycle 22 but fails to reach the normal high values at the top of cycle 23 due to the shearing of the dolorudite. Cycle 24 shows little variation.

Oolites are rare in this megacycle and are present only in cycle 22 and the base of cycle 23. Clasticity and frequency curves are parallel and vary in the normal manner.

Pyrite varies considerably and abnormal relations are exhibited at the top of cycle 22 where the values for microfacies 4 and 5 are reversed. Cycle 23 shows normal variation parallel to the quartz and general clasticity curves. A minimum value appears in the sheared zone. In cycle 24, pyrite frequency closely parallels the quartz frequency trend and the abnormally high peak in the dololutite is duplicated in both curves. Secondary introduction of pyrite in shear zones has probably occurred in cycles 23 and 24. Cycle 25 exhibits normal variation.

The bathymetrical curve oscillates several times in cycle 23 before gradually increasing to microfacies 4.

The remainder of Section 1 contains 10 cycles each of which terminates with the dolorudite of microfacies 4 and therefore provides no basis for further megacycle subdivision. The cycles are relatively thick and are described individually.

Cycle 26 is 16 feet thick and consists of a thick dolarenite overlain by a thin dolorudite. All the parameters of this cycle exhibit normal variation.

Cycle 27 is 7 feet thick and is composed of the same microfacies succession as cycle 26. Quartz frequency shows an abnormal high in the dolarenite. Pyrite frequency is opposed to the normal distribution.

Cycle 28 is 17 feet thick and dolarenite-dolorudite succession is repeated. All the parameters vary in the normal manner except quartz frequency which displays no significant variation.

Superjacent to cycle 28 is an oscillatory succession of microfacies 2, 1, 2, 3, 2 that constitute an incomplete cycle due to the covered interval beginning at 379 feet. This incomplete cycle has a small abnormal peak at 345 feet and shows the quartz clasticity curve to be extremely stable around a value of .15 mm. The crystallinity curve displays extremely high erratic values which have no apparent explanation. Pyrite shows a normal variation parallel to quartz frequency.

Cycle 29 is 11 feet thick and is composed of microfacies 1 overlain by microfacies 4. All the parameters exhibit normal variation.

Cycle 30 is 23 feet thick and is composed of a thick dolarenite unit overlain by a very thin dolorudite. The quartz curves exhibit no significant increase upward and a large abnormal peak is present in the crystallinity curve at 450 feet. Pyrite frequency shows opposite variation and decreases upward.

Cycle 31 is 14 feet thick and contains the microfacies succession 1, 2, 4. The parameters are normal except for quartz and pyrite frequency which are parallel to each other and in general decrease upward.

Cycle 32 is 6 feet thick and has the microfacies succession 3, 2, 4. The parameters are normal except for quartz and pyrite frequency which show little variation.

Cycle 33 is 7 feet thick and has the microfacies succession 1, 2, 4. Pyrite frequency is abnormally low in microfacies 4.

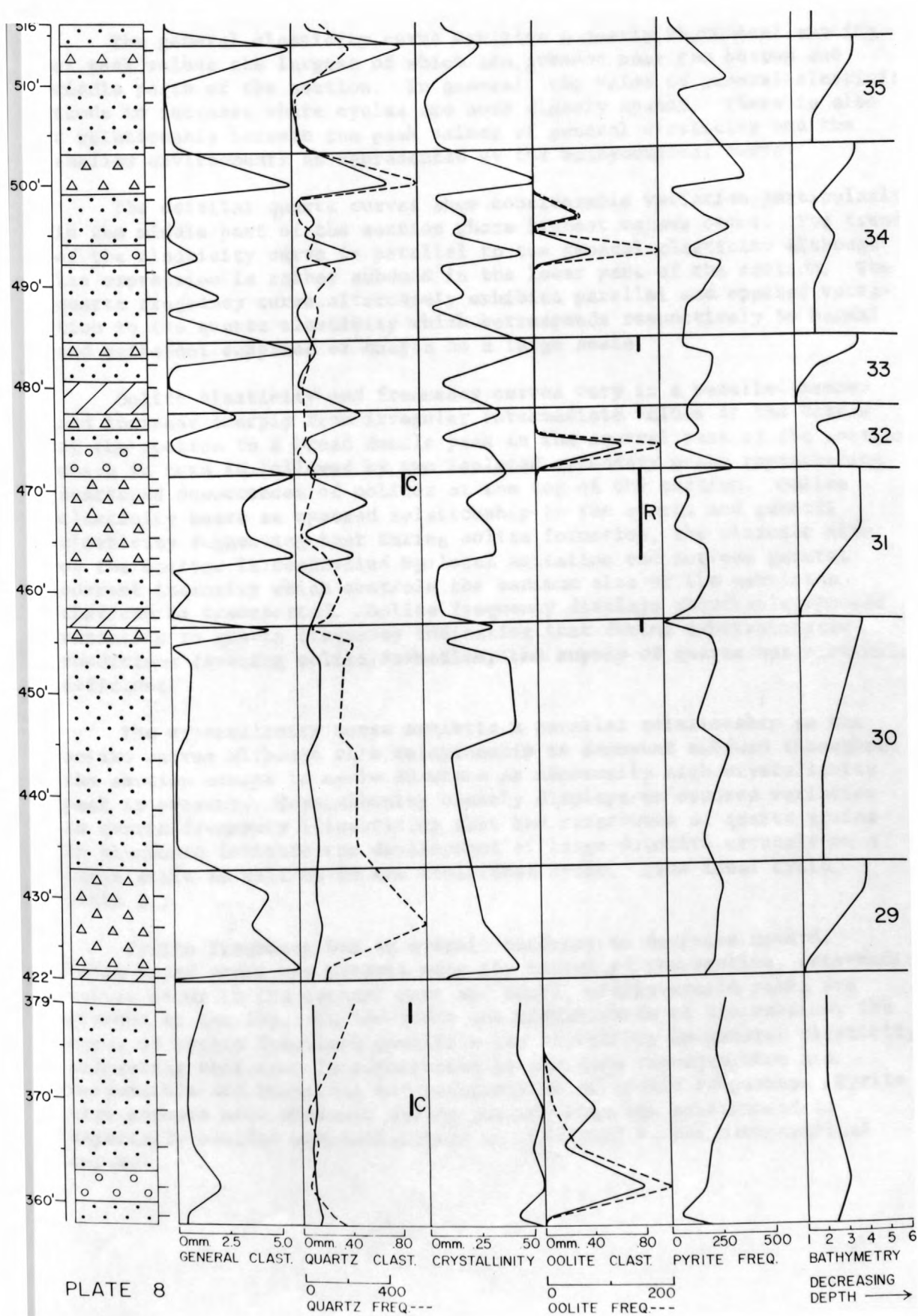
Cycle 34 is 18 feet thick and contains the microfacies succession 2, 3, 2, 4. General clasticity shows an abnormally high peak at 490 feet in microfacies 2.

Cycle 35, the topmost cycle of Section 1, is 10 feet thick and is composed of a dolarenite overlain by a dolorudite. All the parameters vary in the normal manner.

Generalized parameter variations for Section 1

Plate 9 illustrates the general trend of the respective parameters for Section 1. Unlike an envelope curve which connects peak values of a detailed section, this plate was constructed in such a manner to place minimum emphasis on the isolated and repeated peak values so frequently displayed in cyclic environments but to emphasize the average parameter value for a given interval of stratigraphic section.

The exposed part of Section 1 was divided into 20 foot intervals regardless of cycle boundaries. For each interval, an average value for each parameter was computed by adding the respective values regardless of the microfacies and dividing the sum by the total number of thin sections present in that interval. To minimize the effect of reworked oolites, the average oolite clasticity and frequency values were calculated by adding the values which occurred only in microfacies 2, 3 and 5 and dividing the sum by the number of thin sections of these microfacies present in each respective interval. The points for each parameter were plotted on appropriate arithmetic scales and connected by smooth curves. The bathymetry shows the cycles as they appear in plates 5 through 8 except the oscillations within each cycle are not represented. Bathymetry for cycles 10, 12, 14, 16, 18 and 20 are omitted for drafting purposes. Megacycle boundaries are indicated by Roman numerals.



The general clasticity curve exhibits a nearly rhythmical spacing of peak values the largest of which are present near the bottom and middle parts of the section. In general, the value of general clasticity tends to increase where cycles are more closely spaced. There is also a relationship between the peak values of general clasticity and the shallow environments as represented by the bathymetrical curve.

The detrital quartz curves show considerable variation particularly in the middle part of the section where highest values occur. The trend of the clasticity curve is parallel to the general clasticity although its expression is rather subdued in the lower part of the section. The quartz frequency curve alternately exhibits parallel and opposed variation to the quartz clasticity which corresponds respectively to normal and deficient supplies of quartz on a large scale.

Oolite clasticity and frequency curves vary in a parallel manner and increase sharply from irregular intermediate values at the bottom of the section to a broad double peak in the central part of the section which in turn is followed by two isolated secondary peaks representing scattered occurrences of oolites at the top of the section. Oolite clasticity bears an opposed relationship to the quartz and general clasticity suggesting that during oolite formation, the ultimate size of the oolites is controlled by local agitation and not the general current intensity which controls the maximum size of the particles that can be transported. Oolite frequency displays remarkable opposed variation to quartz frequency indicating that during supersaturated conditions favoring oolite formation, the supply of quartz was particularly deficient.

The crystallinity curve exhibits a parallel relationship to the oolite curves although this relationship is somewhat subdued throughout the section except in cycle 29 where an abnormally high crystallinity peak is present. Crystallinity clearly displays an opposed variation to quartz frequency illustrating that the occurrence of quartz grains in abundance inhibits the development of large dolomite crystals on a large scale as well as in the individual cycle. (See ideal cycle, Plate 3.)

Pyrite frequency has an overall tendency to decrease upward. Large broad peaks are present near the bottom of the section, intermediate values occur in the central part and small, widely-spaced peaks are present at the top. In the lower and middle parts of the section, the curve of pyrite frequency parallels the variations in general clasticity suggesting that iron is transported by the same currents that are responsible for reworking and redeposition of lithic fragments. Pyrite also appears most abundant during periods when the environment is especially shallow and oscillatory as indicated by the bathymetrical curve.

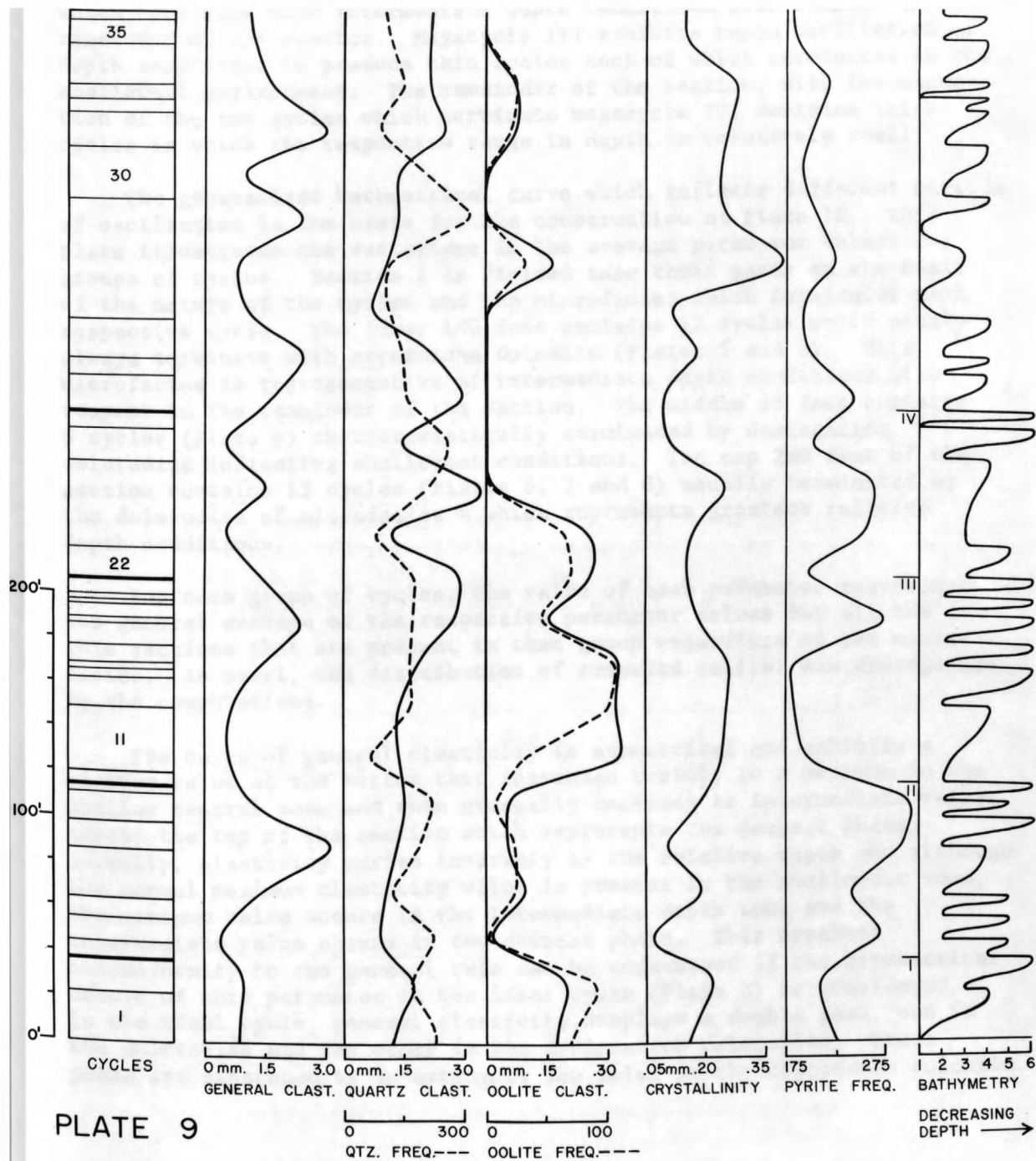


PLATE 9

GENERALIZED PARAMETER VARIATIONS — SECTION I

The bathymetrical curve demonstrates that more or less distinct periods of environmental oscillations exist which correspond in general to the megacycle boundaries. Megacycles I and II show moderate oscillation of the environment producing cycles of irregular thickness most of which terminate with intermediate depth conditions with respect to the remainder of the section. Megacycle III exhibits rapid oscillation of depth conditions to produce thin cycles each of which terminates in the shallowest environment. The remainder of the section, with the exception of the two cycles which terminate megacycle IV, contains thick cycles in which the respective range in depth is relatively small.

The generalized bathymetrical curve which reflects different periods of oscillation is the basis for the construction of Plate 10. This plate illustrates the variations in the average parameter values for groups of cycles. Section 1 is divided into three parts on the basis of the nature of the cycles and the microfacies which terminates each respective cycle. The lower 180 feet contains 12 cycles which nearly always terminate with cryptozoan dolomite (Plates 5 and 6). This microfacies is representative of intermediate depth conditions with respect to the remainder of the section. The middle 35 feet contains 8 cycles (Plate 6) characteristically terminated by desiccation dolorudite indicating shallowest conditions. The top 260 feet of the section contains 15 cycles (Plates 6, 7 and 8) usually terminated by the dolorudite of microfacies 4 which represents greatest relative depth conditions.

For each group of cycles, the value of each parameter represents the general average of the respective parameter values for all the thin sections that are present in that group regardless of the microfacies. As usual, the distribution of reworked oolites was disregarded in the computations.

The curve of general clasticity is symmetrical and exhibits a minimum value at the bottom that increases rapidly to a maximum in the shallow central zone and then gradually declines to intermediate values toward the top of the section which represents the deepest phase. Normally, clasticity varies inversely as the relative depth and although the normal maximum clasticity value is present in the shallowest zone, the minimum value occurs in the intermediate depth zone and the intermediate value occurs in the deepest phase. This apparent nonconformity to the general rule can be understood if the asymmetrical nature of this parameter in the ideal cycle (Plate 3) is considered. In the ideal cycle, general clasticity displays a double peak, one in the dolorudite and the other in the desiccation dolorudite. These peaks are separated by an extremely low value in the cryptozoan dolomite.

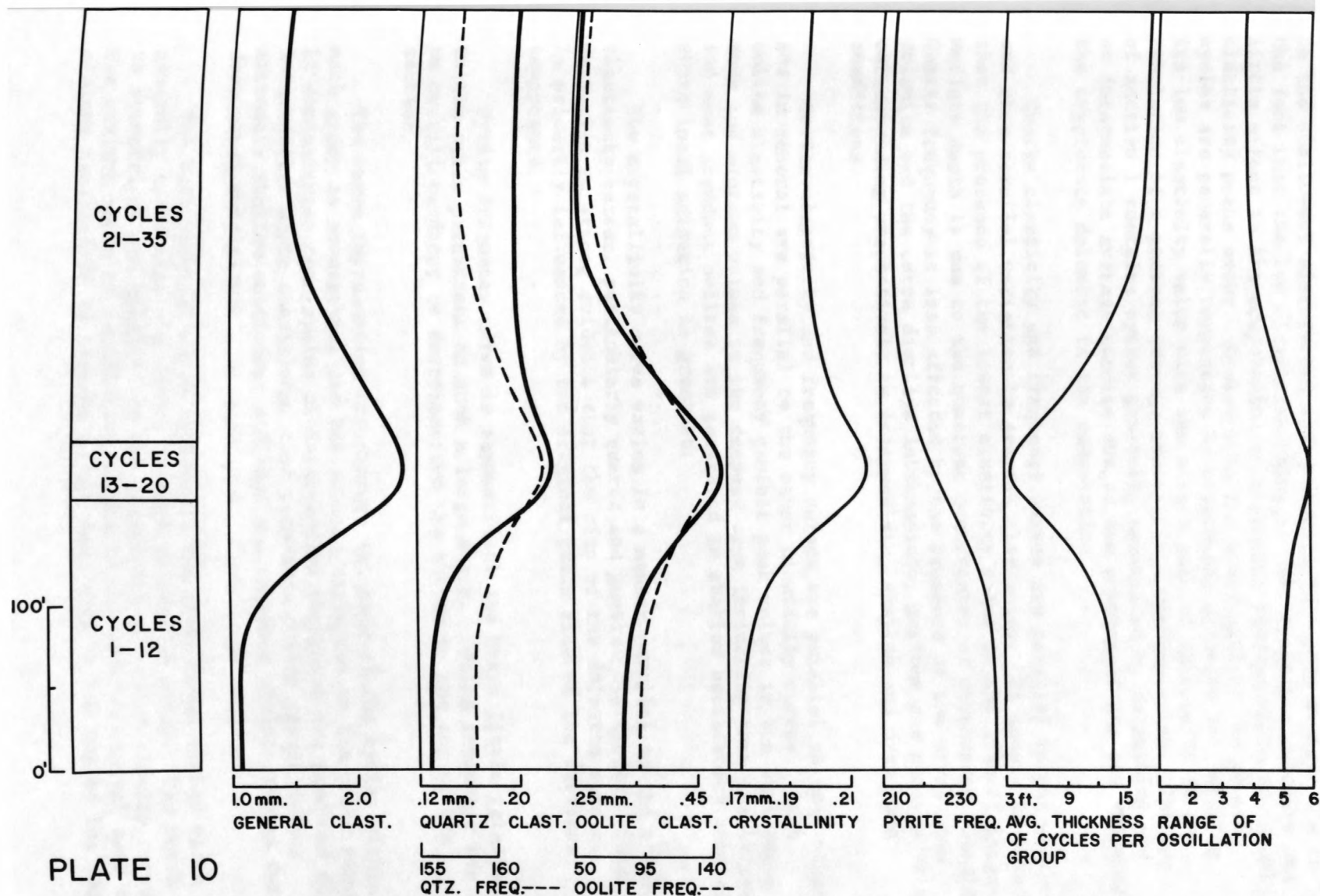


PLATE 10

PARAMETER VARIATIONS FOR GROUPS OF CYCLES — SECTION I

In the middle part of the section, cycles are generally complete to the shallowest microfacies and a normal maximum is present due to the fact that the low clasticity value of the cryptozoan dolomite has little effect in the computation of a general average where the double clasticity peaks occur. However, in the lower part of the section, cycles are generally terminated by cryptocoan dolomite and entering its low clasticity value with the single peak of dolorudite in the tabulation of a general average results in a minimum value. The top of section 1 contains cycles generally terminated by dolorudite and an intermediate average results due to the absence of the low value of the cryptozoan dolomite in the computation.

Quartz clasticity and frequency curves are parallel to one another and show parallel variation to general clasticity. It should be noted that the presence of the lowest clasticity value in the zone of intermediate depth is due to the numerous occurrences of cryptozoan dolomite. Quartz frequency is less affected by the presence of the cryptozoan dolomite and the curve displays intermediate, maximum and minimum values corresponding respectively to intermediate, shallow and deep water conditions.

Oolite clasticity and frequency curves are parallel to each other and in general are parallel to the other clasticity curves. Both oolite clasticity and frequency exhibit peak values in the shallowest zone and minimum values in the deepest zone indicating that the largest and most abundant oolites are generated in shallow oscillatory conditions where local agitation is greatest.

The crystallinity curve varies in a manner parallel to the other clasticity curves, particularly quartz and general clasticity. This variation is strong evidence that the size of the dolomite crystals is primarily influenced by the original grain size of the detrital components.

Pyrite frequency curve is asymmetrical and bears little relationship to the other parameters on such a large scale. Pyrite frequency has an overall tendency to decrease from the bottom to the top of the section.

The curve representing the average thickness of the cycles within each group is symmetrical and has opposed variation to the other curves. It demonstrates that cycles of intermediate thickness are produced during intermediate depth conditions, that very thin cycles result during extremely shallow conditions and that the thickest cycles develop during deep water conditions.

The bathymetrical curve represents the microfacies number which generally terminates the cycles in each respective group. The curve is symmetrical and parallel to the clasticity and crystallinity curves. The maximum range of oscillation occurs in the shallow central zone and minimum oscillation is present in the deep zone at the top of the section.

Description of Section 2

Section 2 is considerably thicker than Section 1 and in general the individual megacycles are better developed as distinct sedimentary units. The description of this section is presented by megacycles in order to avoid repetition. Remarks are confined primarily to the abnormal aspects of each cycle and its variation from the ideal cycle for Section 2 which appears on Plate 4.

Megacycle I

Megacycle I is 88 feet thick and ^{*extends from cycle 1 through 9.*} ~~contains 9 cycles most of which are relatively thin.~~

The general clasticity curve conforms remarkably to the ideal cycle and each cycle displays progressively larger values toward the top. The only exceptions occur in cycle 1 which terminates with the normal low value of cryptozoan dolomite and in cycle 9 which contains two clasticity peaks, one at the bottom and another at the top to make a symmetrical cycle. Symmetrical cycles are extremely rare in these investigated sections and are the result of a gradual deepening of the water after a gradual shallowing. In the typical cycle, deepening is so rapid after the deposition of the shallow water facies of the preceeding cycle that it is left completely unrecorded in the micro-facies succession.

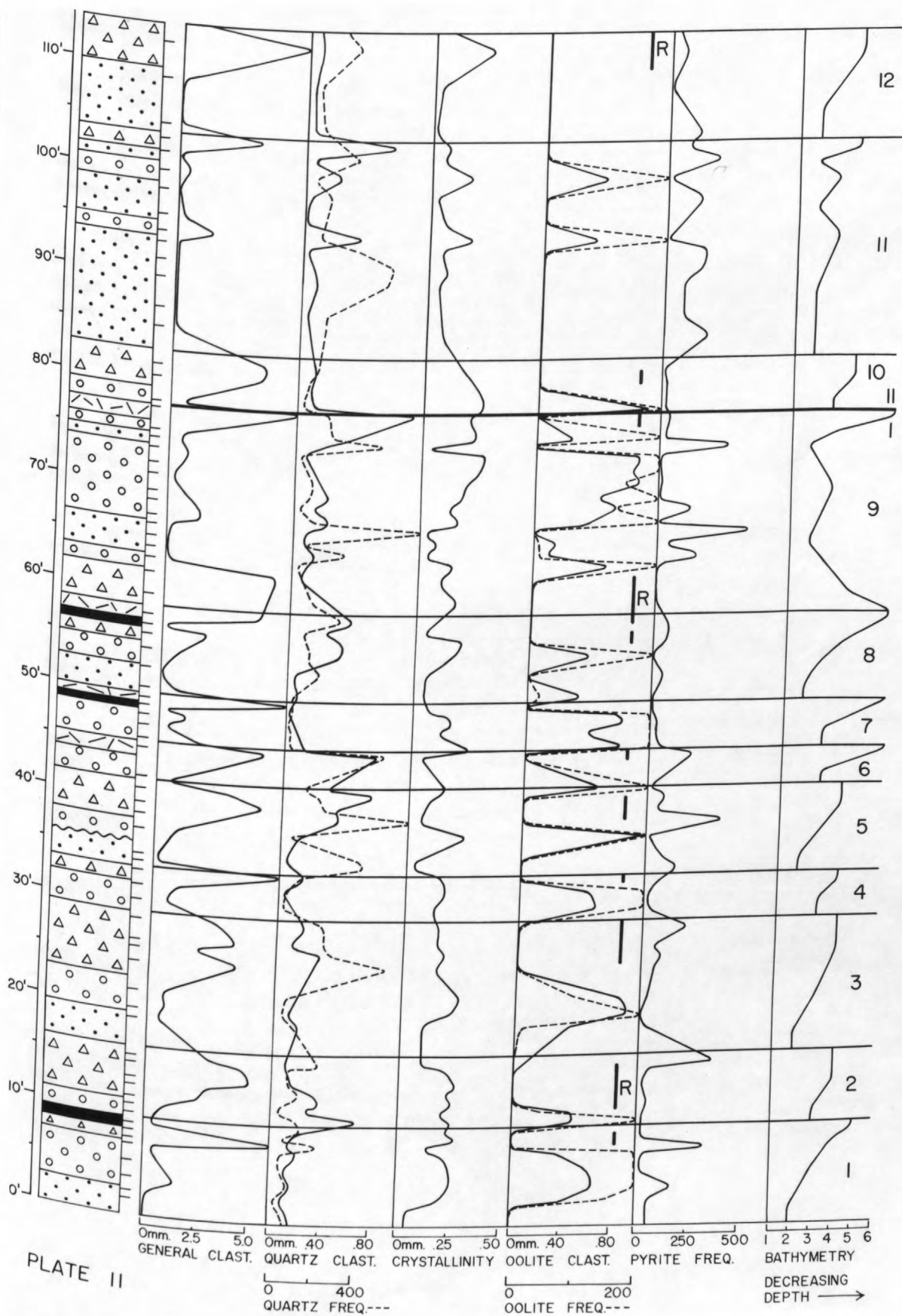
Quartz clasticity and frequency curves are nearly parallel and vary in a manner similar to general clasticity. Quartz clasticity shows abnormal relations in cycle 2 in which values decrease upward due to the presence of scattered quartz sandstone lenses and in cycle 7 where clasticity and frequency are stable around low values. Quartz frequency has abnormally high peaks in the dolarenites of cycles 5 and 9 again due to the presence of scattered bands of quartz sandstone.

Crystallinity displays only slight variation in cycles 2 and 4 but the only incorrect variation is the low value in the dolerudite of cycle 5.

Megacycle I contains abundant normal and reworked oolites indicating particularly concentrated conditions. Oolite values strongly parallel the more subdued variations of the crystallinity throughout this megacycle. Oolite frequency in the oolitic dolarenites generally extends beyond the value on the scale.

Pyrite frequency curve shows remarkable parallel variation to quartz frequency and generally increases upward in each cycle except in cycle 7 and 8 where values are uniformly low.

The bathymetrical curve of cycles 1 to 8 shows normal progressive decrease in depth upward. Cycle 9 is symmetrical and exhibits oscillating conditions in its middle portion.



Megacycle II

Megacycle II, like megacycle I, is 88 feet thick and *extends from cycle 10 through* ~~also contains~~ 9 cycles.]

General clasticity exhibits normal variation throughout with maximum values occurring at the top of each cycle except in cycle 15 which terminates with a normal low value in the cryptozoan dolomite.

The quartz curves in cycles 12 through 14 display opposing variations indicating a deficient supply. In these cycles and in cycles 17 and 18 quartz frequency generally has abnormally high peaks in the dolarenite zones due to scattered lenses of quartz sandstone. The clasticity curve in cycles 15 through 18 varies in the normal manner but the magnitude of variations ~~are~~ very small.

Crystallinity is normal in all the cycles except for the relatively low values in the dolorudites terminating cycles 10, 11 and 13. In general, the crystallinity curve displays marked similarity to the general clasticity curve.

Oolites are scattered and each occurrence is characterized by extremely high frequency values.

Pyrite frequency displays extremely low, abnormal values in cycles 10, 14 and 15. In cycle 11, the curve is normal and directly opposed to quartz clasticity and crystallinity. Cycles 13 and 16 are normal and 17 and 18 oscillate around an average value of 175.

The bathymetrical curve of cycles 10, 12, 14, 15 and 16 shows normal progressive decrease in depth upward. The remaining cycles oscillate before culminating.

Megacycle III

Megacycle III is 84 feet thick including a covered interval of 22 feet beginning at 232 feet. This megacycle ~~contains 7 cycles~~ *extends from cycle 19 through 25.*

General clasticity exhibits good normal variation in each cycle. The single anomalous point is the low value present in the dolorudite of cycle 25 at 255 feet.

Quartz clasticity is extremely stable at approximately .15 mm. throughout this megacycle. The only significant peak occurs in the dolorudite terminating cycle 25. Quartz frequency does not vary considerable but has a general trend parallel to the general clasticity except at 255 feet where the abnormal general clasticity value occurs.

Clast

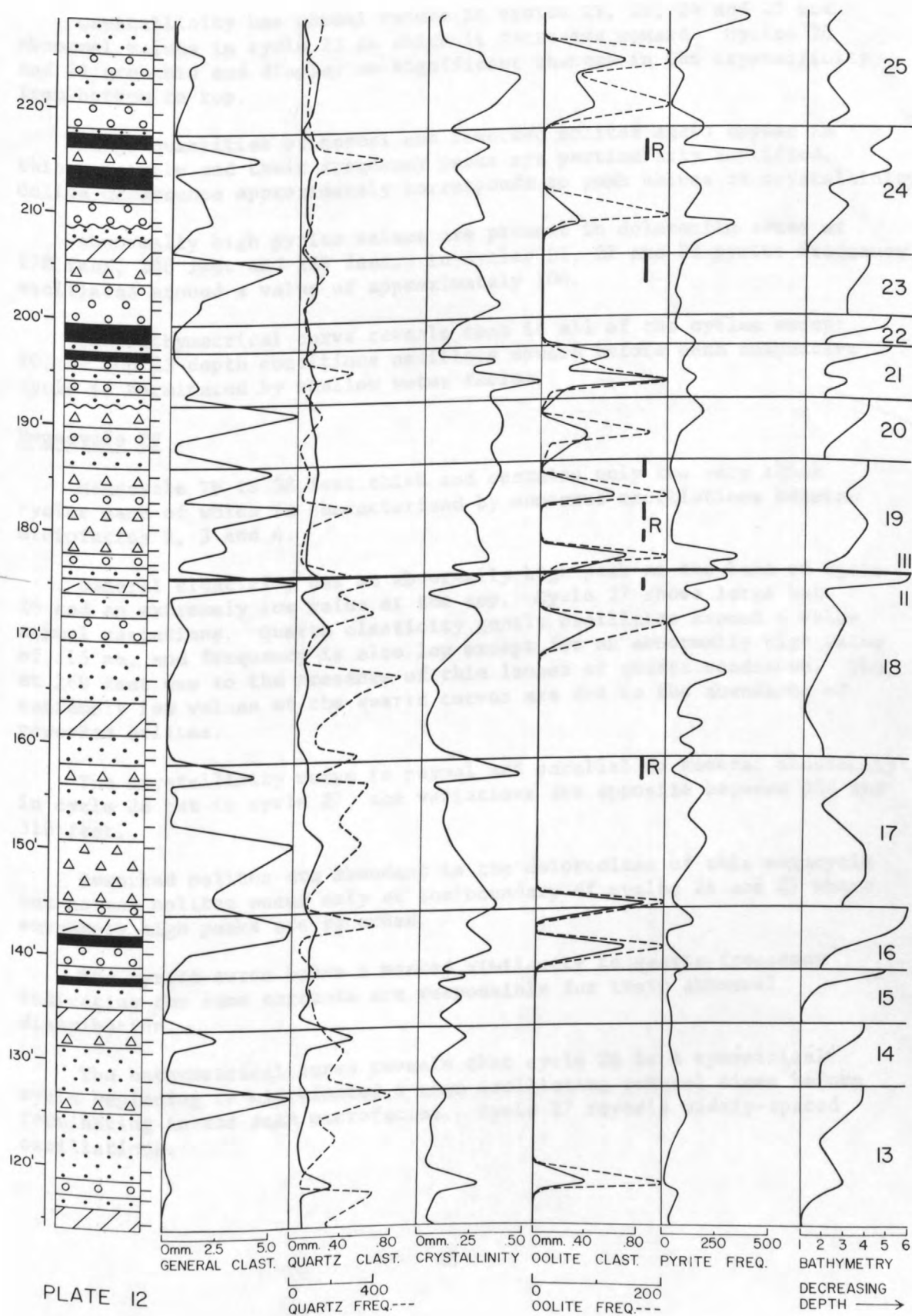


PLATE 12

Crystallinity has normal values in cycles 19, 21, 24 and 25 but abnormal values in cycle 23 in which it decreases upward. Cycles 20 and 22 are thin and display no significant changes in the crystallinity from bottom to top.

Large quantities of normal and reworked oolites again appear in this megacycle and their frequency peaks are particularly amplified. Oolite occurrence approximately corresponds to peak values of crystallinity.

Abnormally high pyrite values are present in dolarenite zones at 178 feet, 208 feet and 229 feet. In cycles 21, 22 and 23 pyrite frequency oscillates around a value of approximately 100.

The bathymetrical curve reveals that in all of the cycles except 20, 22 and 23 depth conditions oscillate upward before each respective cycle is terminated by shallow water facies.

Megacycle IV

Megacycle IV is 58 feet thick and contains only two very thick cycles each of which is characterized by numerous oscillations between microfacies 2, 3 and 4.

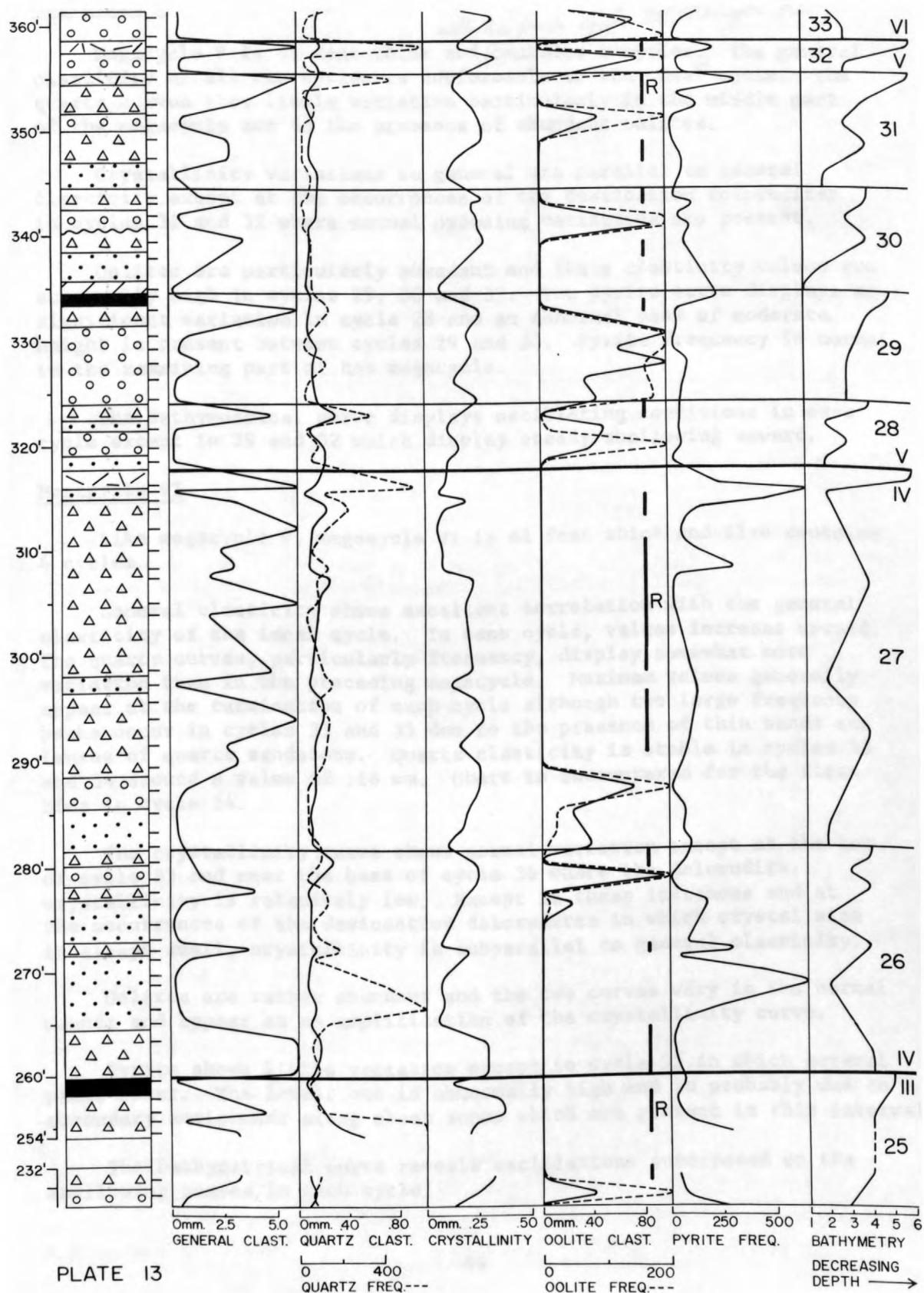
General clasticity has an abnormally high peak at the base of cycle 26 and an extremely low value at the top. Cycle 27 shows large but normal variations. Quartz clasticity gently oscillates around a value of .15 mm, and frequency is also low except for an abnormally high value at 269 feet due to the presence of thin lenses of quartz sandstone. The extremely low values of the quartz curves are due to the abundance of reworked oolites.

The crystallinity curve is normal and parallel to general clasticity in cycle 26 but in cycle 27, the variations are opposite between 308 and 316 feet.

Reworked oolites are abundant in the dolorudites of this megacycle but normal oolites occur only at the boundary of cycles 26 and 27 where extremely high peaks are recorded.

The pyrite curve bears a marked similarity to quartz frequency indicating the same currents are responsible for their abnormal distribution.

The bathymetrical curve reveals that cycle 26 is a symmetrical cycle beginning in microfacies 4 then oscillating several times before terminating in the same microfacies. Cycle 27 reveals widely-spaced oscillations.



Megacycle V

extends from cycle 28 through 32.

Megacycle V is 41 feet thick and contains 4 cycles. The general clasticity of all the cycles is conformable to the ideal cycle. The quartz curves show little variation particularly in the middle part of the megacycle due to the presence of abundant oolites.

Crystallinity variations in general are parallel to general clasticity except at the occurrences of the desiccation dolorudites in cycles 31 and 32 where normal opposing variations are present.

Oolites are particularly abundant and their clasticity values are abnormally high in cycles 29, 30 and 32. The pyrite curve displays no significant variation in cycle 28 and an abnormal peak of moderate height is present between cycles 29 and 30. Pyrite frequency is normal in the remaining part of the megacycle.

The bathymetrical curve displays oscillating conditions in each cycle except in 29 and 32 which display steady shallowing upward.

Megacycle VI

Like megacycle V, megacycle VI is 41 feet thick and also contains 4 cycles.

General clasticity shows excellent correlation with the general clasticity of the ideal cycle. In each cycle, values increase upward. The quartz curves, particularly frequency, display somewhat more variation than in the preceding megacycle. Maximum values generally appear at the termination of each cycle although two large frequency peaks occur in cycles 33 and 35 due to the presence of thin bands and lenses of quartz sandstone. Quartz clasticity is stable in cycles 33 and 34 around a value of 118 mm. Chert is encountered for the first time in cycle 34.

The crystallinity curve shows normal variation except at the top of cycle 33 and near the base of cycle 36 where the dolorudite crystallinity is relatively low. Except in these instances and at the occurrences of the desiccation dolorudites in which crystal size is always small, crystallinity is subparallel to general clasticity.

Oolites are rather abundant and the two curves vary in the normal manner and appear as an amplification of the crystallinity curve.

Pyrite shows little variation except in cycle 35 in which several peaks occur. The lowest one is abnormally high and is probably due to secondary enrichment along shear zones which are present in this interval.

The bathymetrical curve reveals oscillations superposed on the shallowing phases in each cycle.

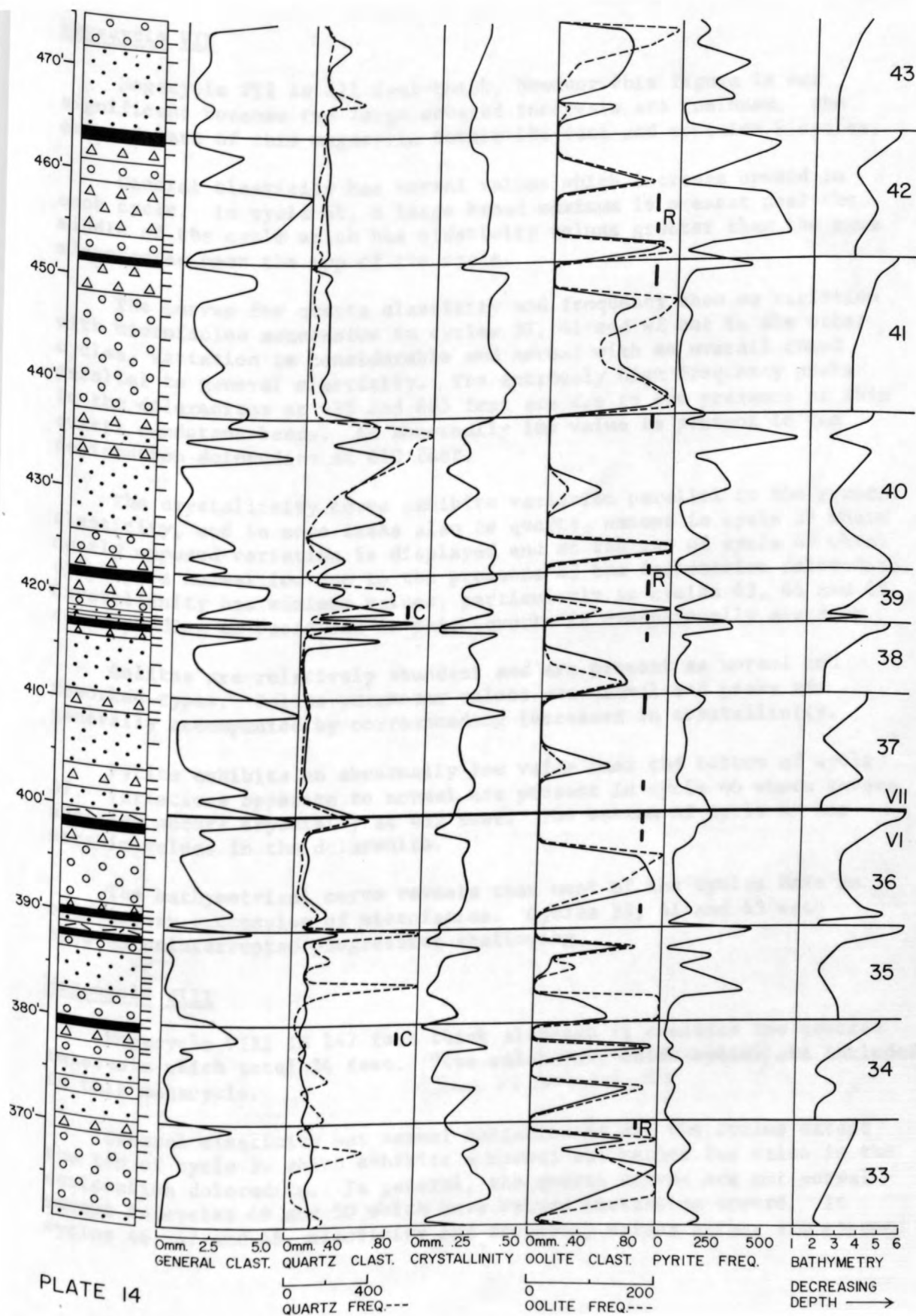


PLATE 14

Megacycle VII

Megacycle VII is 211 feet thick, however this figure is not significant because two large covered intervals are included. The exposed part of this megacycle totals 108 feet and contains 9 cycles.

General clasticity has normal values which increase upward in each cycle. In cycle 41, a large broad maximum is present near the middle of the cycle which has clasticity values greater than the same microfacies near the top of the cycle.

The curves for quartz clasticity and frequency show no variation with microfacies succession in cycles 37, 41 and 42 but in the other cycles, variation is considerable and normal with an overall trend parallel to general clasticity. The extremely high frequency peaks in the dolarenites at 435 and 485 feet are due to the presence of thin quartz sandstone bands. An abnormally low value is present in the desiccation dolorudite at 610 feet.

The crystallinity curve exhibits variation parallel to the general clasticity, and in some cases also to quartz, except in cycle 39 where nearly opposed variation is displayed and at the top of cycle 43 which displays a normal low due to the presence of the desiccation dolorudite. Crystallinity has minimum values, particularly in cycles 43, 44 and 45, corresponding to positions in which quartz is exceptionally abundant.

Oolites are relatively abundant and are present as normal and reworked types. Oolite parameter values are normal and peaks are generally accompanied by corresponding increases in crystallinity.

Pyrite exhibits an abnormally low value near the bottom of cycle 37. Variations opposite to normal are present in cycle 40 where severe shearing occurs especially at 435 feet. The bottom of cycle 43 has erratic values in the dolarenite.

The bathymetrical curve reveals that most of the cycles have an oscillatory succession of microfacies. Cycles 38, 41 and 43 each show an uninterrupted progressive shallowing.

Megacycle VIII

Megacycle VIII is 147 feet thick although it contains two covered intervals which total 34 feet. ~~[Five relatively thick cycles]~~ are included in this megacycle. *Cycles 46 through 50*

General clasticity has normal variation in all the cycles except the top of cycle 50 which exhibits a normal but rather low value in the desiccation dolorudite. In general, the quartz curves are not normal except in cycles 49 and 50 which have values increasing upward. In cycles 46, 47 and 48, elasticity and frequency values either are opposed

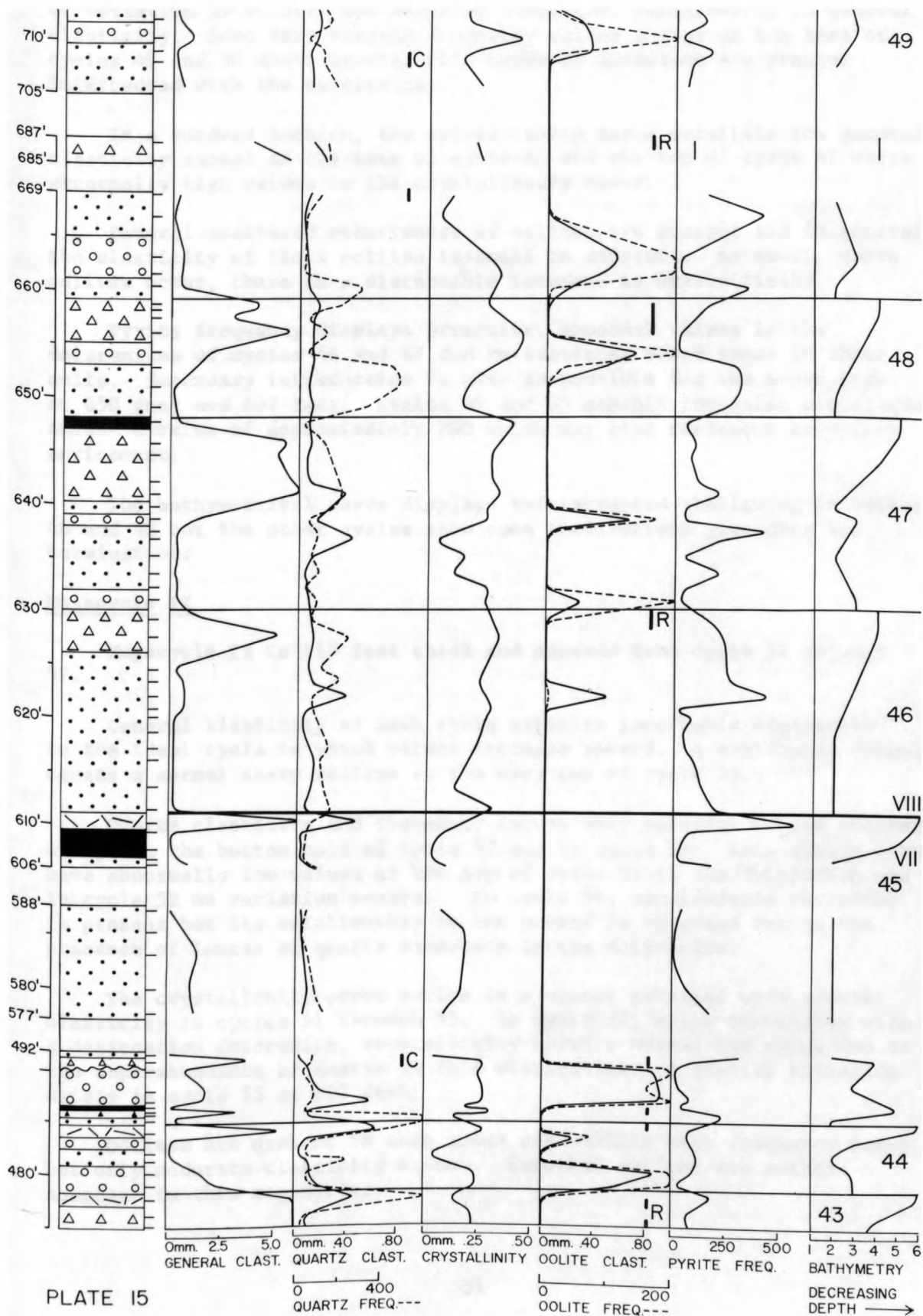


PLATE 15

or variation is erratic and bears no consistent relationship to general clasticity. Some very erratic frequency values appear at the base of cycles 49 and 50 where several thin bands of sandstone are present interbedded with the dolarenite.

In a subdued fashion, the crystallinity curve parallels the general clasticity except at the base of cycle 46 and the top of cycle 47 where abnormally high values in the crystallinity occur.

Several scattered occurrences of oolites are present and in general, the clasticity of these oolites is small to moderate. As usual, where oolites occur, there is a discernable increase in crystallinity.

Pyrite frequency displays irregular, abnormal values in the dolarenites of cycles 46 and 47 due to scattered shear zones in these units. Secondary introduction is also responsible for the broad peak at 650 feet and 667 feet. Cycles 49 and 50 exhibit irregular oscillations around a value of approximately 200 which may also represent secondary enrichment.

The bathymetrical curve displays uninterrupted shallowing in cycles 46 and 48 but the other cycles show some oscillations preceding the termination.

Megacycle IX

Megacycle IX is 115 feet thick and extends from cycle 51 through 57.

General clasticity of each cycle exhibits remarkable similarity to the ideal cycle in which values increase upward. A cryptozoan dolomite causes a normal sharp decline at the very top of cycle 56.

Quartz clasticity and frequency curves vary parallel to one another except in the bottom half of cycle 53 and in cycle 56. Both quartz curves have abnormally low values at the top of cycle 51 in the dolorudite and in cycle 52 no variation occurs. In cycle 54, considerable variation is present but its relationship to the normal is reversed due to the presence of lenses of quartz sandstone in the dolarenite.

The crystallinity curve varies in a manner parallel with general clasticity in cycles 51 through 55. In cycle 57, which terminates with a desiccation dolorudite, crystallinity shows a normal low value due to the superabundance of quartz in this microfacies. A similar situation exists in cycle 53 at 807 feet.

Oolites are present in thin zones and exhibit high frequency peaks but only moderate clasticity values. Reworked oolites are rather abundant in this megacycle.

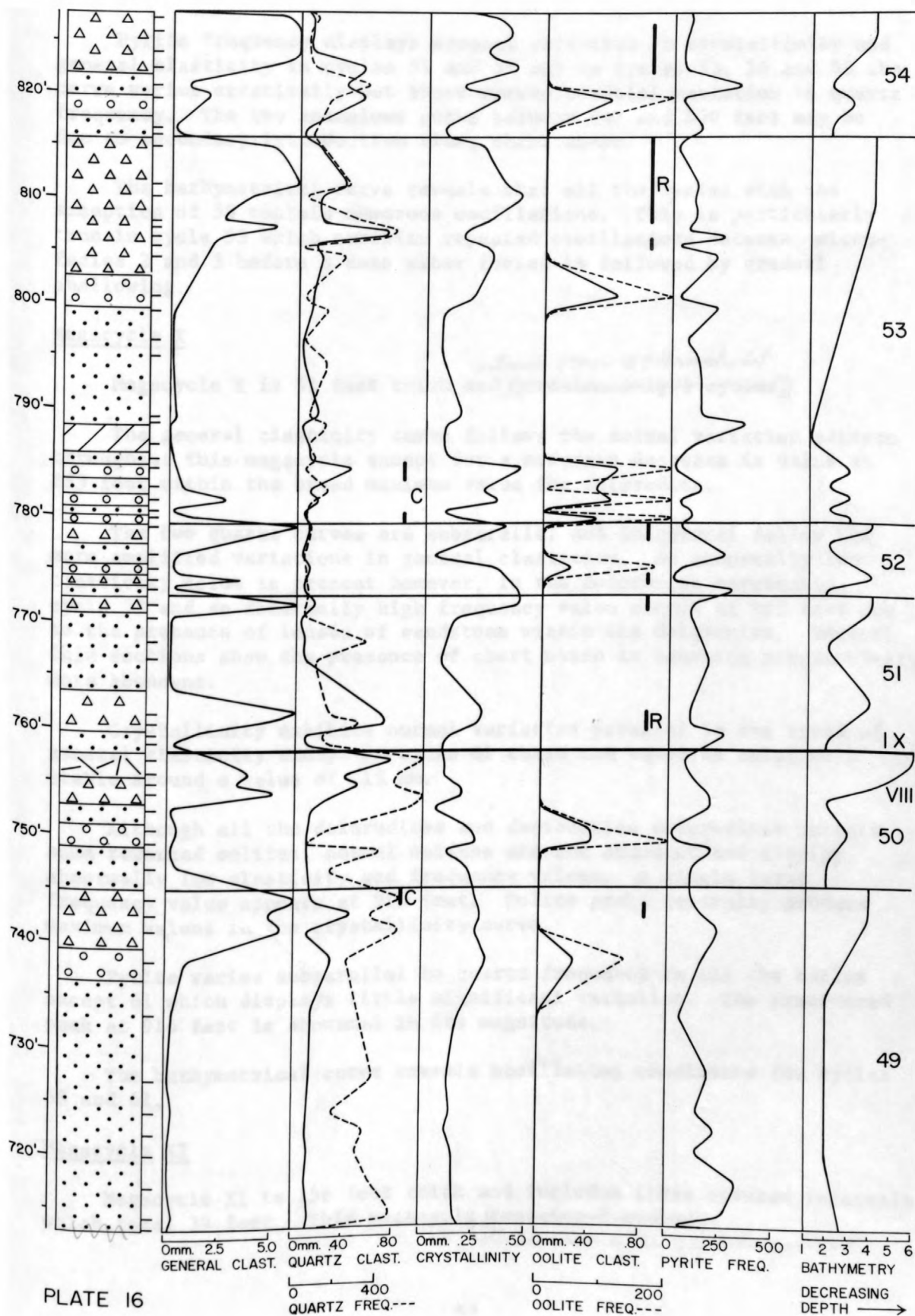


PLATE 16

Pyrite frequency displays opposed variation to crystallinity and general clasticity in cycles 51 and 52 and in cycles 53, 54 and 55 the curve varies erratically but shows marked parallel variation to quartz frequency. The two anomalous peaks between 845 and 850 feet may be due to secondary introduction along shear zones.

The bathymetrical curve reveals that all the cycles with the exception of 55 contain numerous oscillations. This is particularly true in cycle 53 which exhibits repeated oscillations between micro-facies 2 and 3 before a deep water facies is followed by gradual shallowing.

Megacycle X

Megacycle X is 51 feet thick and *extends from 58 through 61.* ~~contains only 4 cycles.~~

The general clasticity curve follows the normal variation pattern throughout this megacycle except for a moderate decrease in value at 883 feet within the broad maximum value for dolorudite.

The two quartz curves are subparallel and in general follow the more amplified variations in general clasticity. An abnormally low clasticity value is present however, in the dolorudite terminating cycle 58 and an abnormally high frequency value occurs at 903 feet due to the presence of lenses of sandstone within the dolarenite. Several thin sections show the presence of chert which is becoming progressively more abundant.

Crystallinity exhibits normal variation parallel to the trend of general clasticity except in cycle 61 where the value is relatively stable around a value of .15 mm.

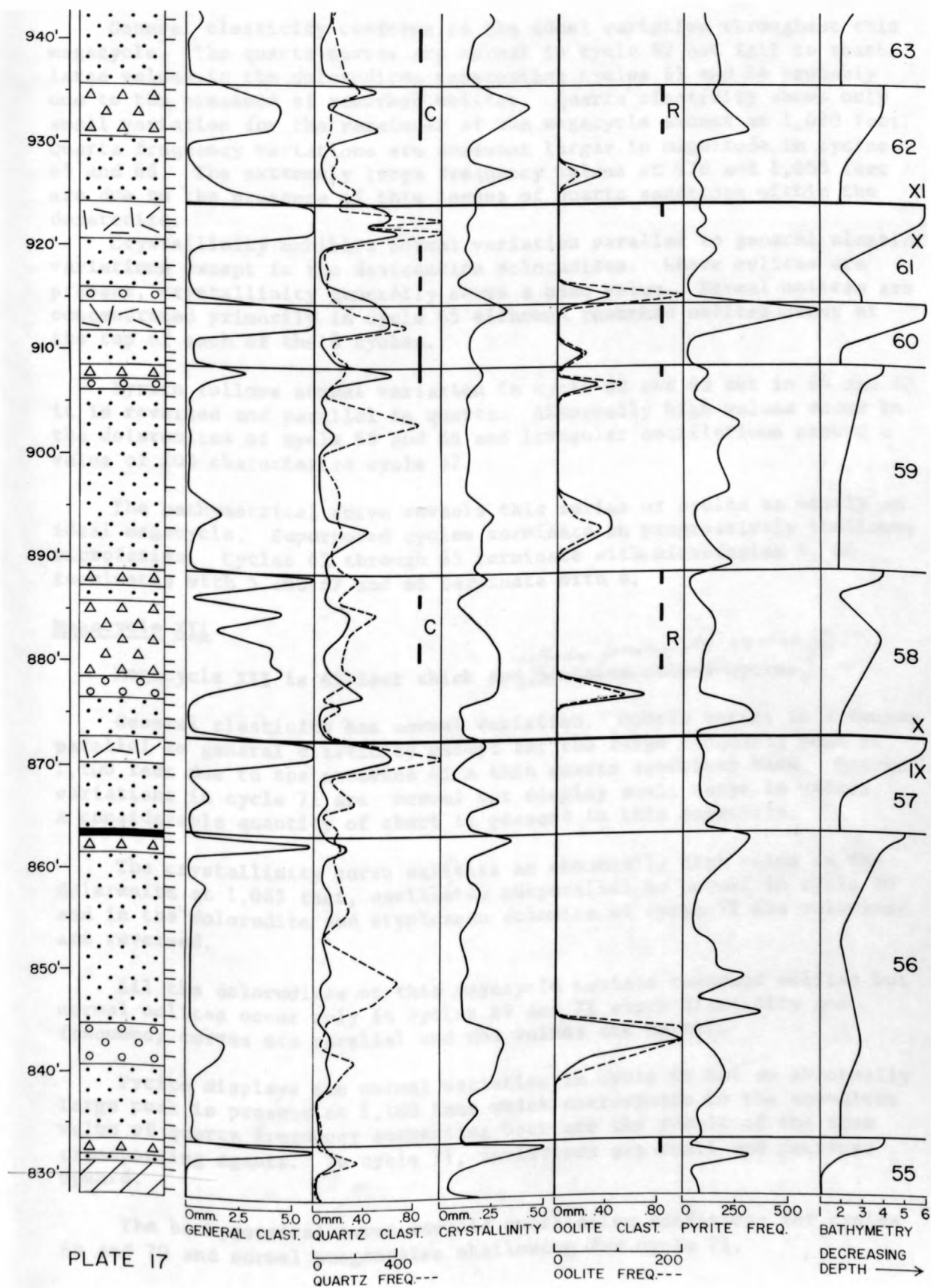
Although all the dolorudites and desiccation dolorudites contain some reworked oolites, normal oolites are not abundant and display abnormally low clasticity and frequency values. A single large frequency value appears at 915 feet. Oolite peaks generally produce maximum values in the crystallinity curve.

Pyrite varies subparallel to quartz frequency in all the cycles except 61 which displays little significant variation. The pronounced peak at 914 feet is abnormal in its magnitude.

The bathymetrical curve reveals oscillating conditions for cycles 58 and 61.

Megacycle XI

Megacycle XI is 156 feet thick and includes three covered intervals which total 39 feet. This megacycle ~~contains 8 cycles.~~ *extends from cycle 62 through 68.*



General clasticity conforms to the ideal variation throughout this megacycle. The quartz curves are normal in cycle 62 but fail to reach large values in the dolorudites terminating cycles 63 and 64 probably due to the presence of reworked oolites. Quartz clasticity shows only small variation for the remainder of the megacycle except at 1,080 feet. Quartz frequency variations are somewhat larger in magnitude in cycles 65 and 66. The extremely large frequency values at 978 and 1,055 feet are due to the presence of thin lenses of quartz sandstone within the dolarenite.

Crystallinity exhibits normal variation parallel to general clasticity variations except in the desiccation dolorudites. Where oolites are present, crystallinity generally shows a peak value. Normal oolites are concentrated primarily in cycle 65 although reworked oolites occur at the top of each of the 8 cycles.

Pyrite follows normal variation in cycle 62 and 63 but in 64 and 68 it is reversed and parallel to quartz. Abnormally high values occur in the dolarenites of cycle 65 and 66 and irregular oscillations around a value of 200 characterize cycle 67.

The bathymetrical curve reveals this series of cycles as nearly an ideal megacycle. Superposed cycles terminate in progressively shallower microfacies. Cycles 62 through 65 terminate with microfacies 4, 66 terminates with 5 and 67 and 68 terminate with 6.

Megacycle XII

Megacycle XII is 42 feet thick and ^{extends from cycle 69 through 71,} ~~contains only 3 cycles.~~

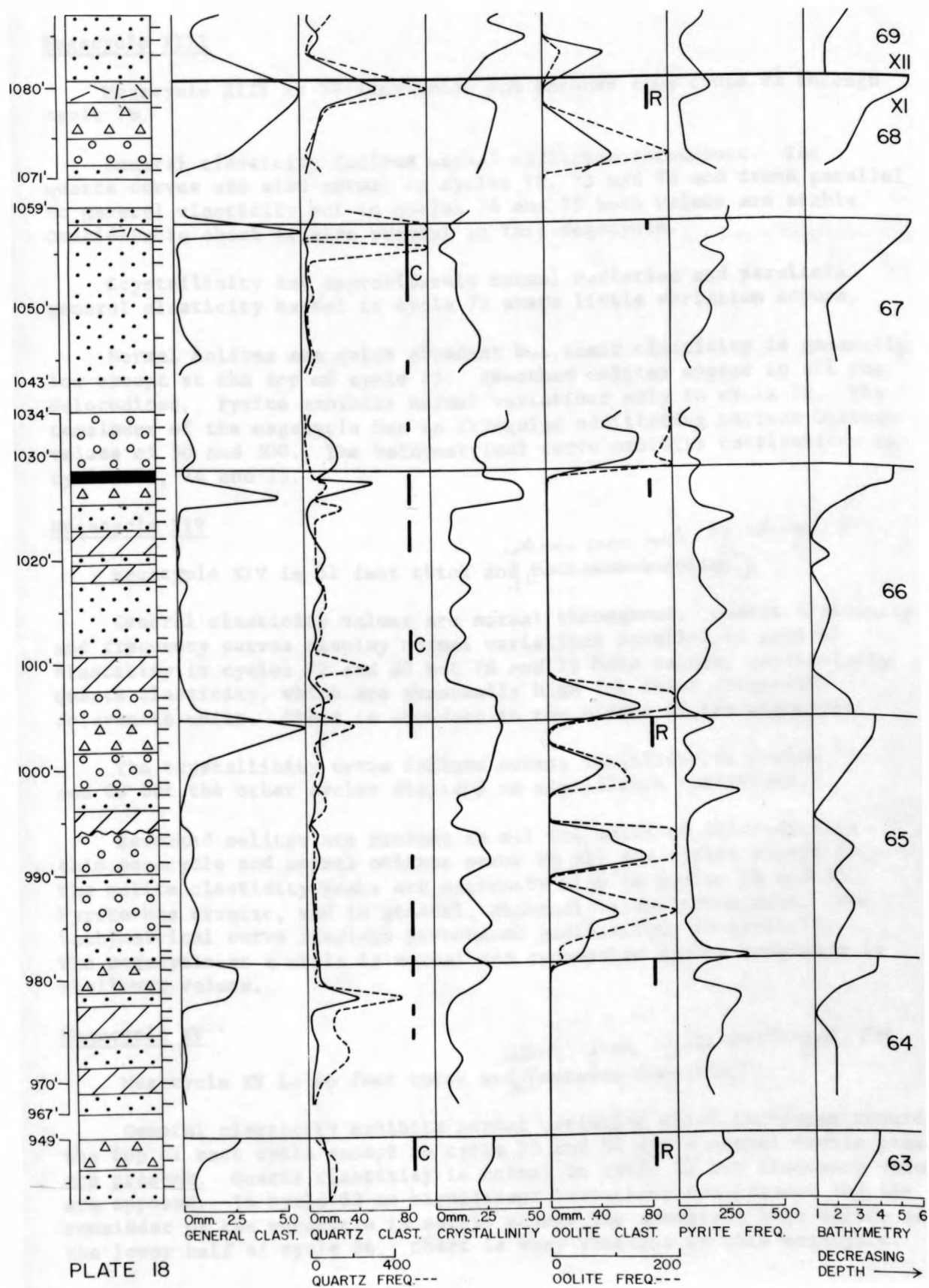
General clasticity has normal variation. Quartz varies in a manner parallel to general clasticity except for the large frequency peak at 1,100 feet due to the presence of a thin quartz sandstone band. Quartz variations in cycle 71 are normal but display small range in values. A considerable quantity of chert is present in this megacycle.

The crystallinity curve exhibits an abnormally high value in the dolarenite at 1,085 feet, oscillates subparallel to normal in cycle 70 and in the dolorudite and cryptozoan dolomite of cycle 71 the relations are reversed.

All the dolorudites of this megacycle contain reworked oolites but normal oolites occur only in cycles 69 and 71 where clasticity and frequency curves are parallel and the values are normal.

Pyrite displays the normal variation in cycle 69 but an abnormally large peak is present at 1,100 feet which corresponds to the anomalous value of quartz frequency suggesting both are the result of the same transporting agents. In cycle 71, variations are small and decrease upward.

The bathymetrical curve reveals oscillating conditions for cycles 69 and 70 and normal progressive shallowing for cycle 71.



Megacycle XIII

Megacycle XIII is 57 feet thick and extends from cycle 72 through cycle 76.

General clasticity follows normal variation throughout. The quartz curves are also normal in cycles 72, 73 and 76 and trend parallel to general clasticity but in cycles 74 and 75 both values are stable. Considerable chert is also present in this megacycle.

Crystallinity has approximately normal variation and parallels general clasticity except in cycle 72 where little variation occurs.

Normal oolites are quite abundant but their clasticity is generally low except at the top of cycle 75. Reworked oolites appear in all the dolorudites. Pyrite exhibits normal variations only in cycle 72. The remainder of the megacycle has an irregular oscillating pattern between values of 50 and 300. The bathymetrical curve exhibits oscillations in cycles 72, 74 and 75.

Megacycle XIV

Megacycle XIV is 51 feet thick and *extends from cycle 77 through 80.*
~~contains 4 cycles.~~

General clasticity values are normal throughout. Quartz clasticity and frequency curves display normal variations parallel to general clasticity in cycles 77 and 80 but 78 and 79 have values, particularly quartz clasticity, which are abnormally high for their respective dolarenite units. Chert is abundant in the middle of the megacycle.

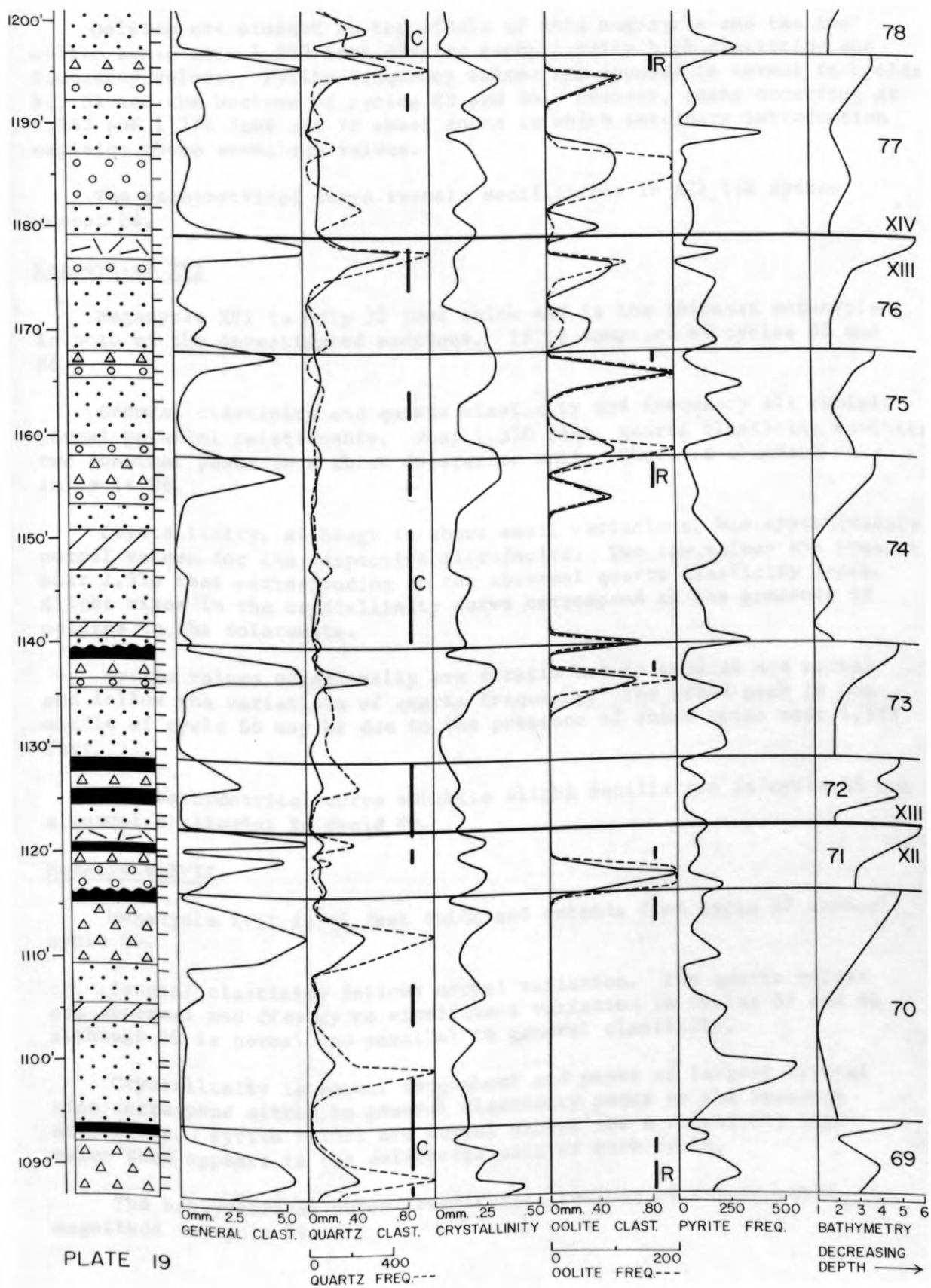
The crystallinity curve follows normal variations in cycles 77 and 80 but the other cycles display no significant variations.

Reworked oolites are present in all the units of dolorudite in this megacycle and normal oolites occur in all the cycles except 79. The oolite clasticity peaks are extremely high in cycles 78 and 80. Pyrite has erratic, and in general, abnormal values throughout. The bathymetrical curve displays pronounced oscillations in cycle 79. The megacycle as a whole is normal and successive cycles terminate in shallower values.

Megacycle XV

Megacycle XV is 66 feet thick and *extends from cycle 81 through 84.*
~~contains 4 cycles.~~

General clasticity exhibits normal variation which increases toward the top of each cycle except in cycle 83 and 84 where normal double peaks are present. Quartz clasticity is normal in cycle 81 but frequency values are opposed. In cycle 82 no significant variations are present and the remainder of the megacycle is normal except for anomalous high values in the lower half of cycle 84. Chert is very abundant in this megacycle.



Oolites are present in the middle of this megacycle and the two oolite zones near 1,250 feet display exceptionally high clasticity and frequency values. Pyrite frequency values are opposed to normal in cycles 81, 82 and the bottoms of cycles 83 and 84. However, peaks occurring at 1,242 and 1,276 feet are in shear zones in which secondary introduction explains these anomalous values.

The bathymetrical curve reveals oscillations in all the cycles except 84.

Megacycles XVI

Megacycle XVI is only 32 feet thick and is the thinnest megacycle in both of the investigated sections. It is composed of cycles 85 and 86.

General clasticity and quartz clasticity and frequency all exhibit normal parallel relationship. Near 1,310 feet, quartz clasticity exhibits two abnormal peaks in a thick dolarenite unit. Chert is abundant only in cycle 86.

Crystallinity, although it shows small variations, has approximately normal values for the respective microfacies. Two low values are present near 1,310 feet corresponding to the abnormal quartz clasticity peaks. Slight rises in the crystallinity curve correspond to the presence of oolites in the dolarenite.

Pyrite values occasionally are erratic but in general are normal and follow the variations of quartz frequency. The broad peak in the middle of cycle 86 may be due to the presence of shear zones near 1,323 feet.

The bathymetrical curve exhibits slight oscillation in cycle 85 but a normal shallowing in cycle 86.

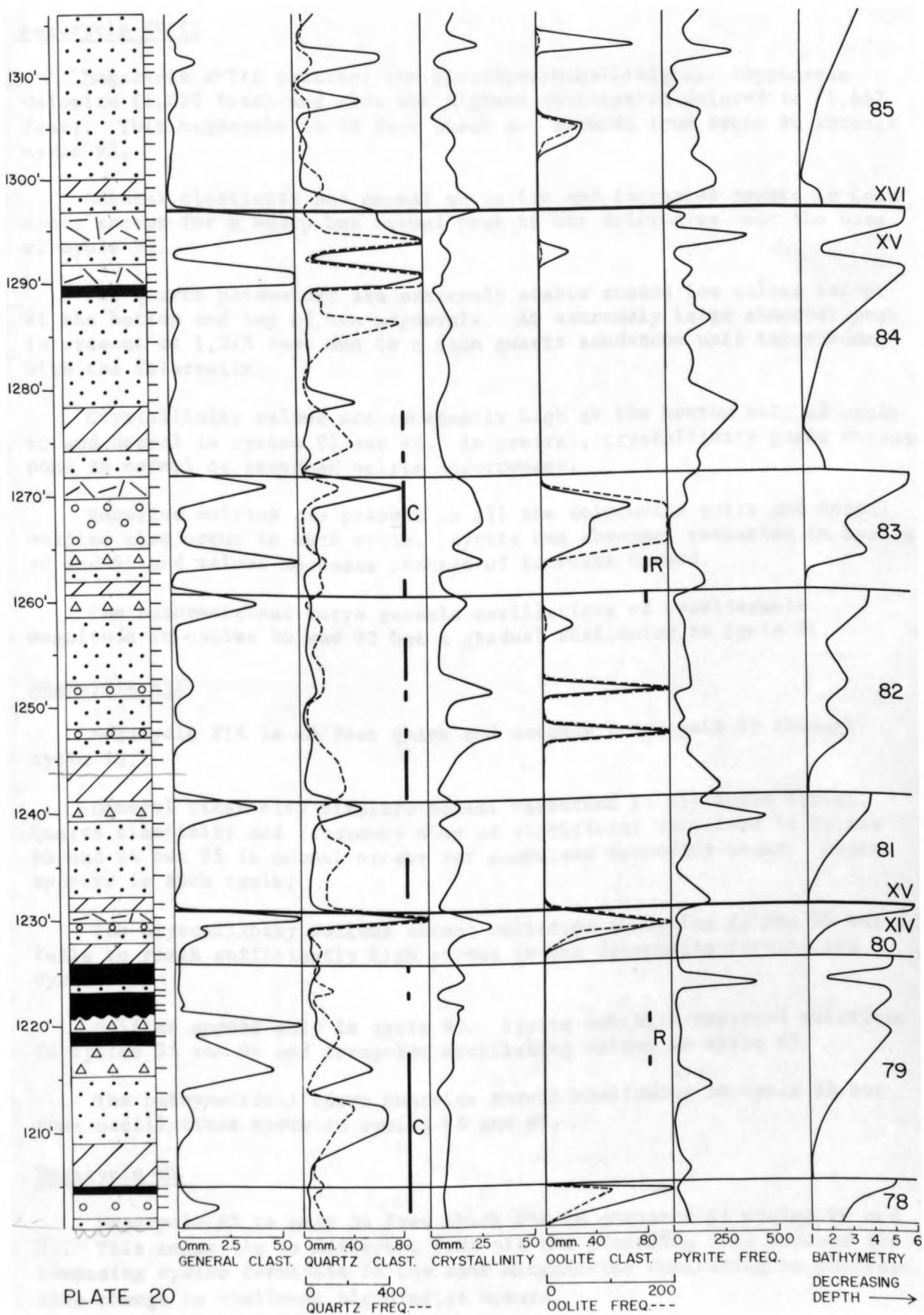
Megacycle XVII

Megacycle XVII is 41 feet thick and extends from cycle 87 through cycle 89.

General clasticity follows normal variation. The quartz curves are abnormal and display no significant variation in cycles 87 and 88 although 89 is normal and parallel to general clasticity.

Crystallinity is normal throughout and peaks of largest crystal size correspond either to general clasticity peaks or the presence of oolites. Pyrite values are normal except for a relatively high value that appears in the dolarenite unit of each cycle.

The bathymetrical curve reveals oscillations of considerable magnitude in cycle 89.



Megacycle XVIII

Megacycle XVIII contains the stratigraphically highest cryptozoan dolomite (1,426 feet) and also the highest desiccation dolorudite (1,457 feet). This megacycle is 48 feet thick and extends from cycle 90 through cycle 92.

General clasticity has normal variation and increases upward in each cycle except for a sharp but normal peak in the dolorudite near the base of cycle 90.

The quartz parameters are extremely stable around low values except at the bottom and top of the megacycle. An extremely large abnormal peak is present at 1,375 feet due to a thin quartz sandstone unit interbedded with the dolarenite.

Crystallinity values are abnormally high at the bottom half of cycle 90 and normal in cycles 91 and 92. In general, crystallinity peaks correspond to normal or reworked oolite occurrences.

Reworked oolites are present in all the dolorudite units and normal oolites also occur in each cycle. Pyrite has abnormal variation in cycles 90 and 91 and values decrease instead of increase upward.

The bathymetrical curve reveals oscillations of considerable magnitude in cycles 90 and 92 but a gradual shallowing in cycle 91.

Megacycle XIX

Megacycle XIX is 40 feet thick and extends from cycle 93 through cycle 95.

General clasticity displays normal variation in all three cycles. Quartz clasticity and frequency show no significant variation in cycles 93 and 94 but 95 is normal except for anomalous secondary peaks. Chert appears in each cycle.

The crystallinity follows normal variation in cycles 93 and 95 but fails to reach sufficiently high values in the dolorudite terminating cycle 94.

Oolites appear only in cycle 93. Pyrite exhibits reversed relations in cycles 93 and 94 and irregular oscillating values in cycle 95.

The bathymetrical curve exhibits normal shallowing in cycle 93 but some oscillations occur in cycles 94 and 95.

Megacycle XX

Megacycle XX is only 36 feet thick and is composed of cycles 96 and 97. This megacycle is different from all the preceding ones because its composing cycles terminate in the same microfacies indicating no progressive change to shallower microfacies upward.

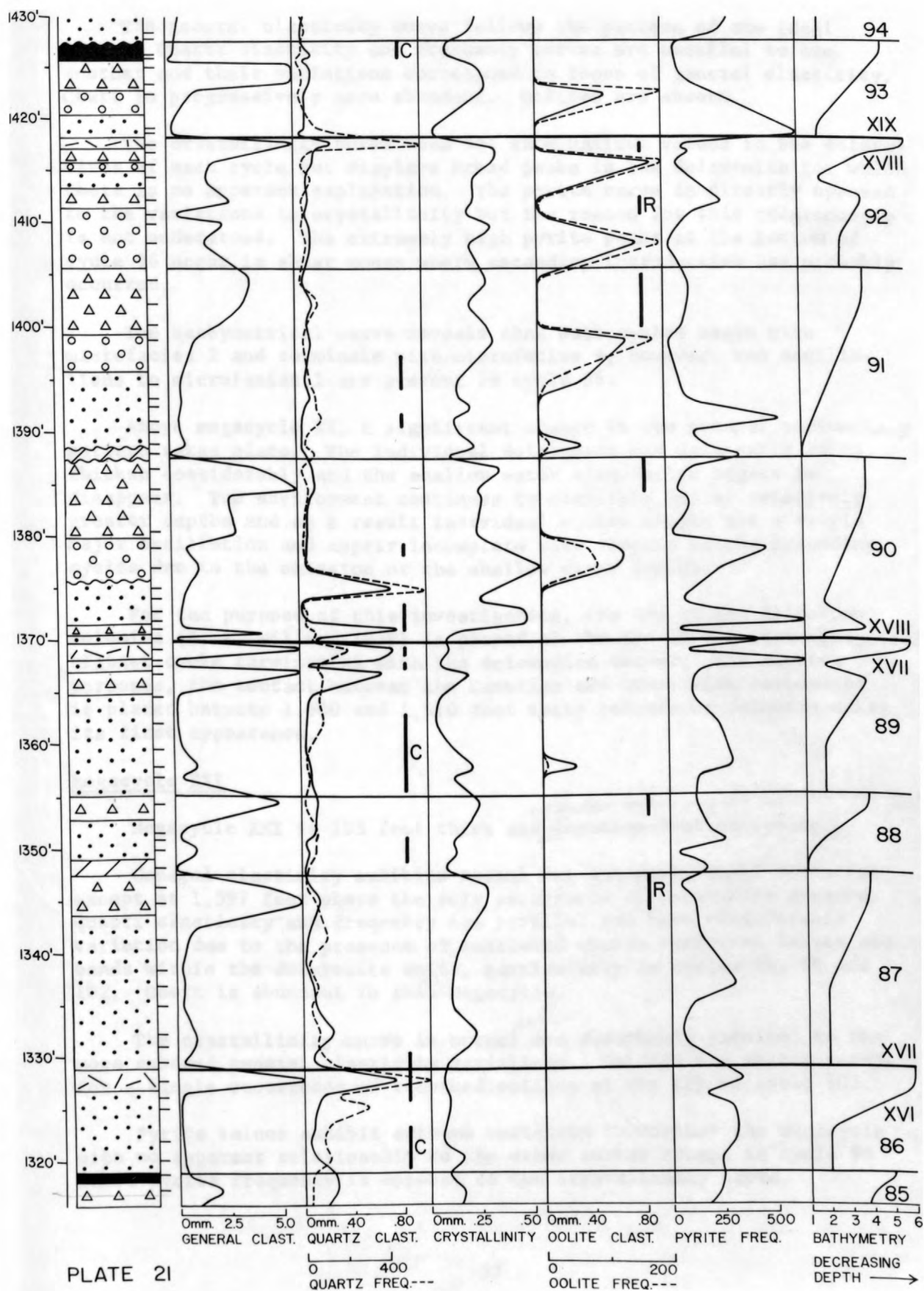


PLATE 21

The general clasticity curve follows the pattern of the ideal cycle. Quartz clasticity and frequency curves are parallel to one another and their variations correspond to those of general clasticity. Chert is progressively more abundant. Oolites are absent.

The crystallinity curve does not show maximum values in the dolorudites of each cycle but displays broad peaks in the dolarenite for which there is no apparent explanation. The pyrite curve is directly opposed to the variations in crystallinity but the reason for this relationship is not understood. The extremely high pyrite peaks at the bottom of cycle 96 occur in shear zones where secondary introduction has probably occurred.

The bathymetrical curve reveals that both cycles begin with microfacies 2 and terminate with microfacies 4, however, two oscillations to microfacies 1 are present in cycle 96.

Above megacycle XX, a significant change in the general sedimentary pattern takes place. The individual dololutite and dolarenite units thicken considerably and the shallow water microfacies begins to disappear. The environment continues to oscillate but at relatively greater depths and as a result individual cycles simply are a single major oscillation and appear incomplete with respect to the preceding cycles due to the omission of the shallow water facies.

For the purpose of this investigation, the top of the Allentown dolomite (B. L. Miller, 1939) is placed at the top of the stratigraphically highest cycle terminating with the dolorudite facies. For mapping purposes, the contact between the Cambrian and Ordovician carbonates is placed between 1,600 and 1,610 feet where calcareous dolomite makes its first appearance.

Megacycle XXI

Megacycle XXI is 103 feet thick and *extends from cycle 98 through cycle 102.* ~~contains 5 thick cycles.~~

General clasticity exhibits normal but extremely small variation except at 1,597 feet where the only occurrence of dolorudite appears. Quartz clasticity and frequency are parallel and have considerable variation due to the presence of scattered quartz sandstone lenses and bands within the dolarenite units, particularly in cycles 98, 99 and 102. Chert is abundant in this megacycle.

The crystallinity curve is normal and remarkably parallel to the more subdued general clasticity variations. Oolites are absent except for a single occurrence of reworked oolites at the top of cycle 102.

Pyrite values exhibit extreme variation throughout the megacycle with no apparent relationship to the other curves except in cycle 98 where pyrite frequency is opposed to the crystallinity curve.

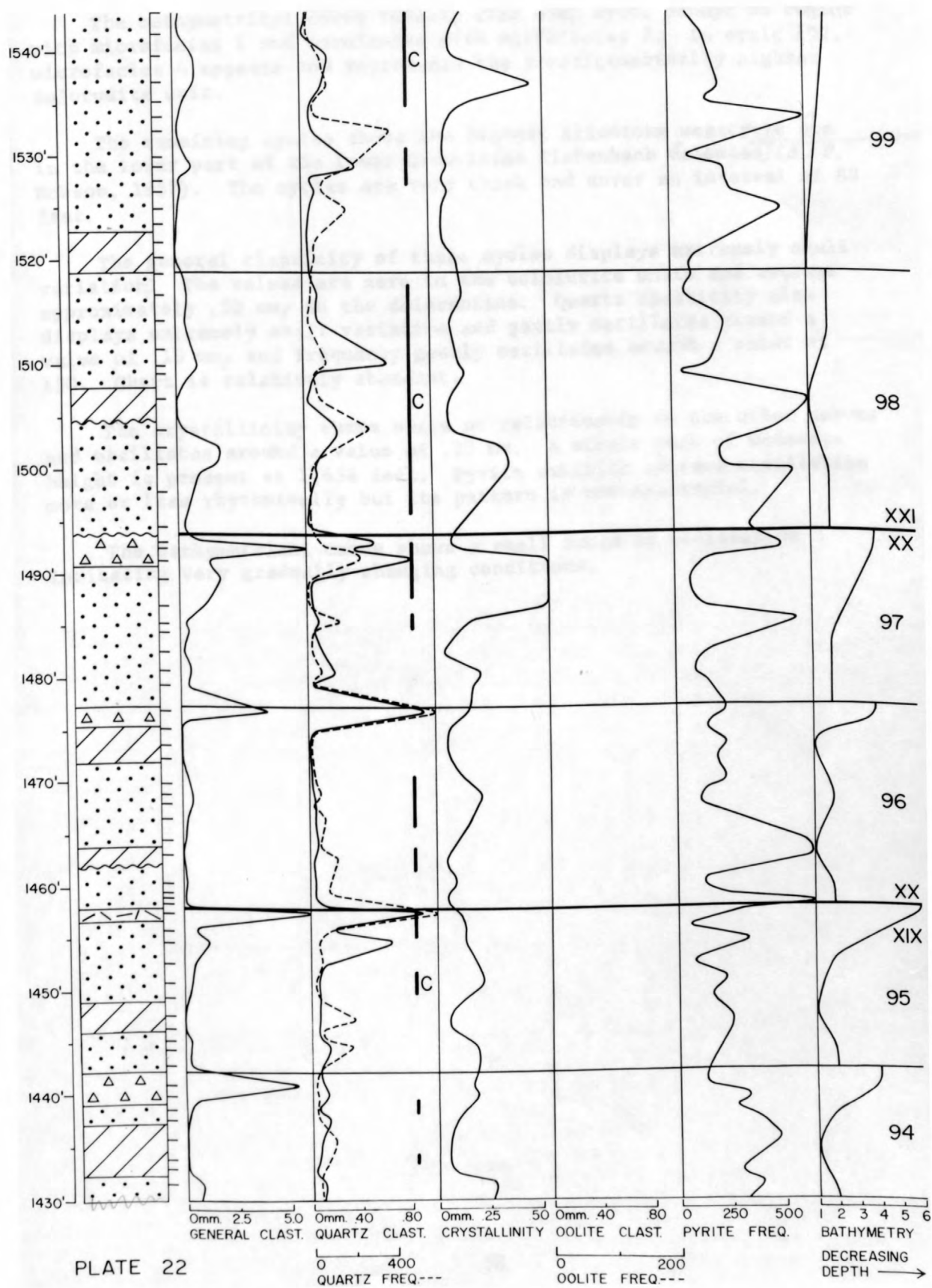


PLATE 22

The bathymetrical curve reveals that each cycle except 98 begins with microfacies 1 and terminates with microfacies 2. In cycle 102, microfacies 4 appears and represents the stratigraphically highest dolorudite unit.

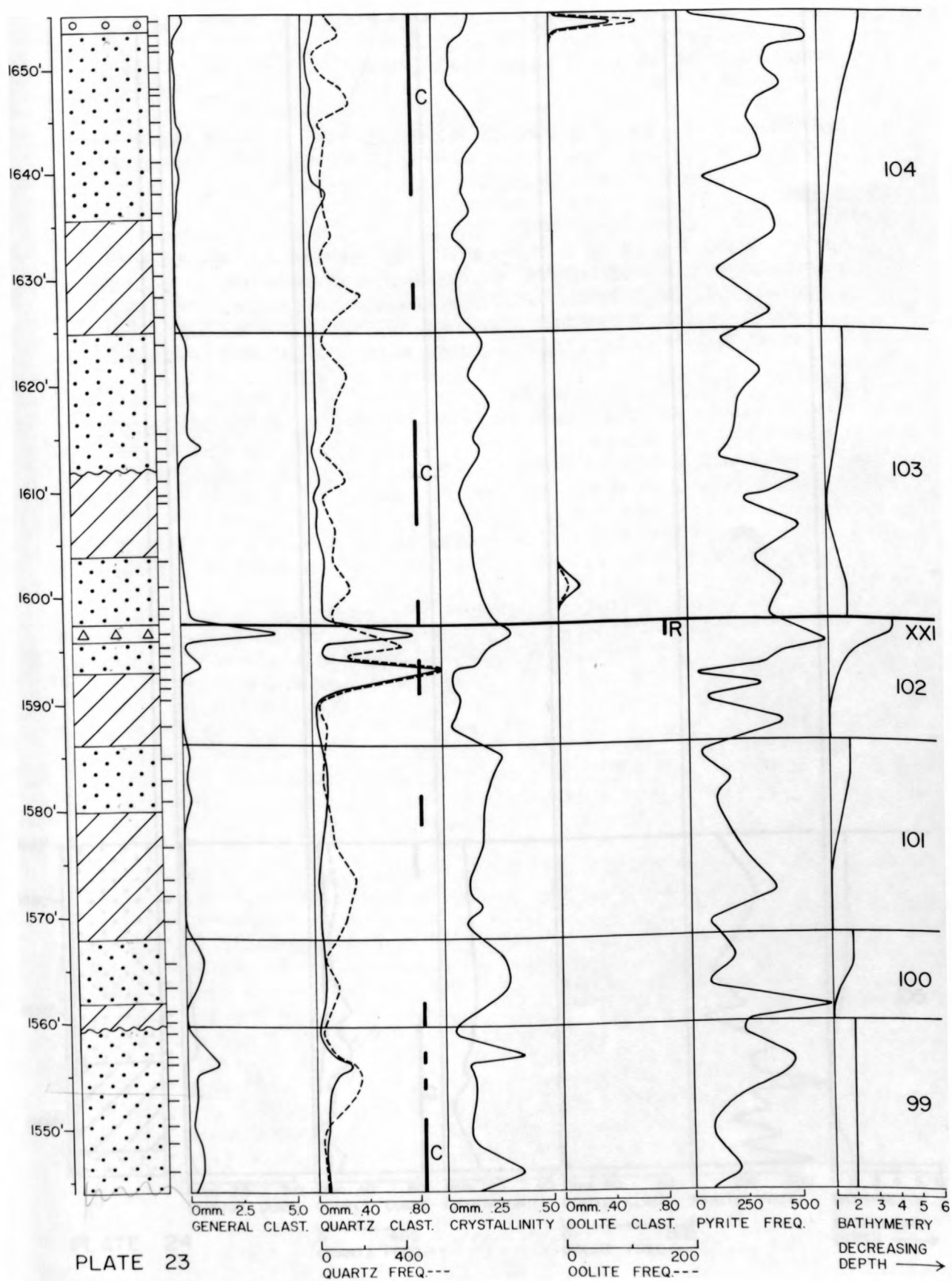
The remaining cycles above the highest Allentown megacycle are in the lower part of the Lower Ordovician Richenbach dolomite *formation* (J. P. Hobson, 1957). The cycles are very thick and cover an interval of 88 feet.

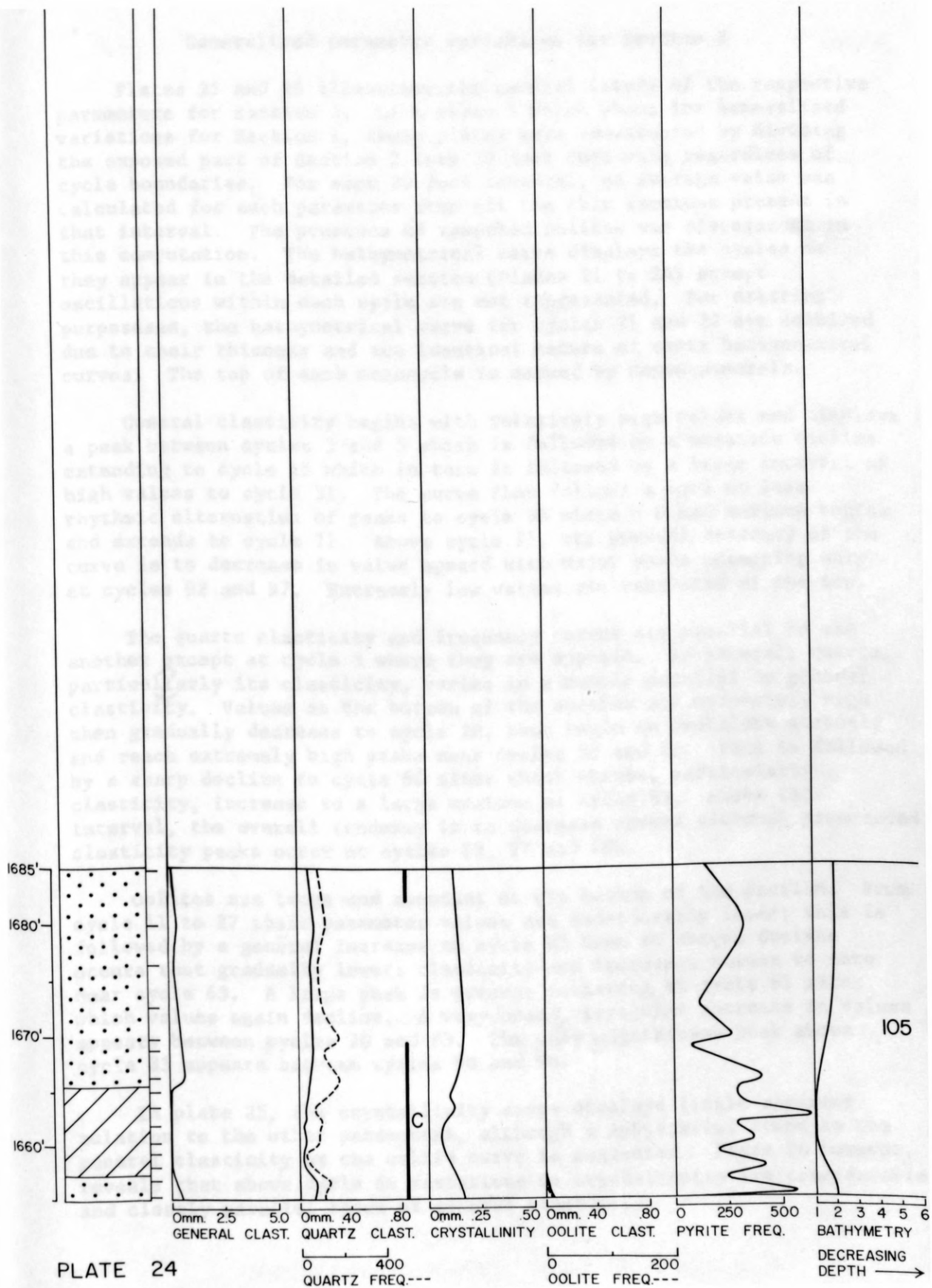
The general clasticity of these cycles displays extremely small variation. The values are zero in the dololutite units and average approximately .50 mm, in the dolarenites. Quartz clasticity also displays extremely small variation and gently oscillates around a value of .10 mm, and frequency gently oscillates around a value of 150. Chert is relatively abundant.

The crystallinity curve bears no relationship to the other curves and oscillates around a value of .20 mm. A single peak of moderate height is present at 1,654 feet. Pyrite exhibits extreme oscillation more or less rhythmically but its pattern is not meaningful.

The bathymetrical curve shows a small range of oscillation indicating very gradually changing conditions.







Generalized parameter variations for Section 2

Plates 25 and 26 illustrate the general trends of the respective parameters for Section 2. Like plate 9 which shows the generalized variations for Section 1, these plates were constructed by dividing the exposed part of Section 2 into 20 foot intervals regardless of cycle boundaries. For each 20 foot interval, an average value was calculated for each parameter from all the thin sections present in that interval. The presence of reworked oolites was disregarded in this computation. The bathymetrical curve displays the cycles as they appear in the detailed section (Plates 11 to 24) except oscillations within each cycle are not represented. For drafting purposes, the bathymetrical curve for cycles 21 and 22 are combined due to their thinness and the identical nature of their bathymetrical curves. The top of each megacycle is marked by Roman numerals.

General clasticity begins with relatively high values and displays a peak between cycles 3 and 5 which is followed by a moderate decline extending to cycle 15 which in turn is followed by a large interval of high values to cycle 31. The curve then follows a more or less rhythmic alternation of peaks to cycle 68 where a broad maximum begins and extends to cycle 71. Above cycle 71, the overall tendency of the curve is to decrease in value upward with major peaks occurring only at cycles 92 and 97. Extremely low values are exhibited at the top.

The quartz clasticity and frequency curves are parallel to one another except at cycle 8 where they are opposed. In general, quartz, particularly its clasticity, varies in a manner parallel to general clasticity. Values at the bottom of the section are moderately high then gradually decrease to cycle 20, then begin to oscillate strongly and reach extremely high peaks near cycles 50 and 62. This is followed by a sharp decline to cycle 66 after which values, particularly clasticity, increase to a large maximum of cycle 85. Above this interval, the overall tendency is to decrease upward although pronounced clasticity peaks occur at cycles 89, 97 and 102.

Oolites are large and abundant at the bottom of the section. From cycle 11 to 27 their parameter values are considerably lower; this is followed by a general increase to cycle 45 then an abrupt decline occurs that gradually lowers clasticity and frequency values to zero near cycle 63. A large peak is present centering at cycle 65 after which values again decline. A very broad, irregular increase in values appears between cycles 70 and 83. The only significant peak above cycle 83 appears between cycles 90 and 94.

In plate 25, the crystallinity curve displays little apparent relation to the other parameters, although a subparallel trend to the general clasticity or the oolite curve is suggested. Plate 26 however, reveals that above cycle 64 variations in crystallinity are considerable and closely parallel those of general clasticity.

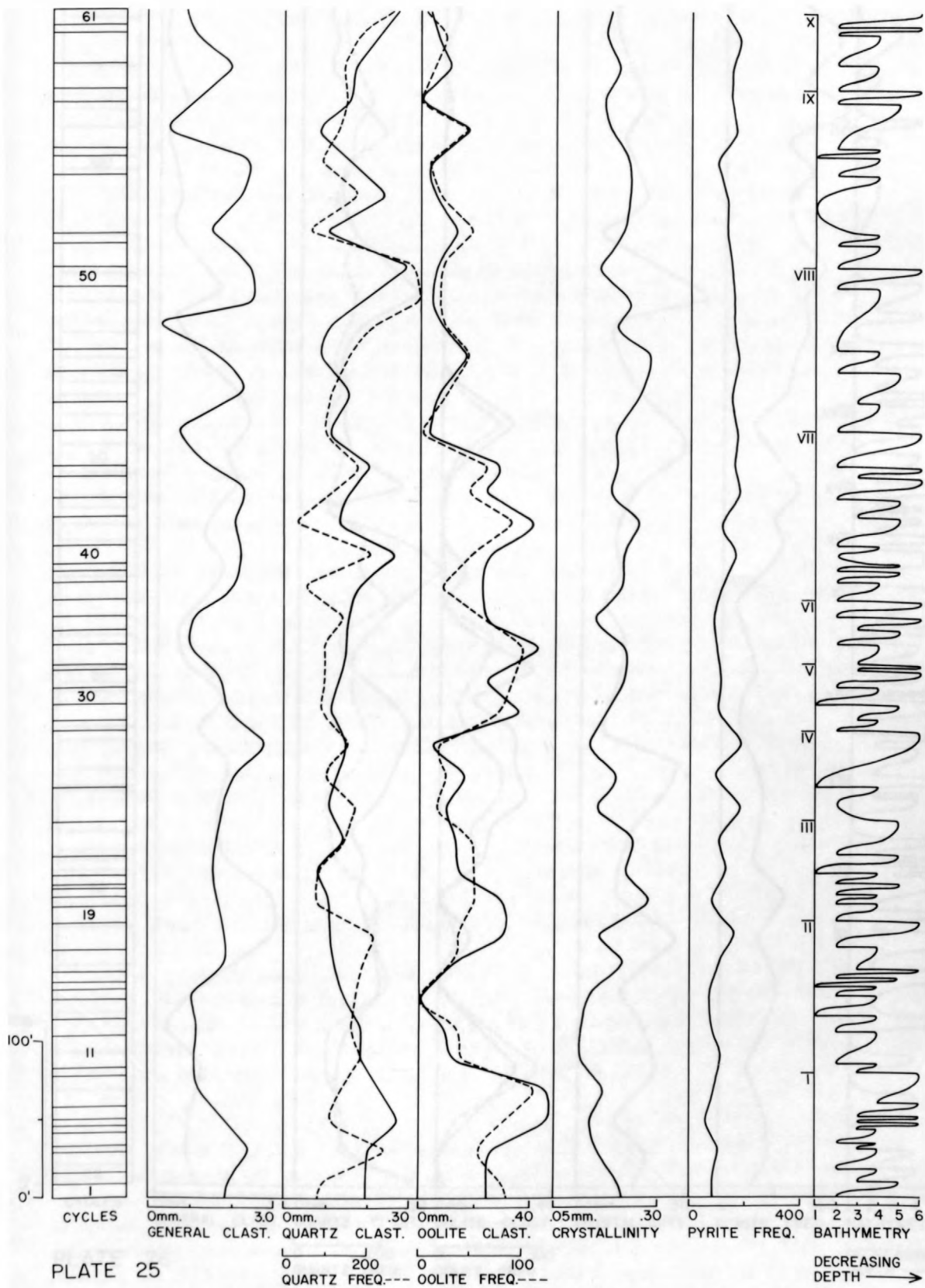


PLATE 25

GENERALIZED PARAMETER VARIATIONS — SECTION 2

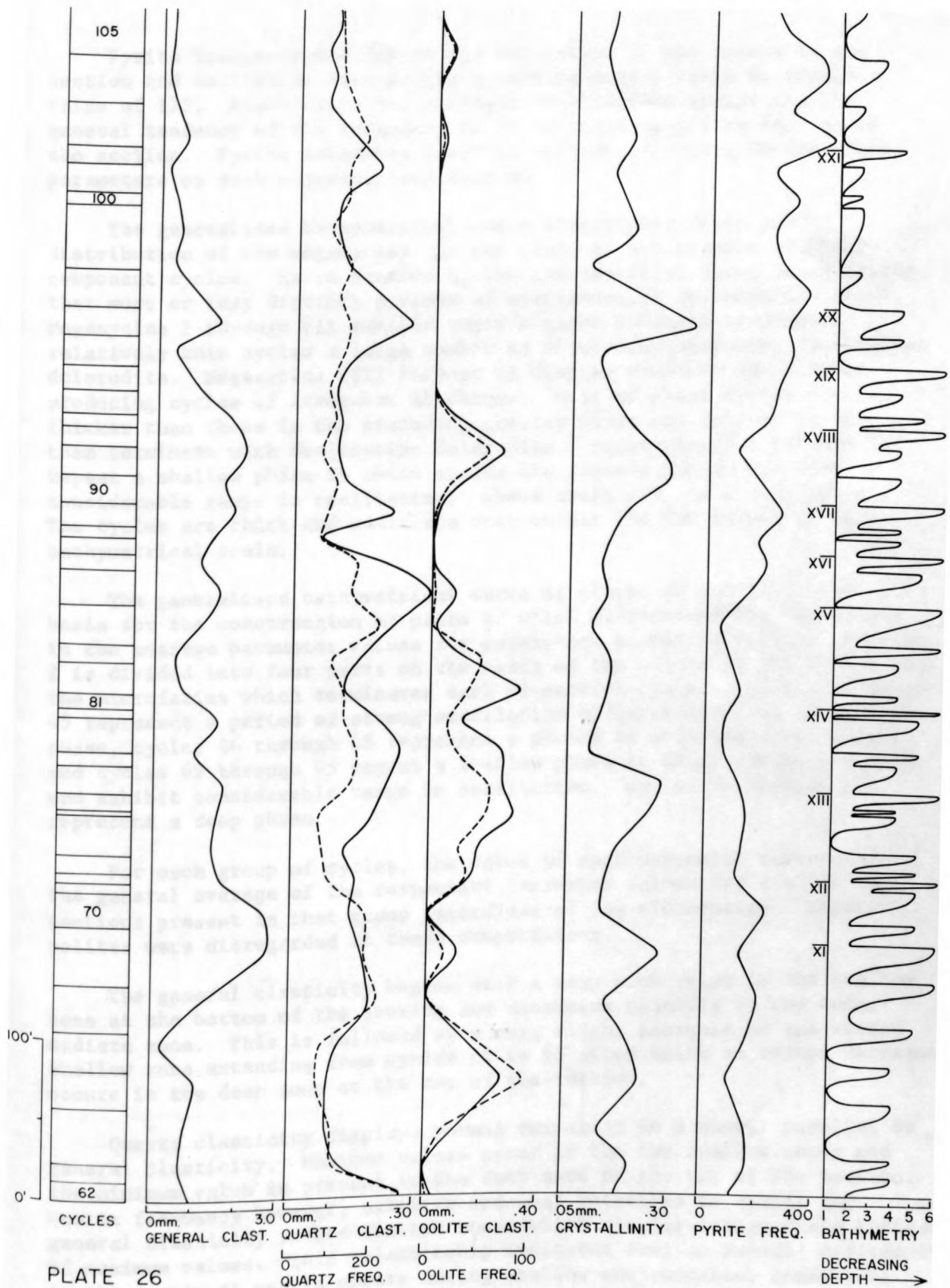


PLATE 26

GENERALIZED PARAMETER VARIATIONS — SECTION 2

Pyrite frequency has relatively low values at the bottom of the section and oscillates very gently to approximately cycle 84 around a value of 175. Above cycle 84, stronger oscillations appear and the general tendency of the frequency is to increase upward to the top of the section. Pyrite frequency bears no apparent relation to the other parameters on such a generalized diagram.

The generalized bathymetrical curve effectively displays the distribution of the megacycles and the range of oscillation of their component cycles. As in Section 1, the bathymetrical curve demonstrates that more or less distinct periods of environmental oscillations exist. Megacycles I through VII exhibit rapid changes in depth to produce relatively thin cycles a large number of which terminate with desiccation dolorudite. Megacycles VIII through XI display moderate oscillation producing cycles of irregular thickness. Most of these cycles are thicker than those in the preceding shallow phase and only a few of them terminate with desiccation dolorudite. Megacycles XII through XIX repeat a shallow phase in which cycles are closely spaced and show considerable range in oscillation. Above cycle XIX, is a deep phase. The cycles are thick and oscillate only within the low values of the bathymetrical scale.

The generalized bathymetrical curve of plates 25 and 26 is the basis for the construction of plate 27 which illustrates the variations in the average parameter values for superposed groups of cycles. Section 2 is divided into four parts on the basis of the nature of the cycles and the microfacies which terminates each respective cycle. Cycles 1 through 45 represent a period of strong oscillation characteristic of a shallow phase, cycles 46 through 68 represent a period of moderate oscillation and cycles 69 through 95 repeat a shallow phase in which cycles are thin and exhibit considerable range in oscillation. Cycles 96 through 105 represent a deep phase.

For each group of cycles, the value of each parameter represents the general average of the respective parameter values for all the thin sections present in that group regardless of the microfacies. Reworked oolites were disregarded in these computations.

The general clasticity begins with a very high value in the shallow zone at the bottom of the section and decreases slightly in the intermediate zone. This is followed by a very slight increase in the second shallow zone extending from cycles 69 to 95 after which an abrupt decrease occurs in the deep zone at the top of the section.

Quartz clasticity displays normal variation in a manner parallel to general clasticity. Maximum values occur in the two shallow zones and the minimum value is present in the deep zone at the top of the section. Quartz frequency however, exhibits abnormal relations to quartz and general clasticity in the shallow zones which display intermediate instead of maximum values. This relationship indicates that an overall deficiency in the supply of quartz occurs during shallow environmental conditions when currents are capable of transporting grains of large size.

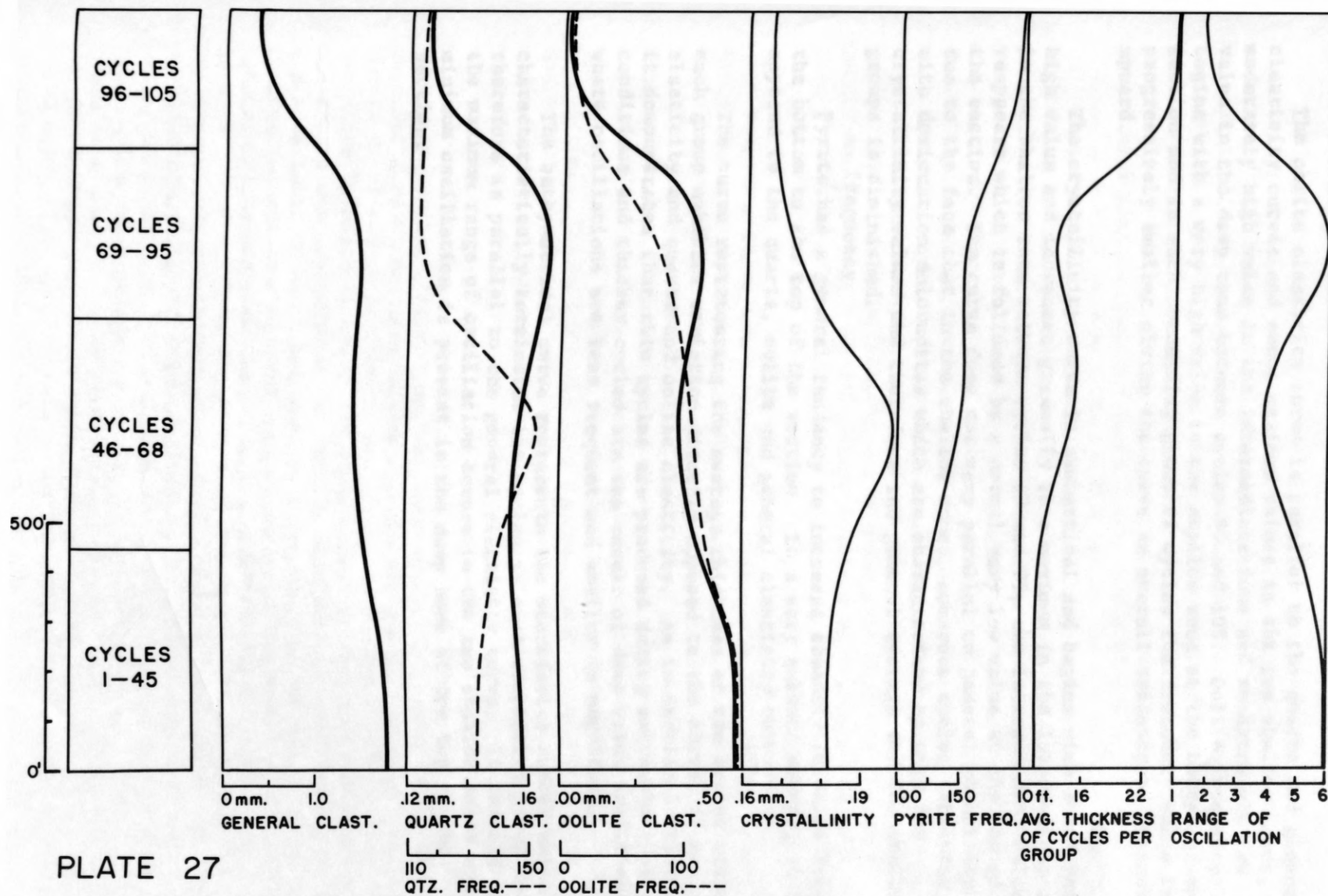


PLATE 27

PARAMETER VARIATIONS FOR GROUPS OF CYCLES — SECTION 2

The oolite clasticity curve is parallel to the quartz and general clasticity curves and shows maximum values in the two shallow zones, a moderately high value in the intermediate zone and an extremely low value in the deep zone between cycles 96 and 105. Oolite frequency begins with a very high value in the shallow zone at the bottom of the section and in each succeeding group of cycles the frequency value is progressively smaller giving the curve an overall tendency to decrease upward.

The crystallinity curve is symmetrical and begins with a moderately high value and increases gradually to a maximum in the intermediate zone. In the shallow zone between cycles 69 and 95, the intermediate value reappears which is followed by a normal very low value at the top of the section. The curve does not vary parallel to general clasticity due to the fact that in the shallow zones, numerous cycles terminate with desiccation dolorudites which are characterized by very low crystallinity values and therefore the general average for the shallower groups is diminished.

frequency

Pyrite has a general tendency to increase steadily in value from the bottom to the top of the section. In a very subdued manner, it is opposed to the quartz, oolite and general clasticity curves.

The curve representing the average thickness of the cycles within each group exhibits variation directly opposed to the curves of general clasticity and quartz and oolite clasticity. As in Section 1 (Plate 10), it demonstrates that thin cycles are produced during extremely shallow conditions and thicker cycles are the result of deep water conditions where oscillations are less frequent and smaller in magnitude.

The bathymetrical curve represents the microfacies number which characteristically terminates the cycles in each respective group and therefore is parallel to the general clasticity curve. It reveals that the maximum range of oscillation occurs in the two shallow zones and minimum oscillation is present in the deep zone at the top of the section.

and in different environments as well (Garrett, 1950, 1958), is still a major unsolved problem and in the present state of our knowledge of the mechanisms of sedimentation can only lead to very tentative interpretations. In one of them, the asymmetrical pattern of the cycles may result from the interplay between continuous subsidence and a variable rate of sedimentation. During part of the time corresponding to a given cycle the rate of sedimentation would be greater than the rate of subsidence, then it would abruptly become smaller for a short interval of time. This could reflect climatic oscillations and the presence of megacycles indicates at least one similar active factor but of different orders of magnitude.

Conclusions

The Upper Cambrian dolomites of eastern Pennsylvania and western New Jersey display great uniformity when inspected megascopically in outcrop. For this reason, considerable difficulty is encountered in field mapping and determining the correct stratigraphic position of isolated exposures which do not display contacts with recognizable sub-jacent or superjacent lithic units.

This investigation represents the first attempt to employ petrographic methods to delineate variations in texture of the carbonate rocks of this area. The statistical treatment of their microscopic components has demonstrated that it is possible to reconstruct, in a detailed manner, the depositional environment of a particular microfacies as well as to delineate changes in the environment through time by the analysis of a succession of superposed microfacies. Repeated series of microfacies, or cycles, are clearly demonstrated and serve as the basis for megacycle subdivision. Also recognizable are large groups of cycles which correspond to rather long periods of distinct oscillation.

The cycles and megacycles described in this investigation appear asymmetrical. Indeed, cycles begin in a relatively deep, quiet environment where structureless dololutite accumulated. This facies is overlain successively by dolarenite, oolitic dolarenite, dolorudite, cryptozoan dolomite and desiccation dolorudite which indicate a slow, gradual shallowing which frequently displays small scale oscillations. Immediately above the shallow facies that terminates each respective cycle is a dololutite that begins a new cycle indicating that the depth increase was so rapid as to eliminate or prevent deposition of intermediate microfacies. This apparently slow decrease in depth followed by a rapid increase does not appear to be an effect of differences in the rate of sedimentation of the microfacies involved because they all belong to the same general very shallow carbonate environment.

The asymmetrical character, which has been observed in many instances and in different environments as well (Carozzi, 1950, 1958), is still a major unsolved problem and in the present state of our knowledge of the mechanisms of sedimentation can only lead to very tentative interpretations. In one of them, the asymmetrical pattern of the cycles may result from the interference between continuous subsidence and a variable rate of sedimentation. During most of the time corresponding to a given cycle the rate of sedimentation would be greater than the rate of subsidence, then it would abruptly become smaller for a short interval of time. This could reflect climatic oscillations and the presence of megacycles indicates at least two similar active factors but of different orders of magnitude.

In a second hypothesis, the asymmetrical pattern may result from the interference of a uniform rate of sedimentation with intermittent subsidence. During the period of stability or of very slow subsidence corresponding to most of the time expressed by a given cycle, sedimentary upbuilding would create a gradual shallowing. During the paroxysm of subsidence the rate of the latter would be greater than sedimentation generating rapid increase in relative depth which would abruptly begin a new cycle. Again the presence of megacycles of similar pattern indicate that several tectonic factors are involved.

The two investigated sections do not overlap stratigraphically and therefore correlation could not be attempted. Although correlation on the basis of individual cycles is probably limited to short distances, the megacycles and major groups of cycles could provide a valuable means of correlation for further work in this general area.

- Deformation of molluscs and pseudomolluscs: *Jour. Sed. Petrology*, v. 5, (in press).
- and Zaslavsky, P. K., 1939, Microfacies of the Mahesh Sand, Mahesh, Indiana: *Jour. Sed. Petrology*, v. 29, p. 144-174.
- Gray, C., Geyer, A. R., and McLaughlin, D. R., 1958, Richland Quadrangle, Geologic Atlas of Pennsylvania, no. 160: Pennsylvania Geol. Survey, 4th ser.
- Hobson, J. F., 1957, Stratigraphy of the northern belt of the Beekmantown group in southeastern Pennsylvania: Pennsylvania State Univ., Ph. D. Thesis (unpublished), 510 p.
- 1957, Lower Ordovician (Beekmantown) succession in Berks County, Pennsylvania: *Am. Association Petroleum Geologists Bull.*, v. 41, p. 2710-2722.
- Howell, B. P., Roberts, Henry, Willard, Bradford, 1950, Subdivision and dating of the Cambrian of eastern Pennsylvania: *Geol. Soc. America Bull.*, v. 61, p. 1355-1368.
- Kimmel, H. B., 1900, Annual Report of the State Geologist: New Jersey Geol. Survey, 1901, 231 p.
- and Waller, Stuart, 1901, Paleozoic limestones of Ricketts Valley, New Jersey: *Geol. Soc. America Bull.*, v. 12, p. 149.
- and Waller, Stuart, 1902, Annual Report of the State Geologist: New Jersey Geol. Survey, 1901, 178 p.
- Osley, J. R., 1883, Geology of Lehigh and Northampton Counties, Pennsylvania: *Second Geol. Survey Report 25*, v. 1, 283 p.

Bibliography

- Bromery, R. W., 1959, Interpretation of aeromagnetic data across the Reading Prong, Pennsylvania: *Geol. Soc. America Bull.*, v. 70, p. 1574-1575.
- Carozzi, A. V., 1950, Contribution à l'étude des rythms de sédimentation: *Archives Sci. [Geneva]*, v. 3, nos. 1 and 2, 75 p.
- _____, 1958, Micromechanisms of sedimentation in the epicontinental environment: *Jour. Sed. Petrology*, v. 28, p. 133-150.
- _____, 1960, Microscopic sedimentary petrography: New York, John Wiley and Sons, 485 p.
- _____, Deformation of oolites and pseudoolites: *Jour. Sed. Petrology*, v. 3, (in press).
- _____, and Zadnik, V. E., 1959, Microfacies of the Wabash Reef, Wabash, Indiana: *Jour. Sed. Petrology*, v. 29, p. 164-171.
- Gray, C., Geyer, A. R., and McLaughlin, D. B., 1958, Richland Quadrangle, *Geologic Atlas of Pennsylvania*, no. 16D: Pennsylvania Geol. Survey, 4th ser.
- Hobson, J. P., 1957, Stratigraphy of the northern belt of the Beekmantown group in southeastern Pennsylvania: Pennsylvania State Univ., Ph. D. Thesis (unpublished), 510 p.
- _____, 1957, Lower Ordovician (Beekmantown) succession in Berks County, Pennsylvania: *Am. Association Petroleum Geologists Bull.*, v. 41, p. 2710-2722.
- Howell, B. F., Roberts, Henry, Willard, Bradford, 1950, Subdivision and dating of the Cambrian of eastern Pennsylvania: *Geol. Soc. America Bull.*, v. 61, p. 1355-1368.
- Kummel, H. B., 1900, Annual Report of the State Geologist: New Jersey Geol. Survey, 1901, 231 p.
- _____, and Weller, Stuart, 1901, Paleozoic limestones of Kittatiny Valley, New Jersey: *Geol. Soc. America Bull.*, v. 12, p. 149.
- _____, and Weller, Stuart, 1902, Annual Report of the State Geologist: New Jersey Geol. Survey, 1901, 178 p.
- Lesley, J. P., 1883, Geology of Lehigh and Northampton Counties, Pennsylvania: Second Geol. Survey Report D3, v. 1, 283 p.

- Miller, B. L., 1934, Limestones of Pennsylvania: Pennsylvania Topog. and Geol. Survey Bull. M20, 729 p.
- Willard, R. 1939, Northampton County, Pennsylvania: Pennsylvania Geol. Survey Bull. C48, 4th ser., 496 p.
- Wolfe, J. B. 1941, Lehigh County, Pennsylvania: Pennsylvania Geol. Survey Bull. C39, 492 p.
- Miller, R. L., 1937, Stratigraphy of the Jacksonburg limestone: Geol. Soc. America Bull., v. 48, p. 1687-1718.
- Nason, F. L., 1890, The Post-Archean Age of the White limestone of Sussex County, New Jersey: New Jersey Geol. Survey Ann. Rept. of 1891, p. 31-98.
- Prime, F., Jr., 1883, Geology of Lehigh and Northampton Counties, Pennsylvania: Second Geol. Survey progress report D3, v. 1, p. 161-214.
- Prouty, C. E., 1959, The Annville, Myerstown, and Hershey formations of Pennsylvania: Pennsylvania Geol. Survey Bull. G30, 4th ser.
- Rodgers, H. D., 1836, First Annual Report of the State Geologist, Pennsylvania.
- _____ 1840, Final Report on the Geology of New Jersey, Philadelphia.
- _____ 1858, Geology of Pennsylvania, v. 1, 586 p.
- Shrock, R. R., 1948, Sequence in layered rocks: New York, McGraw-Hill Book Co., 507 p.
- Stose, G. W., 1908, The Cambro-Ordovician limestones of the Appalachian Valley in southern Pennsylvania: Jour. Geology, v. 16, p. 698-714.
- _____ 1909, Description of the Mercersburg-Chambersburg District: U. S. Geol. Survey Geol. Atlas, Folio 170.
- Tennant, C. B., and Berger, R. W., 1957, X-Ray determination of dolomite-calcite ratio of a carbonate rock: Am. Mineralogist, p. 23-30.
- Walker, T. R., 1957, Frosting of quartz grains by carbonate replacement: Geol. Soc. America Bull., v. 68, p. 267-268.
- Wherry, E. T., 1909, The early Paleozoics of the Lehigh River District, Pennsylvania: Science, v. 30, n.s., p. 416.

1915, A peculiar oolite from Bethlehem, Pennsylvania:
U. S. Nat. Mus. Proc., v. 49, p. 153-156.

Willard, Bradford, 1955, Cambrian contacts in eastern Pennsylvania:
Geol. Soc. America Bull., v. 66, p. 819-834.

Wolff, J. E., and Brooks, A. H., 1898, Age of the Franklin White
the limestone of Sussex County, New Jersey: U. S. Geol. Survey,
18th Ann. Rept., p. 425-457.

Color on both fresh and weathered surfaces herein presented
according to the Rock Color Chart distributed by the G. S. A. The
lithology of each measured unit is dolomite unless otherwise indicated.

Unit	Thickness (feet)
1 Medium gray to light gray mottled with olive gray; medium bedded; silt and clay laminations weathering in ribs; bedding fractured and contorted; shear fractures nearly horizontal. Bedding: N. 82° E., 65° SE.	3.0
2 Light-medium gray, fine grained; severely sheared contorted; silt laminations and sericitic partings.	4.1
3 Medium-dark gray, fine grained dolarenite; massive; limonitic and sericitic partings; weathers pitted.	4.2
4 Interbedded dark-medium gray dolomite, medium gray oolitic dolarenite and dolarenite; lithic fragments deformed with long axes parallel to fracture cleavage; thin to medium bedded; dolomite poorly laminated. Bedding: N. 80° E., vertical.	8.9
5 Dark gray, very fine grained; slightly calcareous dolomite.	2.3
6 Coarsened	17.9
7 Dark-medium gray, medium grained; severely fractured; thin wavy bands of white dolomite.	4.8
8 Olive gray, fine grained dolomite and oolitic dolarenite; medium bedded; limonitic and sericitic partings; severely sheared.	3.5

Appendix

Description of the Stratigraphic Sections

Section 1

Section 1 is located on the east side of the Delaware River along the Pennsylvania Railroad and Carpentersville Road in the north central part of the Riegelsville, Pennsylvania, quadrangle. The section begins approximately 0.26 mile north of the bridge crossing the Delaware River at Riegelsville, New Jersey. Traverse begins 87 feet N. 60° E. of the northeast corner of the Riegel Paper Corporation warehouse along the driveway to an abandoned quarry now used as a garbage dump, and extends stratigraphically upward in overturned strata. Overturning is indicated by Cryptozoons convex-downward, nearly horizontal fracture cleavage in steeply dipping strata and inverted sequence of graded bedding.

Color on both fresh and weathered surfaces herein presented is according to the Rock Color Chart distributed by the G. S. A. The lithology of each measured unit is dolomite unless otherwise indicated.

Unit		Unit Thick- ness (feet)	Cumu- lative Thick- ness (feet)
1	Medium gray to light gray mottled with olive gray; medium bedded; silt and clay laminations weathering in ribs; bedding flexured and contorted; shear fractures nearly horizontal. Bedding: N. 82° E., 65° SE.	3.0	3.0
2	Light-medium gray, fine grained; severely sheared contorted; silt laminations and sericite partings.	4.1	7.1
3	Medium-dark gray, fine grained dolarenite; massive; limonitic and sericitic partings; weathers pitted.	4.2	11.3
4	Interbedded dark-medium gray dolomite, medium gray oolitic dolarenite and dolorudite; lithic fragments deformed with long axes parallel to fracture cleavage; thin to medium bedded; dolomite poorly laminated. Bedding: N. 80° E., vertical.	8.0	19.3
5	Dark gray, very fine grained; slightly calcareous dolomite.	2.5	21.8
6	Concealed	17.9	39.7
7	Dark-medium gray, medium grained; severely fractured; thin wavy bands of white dolomite.	4.0	43.7
8	Olive gray, fine grained dolomite and oolitic dolarenite; medium bedded; limonitic and sericitic partings; severely sheared.	3.5	47.2

9	Olive gray, fine grained; thin bedded; sericitic partings.	1.0	48.2
10	Thinly interbedded dark and light gray dolomite; thin to platy bedded; sericitic and shaly partings; cleavage horizontal. Bedding: N. 85° E., vertical.	2.0	50.2
11	Oolitic dolarenite cut by horizontal gash veins of white coarsely crystalline dolomite and milky quartz.	3.5	53.7
12	Cryptozoan dolomite; <u>Archaeozoon undulatum</u> .	0.7	54.4
13	Medium to olive gray desiccation dolorudite; fragments tabular or convexly lenticular indicating derivation from cryptozoan dolomite.	0.4	54.8
14	Dark-medium gray, medium grained arenaceous dolomite; white dolomite and quartz coats joint surfaces.	1.9	56.7
15	Thinly interbedded oolitic dolarenite and dark gray, fine grained dolomite; thick sericitic partings; unit sheared and flexured.	1.0	57.7
16	Concealed.	2.4	60.1
17	Medium gray cryptozoan dolomite; <u>Cryptozoon fieldii</u> ; weathers light gray; thin bedded; bedding; E-W 75° S.	1.6	61.7
18	Concealed.	0.6	62.3
19	Medium gray to olive gray; extremely sheared; limonite on bedding and cleavage surfaces.	1.8	64.1
20	Olive gray, weathering to chalky light gray; very fine grained; laminated; limonitic stains; sericitic partings; bottom one foot shaly and slightly calcareous.	4.8	68.9
21	Mottled medium gray and grayish red; fine grained; poorly laminated; limonitic; thin discontinuous soft silty bands; bedding flexured.	2.5	71.4
22	Light-medium gray, very fine grained; limonitic partings weather to ribs; poorly bedded; flexured and sheared.	2.4	73.8
23	Cryptozoan dolomite; <u>Archaeozoon undulatum</u> .	0.3	74.1
24	Like unit 22.	4.2	78.3
25	Dark gray oolitic dolarenite; oolites poorly distinguishable and slightly deformed tectonically.	2.7	81.0
26	Cryptozoan dolomite; <u>Archaeozoon undulatum</u> (?); appears argillaceous; veins and patches of white dolomite.	1.6	82.6
27	Yellowish brown, soft, porous, limonitic, silty dolomite; veins of white quartz; unit severely crumpled and sheared.	1.2	83.6
28	Dark gray, fine grained; laminated with limonitic partings; weathers spheroidal; pitted.	4.3	88.1
29	Like unit 28; laminations contorted; thin bedded. Separated from unit 28 by bedding plane fault.	3.5	91.6

30	Dark gray oolitic dolarenite; thin to medium bedded; appears argillaceous; stylolitic partings of limonite.	2.4	94.0
31	Medium gray mottled with light gray; fine grained; laminated.	5.1	99.1
32	Dark gray, very fine grained; weathers light gray thin to medium bedded; lenses of light-medium gray oolitic dolarenite appear on weathered surface.	2.6	101.7
33	Medium to olive gray oolitic dolarenite; weathers to medium-dark gray; locally ruditic textured displayed; medium bedded; limonite coats bedding and fractures.	2.5	104.2
34	Medium to olive gray, very fine grained; thin bedded; beds flexured.	4.0	108.2
35	Like unit 33.	1.0	109.2
36	Dark gray cryptozoan dolomite; <u>Archaeozoon undulatum</u> ; weathers light gray; thinly laminated; thin to platy bedded.	1.4	110.6
37	Dark-medium gray arenaceous desiccation dolorudite; weathers to light gray; limonitic and sericitic partings; pitted.	0.8	111.4
38	Medium gray; silty; slightly calcareous dolomite; shaly to platy bedded. (Bedding plane fault).	0.3	111.7
39	Like unit 37. Some silt and clay present; slightly calcareous; rounded lithic fragments weather in positive relief.	1.8	113.5
40	Thinly interbedded olive gray and tan fine grained dolomite; weathers chalky light gray; scattered lithic fragments; limonite stains on fractures.	2.9	116.4
41	Olive to dark-medium gray; dense; pyrite cubes; limonite pseudomorphs.	0.9	117.3
42	Like unit 40; with scattered oolites and quartz grains. Bedding: N. 88° W. 48° S.	3.3	120.6
43	Light-olive gray, very fine grained; weathers light chalky gray; well laminated; thick limonite stains on joints; top part conglomeratic.	6.0	126.6
44	Mottled medium gray and olive gray, medium grained; fresh surface slightly reddish; weathers earthy, soft and pitted; limonite fills cavities and coats fractures; laced with small veins of white dolomite.	1.8	128.4
45	Cryptozoan dolomite; <u>Cryptozoon fieldii</u> ; poorly bedded; limonite fills cavities; pitted.	1.2	129.6
46	Medium gray, medium grained; upper contact disconformable (?); slickensides; limonite filled cavities; poorly bedded.	2.4	132.0
47	Desiccation dolorudite; fragments thinly laminated, angular and convexly lenticular indicating derivation from cryptozoan dolomite.	1.0	133.0

48	Light-medium gray to light-olive gray, fine grained; weathers light-yellowish gray; scattered oolites(?); limonite; sericitic partings; massive.	4.0	137.0
49	Medium to dark-medium gray mottled with olive gray oolitic dolarenite; limonite partings and cavity fillings; veins of white dolomite.	4.2	141.2
50.	Like unit 48.	3.5	144.7
51	Medium gray, fine grained dolomite; thin to medium bedded; thin crisscrossing veins of white dolomite.	1.2	145.9
52	Like unit 48.	3.5	149.4
53	Interbedded medium gray oolitic dolarenite and fine grained dolomite; oolites vaguely distinguishable; medium bedded; weathers alternately medium and dark gray.	2.3	151.7
54	Olive gray, very fine grained; weathers light chalky gray; laminated; massive.	1.7	153.4
55	Slightly calcareous dolomite; extremely sheared; shaly bedded; bedding plane fault zone.	0.2	153.6
56	Grayish red, fine to medium grained oolitic dolarenite; limonite stains on fractures; thin bedded.	1.4	155.0
57	Like unit 54; thin bedded.	1.6	156.6
58	Like unit 55.	0.5	157.1
59	Medium to dark-medium gray, medium grained; scattered oolites(?); veins of white dolomite and milky quartz.	1.2	158.3
60	Olive gray, fine grained; thinly laminated; laminations in positive relief and slightly displaced by sericitic and limonitic partings..	0.8	159.1
61	Medium gray oolitic dolarenite; interbedded with medium gray, medium grained dolomite; thin to platy bedded.	3.5	162.6
62	Olive gray, very fine grained; conchoidal fracture; dense; massive; limonite stains; sericitic partings weaker in negative relief.	2.6	165.2
63	Dark gray, medium grained dolomite displaying oolites on weathered surface; limonite stains; thin bedded.	2.0	167.2
64	Light-olive gray, very fine grained; laminations broken by thick sericitic partings; limonite stains; thin bedded.	3.1	170.3
65	Grayish red oolitic dolarenite; white dolomite veins; limonite stains; thin bedded.	0.9	171.2
66	Mottled olive gray and medium gray, fine to medium grained; limonite filled cavities and sericitic partings.	2.3	173.5
67	Light-olive gray to olive gray oolitic dolarenite; oolites occur as discontinuous lenses; medium bedded; limonite filled cavities.	2.2	175.7
68	Olive gray, very fine grained; scattered small oolites(?); severely sheared.	1.4	177.1

69	Light-medium gray, fine grained; weathers light gray; sheared and fractured.	1.7	178.8
70	Thinly interbedded olive, medium, and reddish gray dolomite; limonite and sericite coats bedding surfaces. (This unit forms north wall of garbage dump quarry.)	1.4	180.2
71	Like unit 70; veins of white dolomite.	2.1	182.3
72	Light-medium gray oolitic dolarenite; oolites dark gray.	0.3	182.6
73	Olive gray, fine grained cryptozoan dolomite; thin bedded.	0.2	182.8
74	Desiccation dolorudite composed of cryptozoan fragments; silty; scattered oolites. Disconformable to unit 75.	0.7	183.5
75	Dark-medium gray oolitic dolarenite; limonitic stylolites; numerous thin veins of white dolomite.	1.3	184.8
76	Light-olive gray, fine grained cryptozoan dolomite; <u>Cryptozoon fieldii</u> and other types(?) discernable; weathers chalky light gray; laminae of stromatolites distorted and fragmented at top.	1.0	185.8
77	Medium gray, medium grained; vaguely oolitic; abundant large veins of white dolomite and milky quartz.	2.2	188.0
78	Medium gray to olive gray, fine grained; limonitic stains; massive but showing considerable fracturing.	2.7	190.7
79	Medium gray to olive gray, very fine grained; numerous small veins of tan dolomite (limonitic stained) weathering in positive relief. Bedding: N. 84° E., 40° SE.	2.7	193.4
80	Reddish gray to olive gray desiccation dolorudite; fragments elongated or tabular; laminated; scattered quartz grains; limonitic and sericitic partings abundant.	0.3	193.7
81	Medium to dark gray, fine grained dolomite having breccia appearance on weathered surface; limonitic cavity fillings; thin veins of white dolomite; thin to medium bedded.	4.4	198.1
82	Olive gray, very fine grained; like unit 79, massive; pitted.	3.0	201.1
83	Medium gray oolitic dolarenite.	1.2	202.3
84	Light-medium gray, fine grained cryptozoan dolomite; <u>Archaeozoon undulatum</u> ; weathers chalky white to light gray, somewhat pitted; limonite stains, veins of white dolomite.	1.1	203.4
85	Like unit 83.	0.9	204.3
86	Like unit 84; <u>Archaeozoon undulatum</u> .	0.7	205.0

87	Desiccation dolorudite composed of subrounded, laminated dolomite fragments 1/4 to 2 inches long interbedded with lenses of poorly laminated fine grained dolomite and oolitic dolarenite; quartz grains abundant.	0.7	205.7
88	Medium gray oolitic dolarenite.	0.1	205.8
89	Cryptozoan dolomite; <u>Anomalophycus compactus</u> ; individual colonies appear as fingers or tubes 3/8 to 1/2 inch in diameter, 2 to 4 inches high. Base of individual digitate colonies flare out and become joined.	1.1	206.9
90	Shaly, sheared dolomite interbedded with desiccation dolorudite; slightly calcareous; breccia has thin lenses of reddish feldspathic sandstone; thin bedded; discontinuous bands of dark gray chert; scattered quartz grains and oolites.	4.0	210.9
91	Medium gray oolitic dolarenite; thin veins of limonitic stained dolomite.	0.9	211.8
92	Cryptozoan dolomite; <u>Archaeozoon undulatum</u> .	0.6	212.4
93	Desiccation dolorudite; arenaceous; grading upward to oolitic dolarenite.	1.0	213.4
94	Light-olive gray, very fine grained; weathers light gray; sub-conchoidal fracture; massive. Unit contains several large unidentified cryptozoan colonies measuring two feet across, and thinly laminated from bottom to top. (Similar to cryptozoan colonies of unit 317 of Section 2.)	6.6	220.0
95	Shaly bedded dolomite with abundant limonitic laminations; shear zone.	0.8	220.8
96	Interbedded light gray to reddish gray dolomitic sandstone and arenaceous dolomite; scattered tabular dolomite fragments up to 2 inches long.	1.5	222.3
97	Medium to dark-medium gray, medium grained, vaguely oolitic dolarenite; medium bedded; gash veins of white dolomite.	3.7	226.0
98	Light-olive gray, very fine grained; massive.	3.0	229.0
99	Medium gray, medium grained; scattered oolites visible on weathered surface; stylolitic partings of silt; large quartz crystals coat joint surfaces; medium bedded.	6.9	235.9
100	Light-olive gray, very fine grained cryptozoan dolomite; <u>Cryptozoon fieldii</u> ; unit discontinuous and thickens and thins rapidly.	0.5	236.4
102	Light-medium to light-olive gray, fine grained weathers light gray; white dolomite and quartz crystals on joints; massive.	8.2	246.2
101	Medium gray oolitic dolarenite; medium bedded.	1.6	238.0
103	Concealed (Traverse continued 39 feet N. 20° W + 29° from bottom of unit 102)	1.6	247.8

104	Like unit 102.	2.3	250.1
105	Concealed. (Traverse continued: (1) 139 feet S. 70° W -23°, (2) 50 feet N. 48° E. +20°. Section continues in Pennsylvania Railroad cut.)	0.4	250.5
106	Medium gray, medium grained; large veins of white dolomite and milky quartz; limonitic stains on fractures; vaguely oolitic.	1.7	252.2
107	Light-medium gray, fine grained; silty laminations weather in positive relief; thin to platy bedded.	2.2	254.4
108	Dark-medium gray, fine to medium grained; white dolomite and quartz on joints; poorly exposed.	3.6	258.0
109	Light gray, fine grained; limonitic and sericitic partings; large vugs of light blue quartz; massive.	4.2	262.2
110	Dark-medium gray, fine grained; locally calcareous; extremely sheared; shaly bedded.	1.8	264.0
111	Olive gray, fine grained; limonite stains; ribs of concentrated quartz grains parallel to bedding.	2.8	266.8
112	Dark-yellowish orange, slightly calcareous shale; abundant limonite and shiny sericite; soft and porous; sheared.	3.4	270.2
113	Medium gray, very fine grained; sericitic slip surfaces; small vugs of white quartz; thin bedded.	1.7	271.9
114	Like unit 113; arenaceous; limonitic.	3.2	275.1
115	Medium gray, fine grained; scattered quartz; limonitic; sericitic surfaces abundant; shaly to platy bedded; sheared; poorly exposed.	8.2	283.3
116	Light-medium gray to light-olive gray, fine grained; dense; conchoidal fracture; some stylolitic partings of limonite.	4.0	287.3
117	Cryptozoan dolomite; <u>Anomalophycus compactus</u> ; large nodules of dark gray chert.	0.9	288.2
118	Medium to olive gray; abundant sericitic partings; quartz grains scattered and concentrated in 1/2 inch bands.	1.5	289.7
119	Light-olive gray, very fine grained; weathers light gray; some scattered quartz; conchoidal fracture; thin bedded; sheared. Unit disconformable with unit 120.	6.5	296.2
120	Cryptozoan dolomite; <u>Archaeozoon undulatum</u> (?). Unit grades upward to desiccation dolorudite with tabular fragments up to 2 inches long; irregular masses of dark red limonite.	1.3	297.5
121	Medium gray to olive gray, fine grained; white quartz crystals coat joints and fill pockets; massive.	5.3	302.8
122	Dark-medium gray, fine grained; laminated; vugs of light gray quartz; appears argillaceous; medium bedded.	4.2	307.0

123	Light-medium gray, fine grained; irregular partings of limonite weathering in positive relief; massive.	5.4	312.4
124	Reddish gray silty and arenaceous dolomite; weathers soft with dark limonite stains; shaly bedded.	1.2	313.6
125	Light-medium gray, fine grained; irregular patches of white quartz; one discontinuous band of dark gray chert about 1 inch thick; scattered quartz grains; medium bedded becoming platy at top.	4.0	317.6
126	Light gray weathering yellowish gray; slightly calcareous; sericitic; scattered quartz grains; sheared.	2.4	320.0
127	Interbedded dark-medium gray, fine grained dolomite medium gray, medium grained dolomite; the latter contains abundant lenses of dark gray chert; weathered surface shows lithic fragments.	2.4	322.4
128	Dark-medium gray, very fine grained; weathers orange-brown; conchoidal fracture; sheared. This zone shows evidence of bedding plane displacement.	2.5	324.9
129	Medium gray, fine grained dolorudite; fragments subrounded and composed of fine grained dolomite; matrix arenaceous; limonitic; white quartz in irregular patches and on joints.	13.4	338.3
130	Slightly calcareous, shaly to platy bedded dolomite; limonitic; sheared; thin zones are shattered to form fault breccia.	7.7	346.0
131	Medium gray, fine grained; weathered surface laminated; abundant sericitic and limonitic partings; nodules and lenses of dark gray chert.	3.9	349.9
132	Medium gray, fine to medium grained dolomite; stylolitic limonitic partings; transparent quartz coats joints; sericite on bedding surfaces.	7.0	356.9
133	Medium gray, fine grained dolomite interbedded with oolitic dolarenite, oolite zones are lenticular and are crossed by large veins of white dolomite; limonite and sericite; quartz heavily coats joints; massive.	11.3	368.2
134	Medium gray, fine grained; weathers light medium gray; nodules and lenses of chert; thin arenaceous bands; thin bedded.	11.0	379.2
135	Concealed. (Traverse continued: (1) 22 feet west, along strike, (2) 63 feet N 10° E., horizontal.)	41.5	420.7
136	Medium gray, fine grained; limonitic partings; sheared; thin bedded; poorly exposed.	6.5	427.0
137	Concealed. (Traverse continued 26.3 feet N. 35° E. +28°)	4.3	431.3

138	Medium to olive gray, fine grained; slightly calcareous; extremely sheared resulting in thin to shaly bedding; abundant sericitic partings; limonite on joints and fractures.	25.2	456.5
139	Dark-medium gray oolitic dolarenite; abundant irregular veins of white quartz and dolomite.	0.5	457.0
140	Medium gray, fine grained; limonitic and sericitic partings; sheared; platy to shaly bedded; thin zone of fault breccia near top.	4.2	461.2
141	Dark-medium gray to olive gray, very fine grained; weathers light gray; conchoidal fracture; massive.	2.1	463.3
142	Fault zone containing irregular patches coarsely crystalline quartz in contorted, shaly dolomite.	0.3	463.6
143	Dark gray, medium grained; limonitic; arenaceous; vaguely oolitic; irregular nodules of chert.	1.7	465.3
144	Dark gray oolitic dolarenite; massive; irregular veins of white quartz and dolomite.	3.1	468.4
145	Medium gray, very fine grained; weathers light gray; thin bedded; strong development of cleavage.	2.2	470.6
146	Interbedded dark-medium gray oolitic dolarenite and olive gray fine grained dolomite. Limonite-filled cavities; stringers of dark gray oolitic chert.	1.2	471.8
147	Interbedded oolitic dolarenite and light medium gray, medium grained dolomite. Oolitic portions arenaceous; limonitic.	6.0	477.8
148	Light-medium gray, medium grained dolomite; weathers light yellowish gray; thin bedded; sheared.	5.4	483.2
149	Medium gray oolitic dolarenite with breccia fragments; massive.	1.4	484.6
150	Shaly to platy bedded dolomite; beds crumpled; bedding surfaces show black carbonaceous streaks; limonitic.	3.6	488.2
151	Medium gray, fine grained; vugs of light blue quartz; massive.	2.4	490.6
152	Light-medium gray; weathers light-yellow gray; weathered surface locally displays fault breccia appearance; limonitic and sericitic; thin bedded; sheared.	1.6	492.2
153	Medium gray, fine grained; lenses of oolitic dolarenite; graded bedding; thin to medium bedded.	4.5	496.7
154	Medium gray, fine grained; sericitic; arenaceous; beds flexured; lenses of fault breccia.	6.0	502.7
155	Medium gray, fine grained; poorly laminated; irregular, braided limonitic partings in positive relief; vugs of light blue quartz.	2.7	505.4
156	Light-medium gray, fine grained; slightly calcareous; sericitic surfaces; veins of light blue quartz.	8.0	513.4
157	Medium gray to olive gray, fine grained; numerous limonite-filled cavities; small nodules of dark gray chert; clear to white quartz on joint surfaces; massive.	3.1	516.5

Section 2

Section 2 is located along the east side of the Delaware River along the Pennsylvania Railroad and Carpentersville Road in the south central part of the Easton, Pennsylvania, quadrangle. The section begins approximately 0.23 mile south of the crossroads at Carpentersville, New Jersey. Traverse begins 90 feet north of the north wall of a large abandoned quarry and extends stratigraphically downward.

Beds in the north end of the section strike N. 65° E., and dip 68° SE and in the south end of the section strike N. 60° E. and dip 67° SE and are overturned. Overturning is indicated by Cryptozoons convex downward, dip of the fracture cleavage is less than the dip of the strata, orientation of "half-moon" oolites, and inverted sequence of graded bedding.

Color on both fresh and weathered surfaces herein presented is according to the Rock Color Chart distributed by the G. S. A. The lithology is dolomite unless otherwise indicated.

Unit		Unit Thick- ness (feet)	Cumu- lative Thick- ness (feet)
1	Light-olive gray to medium gray, fine to medium grained calcareous dolomite; laminated; shaly partings; massive.	8.3	1685.8
2	Like unit 1; medium bedded.	8.2	1677.5
3	Light-medium gray, medium grained calcareous dolomite; massive to platy bedded.	1.5	1669.3
4	Medium to dark gray, medium grained calcareous dolomite; poorly laminated; massive; large nodular masses of dark gray chert.	2.6	1667.8
5	Light-medium gray calcareous dolomite; laminated; massive to platy bedded; lenses of chert.	3.7	1665.2
6	Light gray interbedded with dark gray; massive to platy bedded.	4.0	1661.5
7	Light gray, very fine grained calcareous dolomite; poorly bedded; small lenses of chert.	3.0	1657.5
8	Light-olive gray, fine grained; arenaceous(?); small veinlets of white calcite and dolomite; two irregular chert beds.	3.2	1654.5
9	Light to medium gray, fine grained; finely laminated; platy bedded; lenses and discontinuous bands of chert.	4.0	1651.3
10	Medium gray, fine grained; well laminated; sericitic partings; platy to shaly bedded; lenses of chert.	4.7	1647.3

11	Medium gray, medium grained; massive to platy bedded; thin lenses of chert parallel to bedding.	4.5	1642.6
12	Light-medium to dark gray calcareous dolomite; weathers light gray; thinly laminated; argillaceous partings.	5.4	1638.1
13	Light to medium gray, fine grained calcareous, arenaceous dolomite; numerous vugs of calcite; somewhat sheared.	5.9	1632.7
14	Medium to dark gray, calcareous dolomite; thin irregular lamination; shaly partings.	12.3	1626.8
15	Light to medium gray, fine to medium grained calcareous dolomite; bedding undulatory, thin to platy bedded; irregular lenses of chert. (Bottom of this bed forms north wall of quarry.)	5.0	1614.5
16	Light-medium gray, very fine grained calcareous dolomite; weathers light gray; massive grading upward to platy bedded and 8 inch shear zone at top; vugs of white calcite.	4.9	1609.5
17	Light-olive to medium gray, fine grained calcareous dolomite; thinly laminated; rather massive.	7.5	1604.6
18	Light- to medium-olive gray, fine to medium grained; poorly laminated; arenaceous; massive; lower contact undulatory.	2.0	1597.1
19	Light gray calcareous dolomite interbedded with dark gray dolomite; laminated; thin, irregular quartz sandstone beds and lenses; nodules and lenses of chert.	2.2	1595.1
20	Interbedded light gray, very fine grained dolomite and dark gray irregularly bedded chert. Dolomite laminated.	1.1	1592.9
21	Light-olive gray, very fine grained; massive; slickensides at bottom contact; two thin chert beds near top.	5.8	1591.8
22.	Medium-dark gray, medium grained; poorly laminated; massive throughout; local slickensides; scattered vugs and small veins of white dolomite; bottom 1 foot is a discontinuous bed of dark gray chert.	25.5	1586.0
23	Medium gray, very fine grained; laminated, unit is undulatory and flexured; massive; (Unit forms south wall of quarry.)	3.2	1560.5
24	Medium gray, medium grained; arenaceous; irregular bands of chert.	1.2	1557.3
25	Light-olive gray, fine grained; wavy laminations; small veins of calcite and white quartz; scattered quartz grains; massive to platy bedded.	5.0	1556.1
26	Light to medium gray, fine grained; abundant small veins of quartz; irregular nodules of chert; scattered quartz grains; massive.	4.6	1551.1
27	Light gray, coarse grained; undulatory shale partings; irregular bands of chert; disconformable with subjacent unit.	1.7	1546.5

28	Interbedded light gray and dark gray dolomite; numerous wavy laminations; continuous 1 inch bands of chert.	10.5	1544.8
29	Light to medium gray, fine grained; weathers tan; poorly laminated; calcareous; drusy quartz vugs; argillaceous(?); thick to medium bedded; dolomite slightly calcareous.	3.2	1534.3
30	Interbedded light to medium gray, medium to platy bedded dolomite and dark gray chert; dolomite arenaceous; chert thins and thickens.	5.2	1531.1
31	Light to dark gray calcareous dolomite; weathers yellowish white; laminated; sheared.	3.2	1525.9
32	Light to medium gray, fine grained; weathers light gray; massive.	5.0	1522.7
33	Like unit 32. Slickensides and sericite at base.	6.5	1517.7
34	Light-medium gray, fine grained; parts weathering light buff; wavy laminations; arenaceous; medium to platy bedded; (Unit forms north wall of 2nd quarry.)	5.6	1511.2
35	Medium gray, fine grained; arenaceous laminations; cherty.	1.4	1505.6
36	Light gray, coarse grained; vugs of white coarsely crystalline dolomite; bedding undulatory; thin chert beds.	7.3	1504.2
37	Light to medium gray, fine grained; laminated; massive.	2.3	1496.9
38	Interbedded light and dark gray, fine grained calcareous dolomite; light dolomite has streaks of quartz grains; nodules of chert; unit undulatory and flexured.	2.7	1494.6
39	Medium gray, coarse grained; poorly bedded; sericitic partings; pyrite cubes; large irregular patches of chert.	4.0	1491.9
40	Light gray, fine to medium grained; weathers alternately light and dark gray; well laminated; oscillation ripple marks.	6.0	1487.9
41	Medium to dark gray, fine grained; weathers nearly white; laminated; shaly partings; massive.	4.9	1481.9
42	Light-olive gray to dark gray, very fine grained; arenaceous; medium to thick bedded; large vugs of calcite.	4.5	1477.0
43	Medium gray, fine grained dolomite; structureless.	0.6	1472.5
44	Light to medium gray, medium grained; stylolites parallel to bedding; rather massive.	5.2	1471.9
45	Medium-dark gray, fine to medium grained; shaly at bottom.	1.5	1466.7
46	Like unit 45. Weathers dark buff.	1.5	1465.2
47	Medium-dark gray, fine grained; thin bedded; bedding flexured; disconformable to subjacent unit; nodules of chert.	1.7	1463.7

48	Dark gray, very fine grained; massive; thin veins of calcite.	2.7	1462.0
49	Interbedded calcareous shale and dark gray, finely laminated, thin bedded dolomite.	1.6	1459.3
50	Light gray; very thinly laminated; irregular thin beds of chert and quartz sandstone.	0.6	1457.7
51	Light gray, medium grained; discontinuous chert bed at top; thin beds of light gray, very fine grained calcareous dolomite at bottom; massive.	8.3	1457.1
52	Light-olive gray, very fine grained; massive.	2.7	1448.8
53	Black, medium grained; poorly bedded; calcite veins.	3.0	1446.1
54	Medium to dark gray, medium grained; stylolites; massive.	6.0	1443.1
55	Dark gray, fine grained; weathers light-olive gray; laminated; platy.	5.0	1437.1
56	Medium gray, medium grained; massive; disconformable with subjacent unit.	4.7	1432.1
57	Dark gray, fine grained slightly calcareous cryptozoan dolomite. <i>Archaeozoon undulatum</i> (?). This unit is the stratigraphically highest cryptozoan-bearing strata.	1.5	1427.4
58	Light gray, very fine grained; weathers dirty white; thin bedded; lenses and discontinuous beds of chert.	1.9	1425.9
59	Medium gray, medium grained; stylolitic bedding contacts; slickensides at top; massive.	3.7	1424.0
60	Light gray, very fine grained; weathers light buff; slickensides at bottom; platy.	2.0	1420.3
61	Light to medium gray, fine grained; laminated; arenaceous; 2 inch quartz sandstone beds near bottom; well bedded.	1.0	1418.3
62	Light to medium gray, medium grained; large horizontal veins of white quartz; discontinuous bed of oolitic dolarenite at top; massive.	5.9	1417.3
63	Like unit 62. Medium bedded to massive.	12.2	1411.4
64	Like unit 62. Massive; gash veins white quartz.	5.9	1399.2
65	Medium gray, fine to medium grained; weathers brownish gray; sericite on bedding surfaces; platy bedded; disconformable to subjacent unit.	2.5	1390.8
66	Medium gray, medium grained; lenses of quartz sandstone.	2.3	1390.8
67	Light-olive gray; poorly laminated; silty; bedding flexured; thin bedded.	1.0	1388.5
68	Medium-dark gray, medium grained; veins of white dolomite; lenses of oolitic dolarenite; shaly partings.	3.3	1387.5
69	Light to medium gray, interbedded fine and coarse grained; shaly partings; poorly laminated; massive; scour and fill features at bottom.	8.6	1384.2

70	Interbedded light to medium gray dolomite and discontinuous quartz sandstone beds.	2.1	1375.6
71	Light-olive gray; quartz grains concentrated in lenses that weather brown; lenses and discontinuous beds of chert.	2.0	1373.5
72	Light to blue gray, fine grained; laminated; silty and arenaceous; quartz grains disseminated throughout.	1.8	1371.5
73	Desiccation dolorudite with arenaceous matrix; fragments tabular, up to 10 inches long, and composed of laminated fine grained dolomite.	2.0	1369.7
74	Light to medium gray, fine grained; thinly laminated; quartz sand scattered throughout and concentrated in thin irregular bands at top; locally conglomeratic.	4.7	1367.7
75	Medium to dark gray, fine grained; weathers light gray; poorly laminated at top; lenses of chert near top oriented parallel to fracture cleavage; disconformable to subjacent unit.	5.6	1363.0
76	Medium-dark gray, fine grained; thin laminations locally broken and displaced.	2.4	1357.4
77	Medium-dark gray, very fine grained; poorly bedded; irregular fracture pattern; abundant horizontal veins of white dolomite; lenses of oolitic dolarenite. (Top of this unit forms south wall of 2nd quarry.)	3.9	1355.0
78	Light-olive gray, fine grained; weathers brownish gray, laminated.	2.1	1351.1
79.	Medium gray, fine grained; weathers light brownish gray; thinly laminated; sheared; platy.	1.5	1349.0
80	Medium to dark gray, medium grained; large veins of white dolomite; massive.	3.8	1347.5
81	Light to medium gray, fine to medium grained; well laminated; vugs of calcite; thin bedded.	3.2	1343.7
82	Light-olive to medium gray, fine grained; pyrite cubes; massive.	6.8	1340.5
83	Light gray, medium grained; lenses and veins of white dolomite, massive.	4.0	1333.7
84	Light gray, fine grained; thinly laminated; quartz grains scattered and concentrated in lenses and streaks.	7.0	1329.7
85	Dark gray, fine grained; weathers chalky buff; poorly laminated; lenses of chert.	1.1	1322.7
86	Light gray, fine grained; poorly bedded; arenaceous dolorudite(?) near bottom; vugs of white calcite; middle of unit has a stromatolite bed 1 foot thick.	5.7	1321.6
87	Light to medium gray, fine grained; stylolites parallel to bedding; vugs of calcite; massive.	4.5	1315.9
88	Light-medium gray, fine grained; finely laminated; quartz grains disseminated and form lenses.	0.8	1311.4
114	Light gray, fine grained; laminated; massive.	3.2	1309.1

89	Dark gray; arenaceous; veins of calcite; massive.	3.2	1310.6
90	Dark gray, very fine grained; weathers to chalky light buff; quartz grains in lenses and bands up to 4 inches thick.	2.0	1307.4
91	Medium gray, fine grained; numerous thin veins of white dolomite.	5.6	1305.4
92	Light gray, fine grained; arenaceous; poorly laminated; stylolites; vugs of calcite.	4.0	1299.8
93	Interbedded light gray, fine grained laminated dolomite and dolomitic quartz sandstone; desiccation dolorudite with arenaceous matrix at top; fragments tabular, up to 3 inches long and composed of fine grained dolomite.	2.7	1295.8
94	Light-medium gray, fine grained; poorly laminated; vugs of white calcite and quartz; massive.	1.3	1293.1
95	Interbedded light gray, fine grained dolomite and thin bands of quartz sandstone, locally appearing ruditic; slickensides at top.	2.0	1291.8
96	Light gray, fine grained cryptozoan dolomite; <u>Cryptozoon fieldii</u> (?); colonies are brecciated at top.	0.6	1289.8
97	Medium to dark gray, fine grained; laminated; massive.	6.0	1289.2
98	Like unit 97. Thin to medium bedded.	3.9	1283.2
99	Light-olive gray; very finely laminated; sheared.	6.0	1279.3
100	Medium gray, fine grained dolomite interbedded with several thin beds of quartz sandstone, locally ruditic; laminated; medium bedded; platy at top due to shear.	5.5	1273.3
101	Medium-dark gray, medium grained; grades upward to oolitic dolarenite; massive.	4.5	1267.8
102	Light gray, very fine grained; weathers light buff; platy.	2.7	1263.3
103	Medium gray, fine grained; sheared; medium bedded to massive.	4.0	1260.6
104	Shear zone; no bedrock exposed.	1.0	1256.6
105	Light to medium gray fine grained; laminated; thin bedded.	2.8	1255.6
106	Shear zone; platy to shaly bedded dolomite.	0.6	1252.8
107	Medium gray oolitic dolarenite; veins of white dolomite.	1.1	1252.2
108	Light-medium gray, very fine grained; finely laminated; thin bedded.	3.2	1251.1
109	Dark gray oolitic dolarenite; thin bedded.	0.7	1247.9
110	Dark gray, fine grained; finely laminated; sheared.	6.0	1247.2
111	Light-olive gray, very fine grained; argillaceous(?); massive.	2.6	1241.2
112	Light to medium gray, fine grained; veins and drusy vugs of white quartz; massive.	6.9	1238.6
113	Dark gray, very fine grained; weathers chalky white; arenaceous; chert nodules; bottom of unit sheared.	2.6	1231.7
114	Light gray, fine grained; laminated; massive.	3.2	1229.1

115	Medium gray, fine grained cryptozoan dolomite; weathers chalky buff; discontinuous bands and lenses of chert.	2.8	1225.9
116	Dark gray, very fine grained; weathers chalky white; poorly laminated; veins of white dolomite.	0.5	1223.1
117	Light-olive gray, fine to medium grained cryptozoan dolomite; <u>Archaeozoon undulatum</u> ; discontinuous bands of chert at top; disconformable to subjacent unit.	1.8	1222.6
118	Light-olive gray, fine grained; discontinuous bands of chert; top vaguely displays ruditic texture; thin bedded.	5.6	1220.8
119	Interbedded medium-dark gray, very fine grained dolomite weathering chalky light buff and light gray, medium grained dolomite weathering dark gray; arenaceous; bands and lenses of chert; somewhat sheared.	10.3	1215.2
120	Light to medium gray, fine grained; top 1.5 foot contains tectonically deformed stromatolites; <u>Cryptozoon fieldii(?)</u> ; lenses of stretched oolites are present within stromatolites; stretching is parallel to cleavage. (traverse continued without stratigraphic break 54 feet S. 47° W. -34°.)	4.0	1204.9
121	Light gray, very fine grained; well laminated; lenses of quartz sandstone; numerous small sericitic, slickensided surfaces.	4.5	1200.9
122	Oolitic dolarenite grading upward to oolitic dolorudite; oolites dark gray in a light gray cement.	3.2	1196.4
123	Light gray, coarse grained; poorly laminated; medium bedded.	3.8	1193.2
124	Interbedded light-olive gray, fine grained dolomite and oolitic dolarenite; dolomite poorly laminated; thin to platy bedded.	10.3	1189.4
125	Light-medium gray desiccation dolorudite; fragments up to 4 inches long; matrix medium grained, arenaceous dolomite.	2.4	1179.1
126	Medium gray, fine to medium grained, slightly calcareous dolomite; laminated; irregular bed of oolitic chert at top; massive.	2.9	1176.7
127	Medium gray, fine grained; medium to thin bedded.	2.5	1173.8
128	Mottled light-medium gray and brownish gray, medium to coarse grained; laminated at bottom; thick bedded.	3.5	1171.3
129	Medium gray oolitic dolarenite; 1 inch band of oolitic chert near center of unit.	2.4	1167.8
130	Like unit 128. Lenses of chert; poorly exposed. (Traverse continued without stratigraphic break 41 feet N. 46° E. +35°.)	6.3	1165.4

131	Medium gray, medium grained; numerous irregular veins of coarsely crystalline dolomite; poorly exposed.	5.8	1159.1
132	Light-medium gray, fine grained; irregular patches and lenses of chert; poorly exposed.	6.4	1153.3
133	Medium gray, medium grained; veins and vugs of dolomite; conchoidal fracture; lenses of chert abundant.	6.5	1146.9
134	Medium gray oolitic dolarenite; oolites best visible on weathered surface; disconformable with subjacent unit.	0.7	1140.4
135	Interbedded oolitic dolarenite and cryptozoan dolomite; <u>Cryptozoon fieldii</u> and other types; oolites present as lenses and in pockets within stromatolite colony.	4.0	1139.7
136	Light to medium gray, fine grained; wavy sericitic partings; massive.	3.6	1135.7
137	Light-medium gray, fine grained; weathers light buff; thin sericitic shale partings along bedding.	3.2	1132.1
138	Medium-dark gray, fine grained; chert abundant as nodules, and lenses; a bed of cryptozoan chert 12 inches thick near top.	3.0	1128.9
139	Light-medium gray, fine grained cryptozoan dolomite; <u>Archaeozoon undulatum</u> and other large varieties;	3.0	1125.9
140	Medium gray, fine grained; thin lenses of chert; platy.	0.8	1122.9
141	Light-medium gray, fine grained cryptozoan dolomite overlain by desiccation dolorudite; <u>Cryptozoon fieldii</u> (?) and other varieties.	2.9	1122.1
142	Dark gray, fine grained oolitic dolarenite.	1.5	1119.2
143	Dark gray, fine grained; weathers vaguely oolitic; laminated.	1.5	1117.7
144	Light-medium gray desiccation dolorudite; weathers dirty gray; wavy laminations; stromatolites(?).	1.0	1116.2
145	Medium gray dolomite interbedded with oolitic dolarenite; bottom has partings of silt; vugs of quartz.	4.0	1115.2
146	Light-medium gray fine to medium grained; weathers chalky buff; well laminated; thin bedded.	5.8	1111.2
147	Light-olive gray, fine grained; numerous sericitic partings; sheared; platy bedded.	1.4	1105.4
148	Medium gray, fine grained; large nodules of chert.	3.6	1104.0
149	Light-olive to medium gray, fine grained; discontinuous bands of chert and quartz sandstone; well bedded to platy; mud cracks.	3.3	1100.4
150	Medium gray, fine grained; nodules and lenses of chert; massive.	3.3	1097.1
151	Medium dark gray fine to medium grained cryptozoan dolomite; <u>Archaeozoon undulatum</u> .	0.9	1093.8
152	Yellow brown, fine to medium grained; cubes of pyrite.	0.8	1092.9

153	Medium gray, medium grained; small wavy silt shale streaks that weather as ribs; 2 inch band of chert at top.	2.9	1092.1
154	Light-medium gray, fine grained; numerous laminations of silt and quartz grains; quartz distributed in intricate manner forming honeycombed pattern on weathered surface.	0.9	1089.2
155	Light-medium gray, coarse grained; arenaceous; poorly laminated.	2.5	1088.3
156	Dark gray, medium grained; crisscrossed by large veins of white dolomite; thin bedded.	7.0	1085.8
157	Like unit 156. Massive.	1.9	1078.8
158	Concealed.	3.0	1076.9
159	Medium gray, medium grained oolitic dolarenite; thin bedded.	1.1	1073.9
160	Medium-dark gray, medium grained; veins of white dolomite.	1.4	1072.8
161	Concealed. (Traverse continued: (1) 28.6 feet S. 37° W., 0°, (2) 58 feet S. 42° W., - 15°, (3) 70.6 feet S. 55 W., -34°.)	12.5	1071.4
162	Medium gray, very fine grained; weathers [chalky] chalky dark buff; well laminated; silty; bottom 6 feet thin bedded; top thicker bedded and arenaceous; sheared; discontinuous bands and nodules of chert.	9.5	1058.9
163	Concealed.	1.2	1049.4
164	Dark-medium gray, fine grained; veins of white dolomite; slickensides parallel to bedding.	5.5	1048.2
165	Concealed.	8.5	1042.7
166	Like unit 164. Massive.	5.0	1034.2
167	Light-medium gray oolitic dolarenite; wavy laminations.	0.8	1029.2
168	Light-medium gray, fine to medium grained cryptozoan dolomite; primitive type(?).	2.8	1028.4
169	Medium-dark gray, fine grained; thinly laminated; calcareous shaly slickensides; severely sheared.	1.5	1025.6
170	Medium gray, fine grained; dark gray to black shale partings along shear zones; nodules of chert; massive.	3.6	1024.1
171	Like unit 170; less massive.	2.5	1020.5
172	Light-medium gray, fine to medium grained; platy to medium bedded; thin veins of white dolomite.	2.8	1018.0
173	Light-olive gray, fine grained; well laminated, platy.	3.4	1015.2
174	Medium gray, fine grained; weathers light brown; thinly laminated; argillaceous; sheared; thin to platy bedded.	4.5	1011.8
175	Light-medium gray oolitic dolarenite; diagonal veins of white dolomite; discontinuous bands of chert; thin to medium bedded; bottom 1.5 foot shaly.	5.6	1007.3

176	Light gray, fine grained; vaguely laminated; pyrite cubes; sheared; medium to platy bedded.	3.5	1001.7
177	Light-medium to olive gray, very fine grained; laminated simulating shale; thin bedded.	2.4	998.2
178	Medium to dark gray, fine grained; laminations in relief; disconformable to subjacent unit.	1.7	995.8
179	Dark gray, fine to medium grained oolitic dolarenite; oolites displayed only on weathered surface.	0.6	994.1
180	Like unit 179. Thin bedded.	0.8	993.5
181	Like unit 179. Diagonal veins of white dolomite.	2.7	992.7
182	Dark gray, very fine grained; sericitic partings; lenses of oolitic chert; thin bedded; sheared.	4.2	990.0
183	Medium gray, fine to medium grained; sericitic partings; veins of white dolomite.	3.3	985.8
184	Light-medium gray, fine grained; laminated; thin bedded.	0.9	982.5
185	Medium to dark gray, fine grained oolitic dolarenite.	2.7	981.6
186	Light-medium gray, very fine grained; weathers chalky light gray; thick laminations; platy bedded.	1.2	978.9
187	Interbedded dark gray sheared dolomite and calcareous shale; weathers light brown; sericitic slickensides.	5.5	977.7
188	Concealed.	1.0	972.2
189	Light-olive gray; silty laminations; massive; poorly exposed.	4.0	971.2
190	Concealed. (Traverse continued 32.4 feet East +37°.)	18.4	967.2
191	Light-olive gray, medium grained oolitic dolorudite; fragments irregularly shaped and oriented at random.	1.5	948.8
192	Mottled light-medium gray, medium grained; wavy laminations; massive; poorly exposed.	6.3	947.3
193	Medium-olive gray, fine grained; silty; sericitic; weathers to irregular pits and grooves; sheared.	5.2	941.0
194	Medium gray, fine to medium grained oolitic dolarenite; arenaceous; sheared; poorly exposed.	11.6	935.8
195	Light-medium to dark gray, fine grained; quartz sandstone lenses and irregular bands weather in positive relief. locally ruditic; platy bedded; sheared.	8.2	924.2
196	Medium gray, medium grained, oolitic dolarenite.	1.4	916.0
197	Desiccation dolorudite with abundant quartz grains in matrix; sandstone portions weather in strong positive relief; fragments up to 4 inches composed of medium gray, very fine grained dolomite weathering chalky white.	2.6	914.6
198	Olive gray, fine to medium grained; silty laminations.	1.5	912.0
199	Medium gray, fine grained; laminated; nodules and lenses of chert; veins of white dolomite; massive.	2.0	910.5
200	Light-olive gray, fine grained; mottled; lower part laminated with silt; quartz grains disseminated; poorly exposed.	18.8	908.5

201	Olive gray; wavy laminations weather in positive relief; irregular patches of white quartz; massive.	2.0	889.7
202	Concealed.	0.5	887.7
203	Like unit 201. Top 6 inches fault breccia. (Traverse continued without stratigraphic break 59 feet S. 42° W., -38°.)	4.4	887.2
204	Medium gray mottled with olive gray, medium grained; vaguely oolitic; sericitic partings; lenses and bands of chert; massive.	6.2	882.8
205	Light medium gray; gash veins of dolomite; thin bedded.	3.8	876.6
206	Medium gray, fine grained; arenaceous; quartz grains weather in positive relief.	2.4	872.8
207.	Olive to yellowish gray, medium grained; sericitic, extremely sheared.	3.9	870.4
208	Light-medium gray, fine grained; vugs of quartz; sericitic; platy bedded; poorly exposed.	12.8	866.5
209	Dark-medium gray, fine grained; shaly; sheared.	1.6	853.7
210	Yellow brown to medium gray silty dolomite; weathers soft with pitted surface.	1.9	852.1
211	Light medium gray, fine grained; laminated; platy; sheared.	5.0	850.2
212	Dark-medium gray, fine to medium grained; thick silt laminations in central part; horizontal veins of white dolomite; massive except for platy central part.	13.2	845.2
213	Medium gray, very fine grained; limonitic and sericitic laminations; thin to platy bedded; sheared.	3.0	832.0
214	Like unit 213. Veins of white dolomite.	3.8	829.0
215	Like unit 213. Medium bedded; poorly exposed.	10.9	825.2
216	Medium to olive gray, fine grained; laminations of silt and clay; poorly exposed.	2.6	814.3
217	Light-medium gray, fine to medium grained; veins of white dolomite; medium to platy bedded; sheared.	3.3	811.7
218	Mottled light-medium and medium gray; arenaceous; poorly exposed.	1.4	808.4
219	Interbedded mottled light-olive gray, fine grained dolomite and oolitic dolarenite; laced with veins of dolomite.	6.8	807.0
220	Olive to medium gray, fine grained; thin to platy bedded; sheared at bottom.	4.5	800.2
221	Concealed.	4.7	795.7
222	Light-medium gray, very fine grained; mottled; irregular streaks of dark gray dolomite.	4.9	791.0
223	Interbedded medium gray, very fine grained laminated dolomite and oolitic dolarenite; poorly exposed.	4.9	786.1

224	Olive gray, fine grained; weathers chalky; laminated; discontinuous bands of chert; center has lenses of oolitic dolarenite.	5.4	781.2
225	Dark gray oolitic dolarenite interbedded with light-medium gray, fine grained dolomite; thin bedded.	4.5	775.8
226	Light-medium to olive gray; thick silty laminations; sheared; veins of white dolomite.	5.0	771.3
227	Concealed.	4.2	766.3
228	Interbedded medium-dark gray, medium grained dolomite and dolorudite vaguely oolitic; fragments angular; arenaceous; sericitic partings; sheared.	3.0	762.1
229	Medium gray desiccation dolorudite; fragments tabular and composed of light gray, very fine grained dolomite; oriented parallel to bedding; large quartz grains occur disseminated throughout.	4.6	759.1
230	Dark-olive to dark-medium gray, very fine grained; thin bands of silt weather in positive relief; sheared; platy.	9.2	754.5
231	Medium-dark gray, very fine grained; wavy slickensides; sericite; sheared; platy.	12.8	743.3
232	Concealed.	4.2	732.5
233	Like unit 231. Poorly exposed. (Traverse continued without stratigraphic break 47 feet N. 60° E. +40°.)	14.6	728.3
234	Mottled olive gray and medium gray, fine to medium grained; silty and argillaceous laminations weather in positive relief; thin bedded; poorly exposed.	8.6	713.7
235	Concealed. (Traverse continued 20.8 feet N. 25° W., 0°.)	18.0	705.1
236	Mottled light-medium gray and olive gray; vague ruditic texture; oolites; massive.	2.5	687.1
237	Concealed. (Traverse continued 18 feet N. 24° W. 0°.)	15.6	684.6
238	Medium to dark gray, fine grained; poorly laminated; very poorly exposed.	2.8	669.0
239	Concealed.	2.6	666.2
241	Oolitic dolarenite grading upward to light-medium gray, fine grained arenaceous dolomite; locally texture is ruditic.	5.2	658.0
240	Dark-medium gray, medium to coarse grained; limonitic stained sericitic partings.	5.6	663.6
242	Mottled olive gray and medium gray, fine grained; pyrite cubes; massive; very poorly exposed.	8.0	652.8
243	Mottled olive gray; limonitic-stained sericitic partings that weather in lacy patterns in positive relief; massive; poorly exposed.	3.6	644.8
244	Olive to medium gray, very fine grained; cleaved; thick bedded.	4.4	641.2

245	Mottled light-olive gray and light-medium gray dolomite interbedded with thin 1 inch bands of oolitic dolarenite; slickensides on bedding planes.	2.4	636.8
246	Dark gray, very fine grained; conchoidal fracture; massive.	2.0	634.4
247	Medium-olive gray, medium grained; locally mottled with medium gray; small veins and vugs of white dolomite.	11.5	632.4
248	Light-olive gray, fine grained; grades upward to shaly, sheared zone; thin veins of white dolomite.	0.7	620.9
249	Mottled light-medium gray and olive gray, fine grained; joints coated with white quartz; veins of dolomite; weathered surface knobby; thick bedded.	11.0	620.2
250	Light-medium gray, fine grained; weathers to chalky light gray; several discontinuous bands chert; top half of unit contains stromatolites; <u>Archaeozoon undulatum</u> (?) and other varieties.	3.5	609.2
251	Concealed. (Traverse continued 24.6 feet S. 67° E. +30°.)	17.5	605.7
252	Medium gray, fine grained; bedding appears massive; weathers hackly; poorly exposed.	10.7	588.2
253	Concealed. (Traverse continued 94 feet S. 40° E. 0°.)	85.0	577.5
254	Medium-dark gray, fine grained; weathers soft; thin shaly and silty partings; some parts displaying ruditic texture; platy, disconformable to subjacent unit.	1.4	492.5
255	Light to medium gray oolitic dolarenite, yellow and red limonite stains on bedding surfaces, oolites best displayed on weathered surface. (Unit forms north face of large quarry behind three kilns.)	3.2	491.1
256	Interbedded light-medium gray oolitic dolarenite and desiccation dolorudite with light gray arenaceous matrix; fragments tabular and up to 2 inches long.	1.2	487.9
257	Thinly interbedded dark-medium gray, fine grained dolomite, light gray medium grained silty dolomite and argillaceous, limonitic quartz sandstone; middle 8 inches is arenaceous desiccation dolorudite; oscillation ripple marks (2 inches crest to crest) in thin bedded dolomite near top.	3.3	486.7
258	Light-medium gray, very fine grained; weathers yellow gray; conchoidal fracture; sericitic partings; thin bedded; ripple marks and "fucoids" present.	1.6	483.4
259	Dark-medium gray oolitic dolarenite; oolites seen on weathered surface; vugs drusy quartz; lenses of chert; massive.	2.8	481.8

260	Desiccation dolorudite; tabular fragments up to 7 inches long of medium gray, fine grained dolomite; oriented parallel to bedding; matrix silty, arenaceous; unit weathers yellow tan.	1.0	479.0
261	Light-medium to medium gray, fine grained; oolites vaguely distinguished on weathered surface.	4.0	478.0
262	Like unit 261. No oolites distinguishable.	1.6	474.0
263	Light-medium to light-olive gray, very fine grained; weathers light blue; subconchoidal fracture; sericitic partings; vaguely oolitic near bottom; massive.	18.2	472.4
264	Light-medium gray oolitic dolarenite.	1.4	454.2
265	Interbedded dark gray laminated dolomite and cryptozoan dolomite; <u>Cryptozoon fieldii</u> ; bioconstructed colonies thin and thicken; oolites in pockets within colonies and between adjacent growths.	0.6	452.8
266	Dark-medium gray oolitic dolarenite; massive.	4.0	452.2
267	Light-medium gray, fine grained dolomite with lenticular beds of oolitic dolarenite; subconchoidal fracture.	5.8	448.2
268	Olive gray oolitic dolarenite; weathers light buff; stylolitic partings of limonite; sericite on bedding planes.	4.1	442.4
269	Medium gray dolomitic quartz sandstone weathering yellowish orange; cross bedded; locally ruditic with small fragments composed of light gray laminated dolomite.	1.8	438.3
270	Interbedded silty calcareous shale, thin bands of siltstone and quartz sandstone, and finely laminated gray, fine grained dolomite; argillaceous throughout(?); weathers dark yellowish orange; sheared; platy bedded.	5.8	436.5
271	Fault zone; no bedrock exposed.	1.5	430.7
272	Light olive gray; weathers to chalky dirty white; laminated; limonitic and sericitic partings.	2.5	429.2
273	Medium gray, oolitic dolarenite; argillaceous; corners weather rounded and smooth; veins of white quartz.	3.3	426.7
274	Medium gray, fine grained cryptozoan dolomite; stromatolite structure seen on weathered surfaces; argillaceous.	0.8	423.4
275	Interbedded medium gray dolomite, friable dolomitic quartz sandstone and lenses of oolitic dolarenite; argillaceous; sandstone crossbedded and stained with limonite; thin bedded.	3.1	422.6
276	Interbedded medium gray dolomite, oolitic dolarenite and arenaceous dolorudite; fragments in dolorudite tabular, up to 1 inch long; limonite partings.	0.7	419.5

277	Olive yellow, calcareous shale interbedded with light-medium gray dolomite; sericitic partings.	0.4	418.8
278	Light-medium gray, very fine grained cryptozoan dolomite; <u>Anomalophycus compactus</u> and larger variety; locally stromatolites are brecciated and reworked.	1.0	418.6
279	Medium-dark gray, medium grained; laminated; vaguely oolitic.	0.4	417.6
280	Light-olive to medium gray, fine grained; orange red limonite partings; oolitic; massive.	7.2	417.2
281	Like unit 280. No oolites.	7.3	410.0
282	Medium gray, fine grained; lenses of limonitic-stained oolites; some stylolitic limonite partings.	2.1	402.7
283.	Light-medium gray, very fine grained cryptozoan dolomite; <u>Cryptozoon fieldii</u> (?); some colonies brecciated and reworked in overlying desiccation dolorudite; quartz grains abundant in desiccation dolorudite.	1.6	400.6
284	Medium gray oolitic dolarenite interbedded with dolorudite; fragments barely discernable and oriented parallel to bedding.	3.0	399.0
285	Shear zone. No bedrock exposed.	0.8	396.0
286	Like unit 284.	3.2	395.2
287	Shear zone. Sericitic shale and mylonite.	0.2	392.0
288	Like unit 283.	0.9	391.8
289	Like unit 284.	1.0	390.9
290	Heterogeneous desiccation dolorudite composed of angular to subrounded fragments of dolomite in arenaceous dolomite matrix; limonite and sericite partings.	0.7	389.9
291	Dark gray, very fine grained cryptozoan dolomite; stromatolites poorly preserved and brecciated; partings of limonite and silt; thin bedded.	0.6	389.2
292	Medium gray, very fine grained oolitic dolarenite.	0.9	388.6
293	Light-medium gray, fine grained; weathers light gray; poorly laminated; partings of sericite and limonite.	2.1	389.7
294	Interbedded dark-medium gray, very fine grained dolomite and calcareous shale; stained with limonite; sheared.	1.3	385.6
295	Light-olive gray arenaceous dolomite; stylolitic limonite partings; finely laminated.	1.7	384.3
296	Fine grained oolitic dolarenite; limonitic.	1.8	382.6
297	Light-medium gray, very fine grained cryptozoan dolomite.	0.7	380.8
298	Light-medium gray, fine grained; weathers to light gray; many irregular sericitic and limonitic partings; vugs of white dolomite.	1.5	380.1
299	Light-medium gray oolitic dolarenite; limonitic stains.	0.2	378.6
300	Like unit 298.	2.5	378.4

301	Light-medium gray shaly dolomite; weathers light yellow; extremely sheared; limonitic.	0.7	376.9
302.	Medium gray oolitic dolarenite; locally fragments are present to give ruditic texture.	1.3	375.2
303	Interbedded light-olive gray and dark-medium gray; former weathers chalky light gray; limonitic; platy.	3.7	373.9
304	Medium gray oolitic dolarenite; oolites weather dark gray in light gray cement; limonitic.	1.1	370.2
305	Interbedded medium gray, very fine grained dolomite and oolitic dolarenite; oolites occur in lenses and discontinuous bands; limonitic.	6.2	369.1
306	Medium gray, fine grained; weathers chalky yellow; thick partings of limonite and sericite.	2.4	362.9
307	Oolitic dolarenite; sericitic; limonitic.	1.5	360.5
308	Olive to medium gray, very fine grained; laminated; grading upward to desiccation dolorudite; sericitic; limonitic.	2.3	359.0
309	Dark-medium gray, fine grained; vaguely oolitic; stylolitic partings of limonite.	1.0	356.7
310	Like unit 308. Platy bedded.	2.1	355.7
311	Olive gray, fine grained; sericitic; limonitic; massive.	1.6	353.6
312	Medium gray oolitic dolarenite; limonite; thin veins of white dolomite.	0.6	352.0
313	Light-olive gray, fine grained dolomite interbedded oolitic dolarenite; vaguely laminated; large veins of white dolomite; massive.	4.1	351.2
314	Dark-medium to olive gray, fine grained; subconchoidal fracture; arenaceous; limonitic; massive.	3.6	347.3
315	Medium gray oolitic dolarenite; oolites discernable only on weathered surface; pyrite cubes; stylolitic limonitic partings; conchoidal fracture; massive; disconformable with subjacent unit.	2.8	343.7
316	Interbedded medium gray, fine grained dolomite and dolorudite; arenaceous; unit has 1 inch pinkish red dolomitic quartz sandstone at bottom. Large irregular nodules of limonite occur in the center of unit.	6.2	340.9
317	Medium gray, fine grained cryptozoan dolomite; several very large colonies visible on south wall of quarry in southeast corner. These colonies measure 4 feet across and 10 inches high and appear as large inverted bowls with knobby surfaces.	0.9	334.7
318	Dark gray, fine grained oolitic dolarenite; dense.	4.0	333.8
319	Medium gray, fine grained, weathered surface vaguely displays oolites; subconchoidal fracture; thin bedded.	6.9	329.8
320	Light-medium gray, fine grained; stylolitic partings of shaly material; conchoidal fracture.	3.5	322.9

321	Like unit 320. Thin bedded.	1.3	319.4
322	Light-medium gray, fine grained; finely laminated; grades upward to desiccation dolorudite; sericitic partings.	2.8	318.1
323	Dark gray, fine grained dolorudite; laminated; silty; platy.	0.4	315.3
324	Olive to medium gray, very fine grained dolorudite; fragments are small; limonitic and sericitic partings.	6.1	314.9
325	Interbedded oolitic dolarenite and arenaceous dolorudite; fragments of dolorudite of various peculiar shapes; thick limonitic partings; unit broken by thick veins of white dolomite.	12.0	308.8
326	Interbedded light-medium gray, fine grained dolomite and oolitic dolarenite; oolitic dolarenite zones lenticular; veins of white dolomite; limonite.	4.1	296.8
327	Olive- to dark-medium gray, fine grained; poorly laminated; limonitic, veins of white quartz and dolomite; massive.	11.1	292.7
328	Light-medium gray, fine grained; locally zones of fault breccia are present; abundant limonite in partings and stains on joint surfaces; platy bedded.	1.2	281.6
329	Interbedded medium gray, fine grained dolomite and oolitic dolarenite; oolitic dolarenite occurs in lenses; unit laced with thin veins of white dolomite.	3.2	280.4
330	Interbedded tannish gray and medium gray; fine grained dolomite; limonitic partings, laminations and ribs.	3.0	277.2
331	Olive to dark-medium gray, very fine grained; laminated; limonitic; thin bedded.	2.3	274.2
332	Light-olive gray fine grained; laminated; limonitic; platy.	6.2	271.9
333	Olive to medium-dark gray, fine to medium grained; thin veins of white dolomite; limonitic; poorly exposed.	5.8	265.7
334	Medium gray cryptozoan dolomite; <u>Cryptozoon fieldii</u> ; Very well preserved and displays excellent cross section and knobby top bedding surface formed by tops of individual growths.	1.5	259.9
335	Oolitic dolarenite; medium bedded.	2.4	258.4
336	Interbedded light-medium gray, fine grained; laminated; locally ruditic with thin lenses of quartz sandstone.	2.0	256.0
337	Concealed. (Traverse continued; (1) 8.0 feet S. 28° E +25°, (2) 15.5 feet S. 14° E. 0°.)	21.0	254.0
338	Medium to dark gray oolitic dolarenite; limonitic, veins of white dolomite; slickensides on bedding. (Unit forms north wall of quarry in park-like area behind Mary-Mar-Jon house.)	4.2	233.0

339	Orange red shaly dolomite; limonite concentrated in thin bands; extremely sheared.	1.1	228.8
340	Mottled light-medium gray and light-olive gray, medium grained; some thin interbeds argillaceous fine grained dolomite; veins of white dolomite.	2.6	227.7
341	Dark gray, medium grained; dense.	0.9	225.1
342	Medium gray oolitic dolarenite; limonitic stained sericite partings.	1.2	224.2
343	Like unit 340. No veins of dolomite.	2.0	223.0
344	Fault zone. No bedrock exposed.	1.0	221.0
345	Mottled dark gray and olive gray oolitic dolarenite; weathers to knobby irregular surface; limonitic.	2.2	220.0
346	Light-olive gray slightly calcareous shale interbedded with oolitic dolarenite.	0.4	217.8
347	Light-olive gray, very fine grained; limonite stains on joints; bottom 7 inches cryptozoan dolomite; <u>Cryptozoon fieldii</u> .	1.1	217.4
348	Dark gray, medium grained; vaguely oolitic on weathered surface; limonitic.	0.9	216.3
349	Light-medium gray, very fine grained dolomite interbedded with lenses of oolitic dolarenite; platy.	1.0	215.4
350	Like unit 317. Cryptozoan dolomite with colonies measuring 4 feet in diameter; thin bedded.	2.0	214.4
351	Light-olive gray, soft, porous dolomite; abundant limonite partings and cavity fillings.	1.2	212.4
352	Dark-medium gray, medium grained dolomite interbedded with olive gray silty dolomite.	2.5	211.2
353	Light-olive gray, fine grained; laminated; shaly partings; limonitic; disconformable to subjacent and superjacent units.	1.3	208.7
354	Dark-medium gray, very fine grained; laminated; sericitic and limonitic partings.	2.0	207.4
355	Light-medium gray, fine grained; limonitic; white quartz coats joints.	2.0	205.4
356	Dark-medium gray, fine grained oolitic dolarenite; dense; stylolitic partings of limonite.	2.0	203.4
357	Dark-medium gray, very fine grained oolitic dolarenite with cryptozoan dolomite at bottom.	3.6	201.4
358	Olive gray, very fine grained; limonitic partings.	0.9	197.8
359	Oolitic dolarenite with patchy discontinuous development of small stromatolite colonies. Oolites are subjacent and packed between adjacent colonies.	1.6	196.9
360	Mottled light-olive gray and medium gray, medium grained; limonitic stains; shaly partings.	1.2	195.3
361	Light-medium gray, coarse grained oolitic dolarenite; oolites display peculiar "half-moon" aspect; individual oolites are large and are divided into a light upper half and dark lower half; oolites weather to negative relief resulting in a pitted surface.	1.0	194.1

362	Dark gray oolitic dolarenite; unit laced with large veins of white dolomite; disconformable to subjacent unit.	1.2	193.1
363	Mottled medium and olive gray, fine grained; limonitic.	5.9	191.9
364	Mottled dark-medium and olive gray; argillaceous partings; massive.	3.8	186.0
365	Dark to olive gray, very fine grained; top vaguely laminated; conchoidal fracture; massive.	3.5	182.2
366	Olive gray, fine grained; laminated; calcareous shale partings; platy bedded.	0.9	178.7
367	Dark-medium gray oolitic dolarenite; bottom 3 inches dark gray, coarse grained dolomite.	2.4	177.8
368	Medium gray, fine grained; finely laminated; sericitic; platy; top 12 inches desiccation dolorudite.	2.5	175.4
369	Dark gray, very fine grained; wavy laminations of silt; sericitic partings; center of unit has 6 inch bed dark gray, coarse grained dolomite.	5.0	172.9
370	Thinly interbedded medium gray, fine grained dolomite and sericitic, limonitic shale; weathers yellow orange; shaly to platy bedded.	6.3	167.9
371	Dark gray, very fine grained; sericitic partings; conchoidal fracture.	0.9	161.9
372	Like unit 370. Argillaceous.	2.8	160.7
373	Dark-medium gray, fine grained; sericitic; limonitic; platy; sheared.	2.0	157.9
374	Like unit 370.	4.2	155.9
375	Mottled olive gray and medium gray, medium grained dolomite; thick limonitic partings; poorly exposed.	3.7	151.7
376	Concealed.	1.7	148.0
377	Mottled dark-medium gray and olive gray, fine grained dolomite; limonitic; sericitic; poorly exposed.	1.6	146.3
378	Medium gray oolitic dolarenite; limonitic stains.	0.9	144.7
379	Dark-medium gray, very fine grained; bottom mottled with light-olive gray, fine grained dolomite.	1.9	143.8
380	Light-olive gray, very fine grained cryptozoan dolomite; <u>Cryptozoon fieldii</u> .	0.9	141.9
381	Medium gray oolitic dolarenite; limonite stains on bedding; veins of white dolomite.	3.2	141.0
382	Like unit 380.	0.4	137.8
383	Medium-dark gray, very fine grained; arenaceous.	10.6	137.4
384	Light-medium gray, fine grained; stylolitic sericite and limonite partings; some discontinuous beds and lenses of oolitic dolarenite.	3.6	126.8

385	Like unit 384. Sheared.	4.8	123.2
386	Medium-dark gray, fine to medium grained; vaguely oolitic on weathered surface; poorly exposed.	4.4	118.4
387	Mottled light- and dark-medium gray, medium to coarse grained; limonitic; poorly exposed.	3.6	114.0
388	Concealed.	1.1	110.4
389	Medium gray, very fine grained; wavy partings of limonitic, argillaceous material weathering in positive relief; vaguely laminated; sheared; poorly exposed.	5.9	109.3
390	Medium gray, very fine grained; weathers dark gray; limonitic stained stylolitic shale partings; massive.	9.8	103.4
391	Olive gray, very fine grained; weathers light buff; well laminated; argillaceous.	5.3	93.6
392	Medium gray, fine grained; laminated; limonitic partings; fault breccia zone 7 inches thick near top.	4.4	88.3
393	Olive gray, fine grained; small veins and vugs of white dolomite; massive.	3.2	83.9
394	Dark-medium gray oolitic dolarenite; massive.	3.3	80.7
395	Medium gray, fine to medium gray oolitic dolarenite; arenaceous; top 12 inches displays desiccation dolorudite with subrounded fragments up to 1 inch long and composed of dark gray dolomite.	2.7	77.5
396	Yellow, calcareous, shaly bedded dolomite; abundant sericite; severely sheared.	0.9	74.8
397	Interbedded medium gray, fine grained dolomite and oolitic dolarenite; silty, limonitic partings; massive.	5.8	73.9
398	Dark-medium gray, fine grained; limonitic.	1.6	68.1
399	Like unit 398. Platy bedded; sheared.	3.3	66.5
400	Interbedded medium gray, fine grained dolomite, oolitic dolarenite and arenaceous dolomite; oolite beds are up to 12 inches thick and lenticular. Bottom 2 feet composed of desiccation dolorudite.	6.0	63.2
401	Medium gray, fine grained cryptozoan dolomite; weathers light gray; argillaceous.	1.0	57.2
402	Light-medium gray, fine grained; irregular partings composed of silt, quartz grains and limonite; vaguely oolitic.	4.8	56.2
403	Medium to olive gray, fine grained dolomite.	1.6	51.4
404	Desiccation dolorudite overlying cryptozoan dolomite; bottom 1 inch oolitic dolarenite; limonitic.	1.3	49.8
405	Dark-medium gray dolomite; veins of white dolomite.	1.1	48.5

406	Medium gray dolomite interbedded with oolitic dolarenite; thin 3 inch band of desiccation dolorudite in center and 5 inches of tannish silty shale at bottom; sericitic slickensides; limonitic stained argillaceous partings.	7.2	47.4
407	Medium gray, fine grained oolitic dolarenite; quartz grains scattered throughout.	1.5	40.2
408	Tan to light-olive gray, very fine grained araneaceous dolomite; limonitic stains; sheared.	0.6	38.7
409	Dark-medium gray oolitic dolarenite; conchoidal fracture; disconformable with subjacent unit.	2.3	38.1
410	Olive to medium gray, fine grained; weathering to knobby irregular surface; limonitic; thin bedded.	2.5	35.8
411	Medium gray oolitic dolarenite; oolites visible on weathered surface only.	3.3	33.3
412	Light-medium gray, fine grained; poorly laminated; numerous sericitic partings stained with limonite; massive.	4.1	30.0
413	Medium to olive gray, fine grained dolorudite; fragments subrounded up to 1 inch long of light gray dolomite; scattered oolites; bottom 10 inches shaly, sheared dolomite; limonitic.	3.1	25.9
414	Medium gray oolitic dolarenite; thin veins of white dolomite in positive relief.	3.4	22.8
415	Light-medium to light-olive gray, very fine grained; limonitic and argillaceous partings; massive.	3.3	19.4
416	Like unit 415. Platy bedded.	2.8	16.1
417	Mottled dark- and light-olive gray oolitic dolarenite; limonitic stains; sericitic partings.	0.4	13.3
418	Light-medium gray, fine grained; partly mottled with light-olive gray; bottom 12 inches vaguely oolitic.	1.8	12.9
419	Like unit 418. Oolitic; limonitic.	1.0	11.1
420	Medium gray; weathers to buff; scattered quartz grains.	0.8	10.1
421	Light-olive gray, very fine grained dolomite; central 5 inches contains cryptozoan dolomite; <u>Archaeozoon undulatum</u> (?).	1.0	9.3
422	Dark gray oolitic dolarenite; limonitic partings; joints coated with white dolomite.	0.8	8.3
423	Olive gray, very fine grained dolomite interbedded with oolitic dolarenite.	0.4	7.5
424	Interbedded medium gray, very fine grained dolomite and oolitic dolarenite; limonitic partings and stains on bedding surfaces.	4.5	7.1
425	Light-olive gray to olive gray, very fine grained; laminated; thin to platy bedded.	0.6	2.6
426	Medium to olive gray, very fine grained; numerous partings of limonite-stained argillaceous material weathering in positive relief. (Unit forms south wall of quarry behind Mary Mar-Jon house.)	2.0	2.0

VITA

The author was born in Cleveland, Ohio on February 14, 1934. He received his elementary and secondary education in Auburn, Ohio. He entered St. Meinrad Seminary, St. Meinrad, Indiana, for one year and in September, 1953, transferred to Western Reserve University, Cleveland, Ohio. In May, 1957, he was elected to the Phi Beta Kappa Honorary Society and in June, 1957, was awarded the Bachelor of Arts Degree in Geology graduating magna cum laude.

In September, 1957, the author began graduate study in geology at the University of Illinois under a University Fellowship and received the Master of Science Degree in Geology in August, 1958. Graduate study was continued under successive University Fellowships of and the Degree of Doctor/Philosophy in Geology was conferred upon him in October, 1960. His dissertation was entitled, "Petrography of the Upper Cambrian Dolomites of Warren County, New Jersey."

The author, with Prof. Albert V. Carozzi, published his Masters Degree thesis entitled, "Microfacies of the Wabash Reef, Wabash, Indiana," in the Journal of Sedimentary Petrology, Vol. 29, pp. 164-171, June, 1959.

USGS LIBRARY - RESTON



3 1818 00083247 5